DISSERTATION

PLASMA FLUCTUATIONS IN ION THRUSTERS UTILIZING HOLLOW CATHODES

Submitted by
Dennis J. Fitzgerald
Department of Mechanical Engineering

In partial fulfillment of the requirements
for the Degree of Doctor of Philosophy
Colorado State University
Fort Collins, Colorado
Summer, 1983

COLORADO STATE UNIVERSITY

July 15, 1983

WE HEREBY RECOMMEND THAT THE THESIS PREPARED UNDER OUR SUPERVISION BY DENNIS J. FITZGERALD ENTITLED "PLASMA FLUCTUATIONS IN ION THRUSTERS UTILIZING HOLLOW CATHODES" BE ACCEPTED AS FULFILLING IN PART REQUIREMENTS FOR THE DEGREE OF DOCTOR OF PHILOSOPHY.

Committee on Graduate Work

Harold R. Kaufman

Virgil H. Sandborn

Charles E. Mitchell

Paul J. Wilbur
Advisor

Paul J. Wilbur
Department Head

ABSTRACT

PLASMA FLUCTUATIONS IN ION THRUSTERS UTILIZING
HOLLOW CATHODES

Experiments and analysis have been performed to determine the cause of certain electrical fluctuations found to be present in the main discharge of a mercury ion thruster equipped with a hollow cathode. The fluctuation frequency was in the range of 10 to 30 kilohertz. The peak to peak magnitude of the discharge current and voltage were of the same order as the respective DC levels. The frequency was found to increase with increasing discharge current, discharge voltage, and magnetic field intensity. Extensive plasma measurements were made in a bell-jar ion source with a similar geometry to the ion thruster. Langmuir probes were used to evaluate average plasma characteristics such as the electron temperature and plasma potential distribution. Dynamic measurements were also made to determine the phase relationships between fluctuations in the plasma potential, electron density, and the discharge current and voltage. A detailed description of these measurements is given. A survey was made of fluctuation mechanisms common to this type of ion source. A mechanism was proposed after due consideration to both theory and the plasma measurements. The proposed mechanism has two parts; i.e., the launching of an ion acoustic wave at the interface between the keeper and main discharge plasma towards the cathode, and a feedback mechanism which triggers the next wave. There is evidence given that the ion acoustic wave is produced by an ion beam-plasma instability condition which is

present during part of the fluctuation cycle. An expression is derived which includes the critical parameters determining the fluctuation frequency. The frequency calculated from the derived expression was found to compare well with the measured fluctuation frequency over a broad range of discharge parameters and keeper discharge chamber geometries.

Dennis J. Fitzgerald
Department of Mechanical Engineering
Colorado State University
Fort Collins, Colorado 80523
Summer, 1983

ACKNOWLEDGMENTS

This dissertation is dedicated to the memory of my wife Judith who gave me encouragement and unflagging support over the years required to perform this research. I would like to thank Daniel Kerrisk and Eugene Pawlik for allowing me to use facilities at the Jet Propulsion Laboratory for this work. I would also like to thank my committee members for their helpful comments and suggestions over the past several years. In particular, I would like to express my sincere gratitude to my advisor, Dr. Paul J. Wilbur, for his assistance, guidance, and patience during the preparation of this dissertation and during the preceeding years of research. Finally, I would like to thank Dorothy Sanders for her enthusiasm and encouragement during the typing of this work.

TABLE OF CONTENTS

I. INTRODUCTION

The following dissertation is an account of experiments and analyses which were performed to determine the cause of certain electrical fluctuations which have been observed in the main discharge of ion thrusters utilizing a hollow cathode. The ion thruster is a space propulsion device which produces thrust by the expulsion of ions which have been accelerated to very high velocities by means of an electric field. The ions are produced within a container by flowing gas through an electrical discharge. The electrical discharge in the hollow cathode ion thruster was found to be characterized by the presence of large, high frequency voltage and current fluctuations!

There were two reasons for studying these discharge fluctuations. First, plasma fluctuations are very often indicative of an enhanced electron diffusion loss from the plasma and consequently may represent an inefficient mode of ion source operation. It has been shown[2,3] that discharge fluctuations in ion sources using refractory cathodes can be reduced and in some cases the ion source efficiency increased by relatively simple changes in the magnetic field geometry. Secondly, plasma fluctuations in the ion thruster could be a potential source of electromagnetic noise which may detrimentally interact with other systems on the spacecraft. The concern for these interactions has prompted studies[4,5] to determine the amount of conducted and radiated electromagnetic interference (EMI) produced by the ion thruster and its associated controls and power supplies (thrust subsystem). These studies indicate that the EMI generated

by the thrust subsystem should not interfere with critical spacecraft subsystems; ie, the computer, attitude control, communications, etc., but it may disturb the more sensitive science instruments such as plasma wave detectors and low energy particle spectrometers. Therefore, the fluctuations are not viewed as a critical problem. However, a better understanding of the physical mechanism causing the electrical fluctuations may lead to appropriate changes in ion thruster design which may affect a reduction in EMI and an improvement in thruster efficiency.

This dissertation is divided into four parts. Chapter II will begin with some general background information on electric propulsion with particular emphasis being given to the design and operation of the ion thruster. This will be followed by a description of the observed electrical fluctuations in terms of externally measurable quantities such as the discharge voltage and current. There will be a critical review of several fluctuation processes which have been commonly found to be present in laboratory plasmas similar to the ion thruster. The review produced two candidates which appeared to be in the proper frequency range, i.e., the so-called Cohen instability and the ion acoustic resonance. Chapter II will include a description of an experiment which was performed on the ion thruster to check for the presence of the Cohen instability. It will be shown that the experiment did not support this hypothesis.

Chapter III will contain a description of a series of experiments which were conducted using a bell-jar ion source. The first series of bell-jar experiments focused on the relationship between various plasma parameters in the main discharge and the fluctuation frequency. The results of these experiments raised doubts as to the possibility of an ion acoustic resonance in the main discharge. However, these data showed some

promise for such a resonance in the keeper discharge region. Consequently, a second series of bell jar experiments were conducted to investigate the effects of certain geometrical and electrical parameters in the keeper plasma region on the observed plasma fluctuations. These experiments produced detailed information on the dynamics which take place in the plasma during the fluctuation cycle.

Chapter IV will begin with a general qualitative description of a mechanism which is proposed to be responsible for the plasma fluctuations in the ion thruster. This will be used to explain the results of some of the experiments described in Chapters II and III. The dispersion equation for the plasma in the keeper region will be derived and it will be shown that an ion acoustic wave can be produced in that region under the proper conditions. The ion acoustic wave hypothesis will then be factored into a model which describes the sequence of events during a fluctuation cycle. The model will lead to the derivation of a simple expression which gives the fluctuation frequency in terms of several critical parameters. The theoretical expression will then be directly compared to the experimental results. The conclusions will then be summarized in Chapter V.

II - BACKGROUND

Electric Propulsion Technology

Electric propulsion covers a broad range of technology which is used to convert electrical power into thrust for space propulsion[6,7,8,9]. Some of the sources of electrical power which have been considered include solar cells, thermoelelectric, and thermionic generators. Electric propulsion can be divided into three categories, ie, electrostatic (ion thrusters), electrothermal (arcjets), and electromagnetic (magnetoplasma-dynamic and pulsed plasma thrusters). In general, electric propulsion is capable of producing higher exhaust velocities than conventional chemical rocket propulsion. Consequently the propellant mass required for a given change in vehicle velocity is less with electric propulsion. However, the thrust produced by an electric propulsion system is limited to a fraction of the power plant weight in the Earth's gravitational field. Therefore, electrical propulsion is restricted to operating in space where the thrust is greater than the gravitational forces on the spacecraft. In spite of these limitations, many missions have been identified[10,11] which would benefit from this form of propulsion.

To date, most of the work in electric propulsion has concentrated on the development of the electrostatic ion thruster. The ion thruster produces ions (ion source), accelerates the ions by means of an electric field (electrostatic grids) to produce thrust, and ejects sufficient electrons into the ion beam to maintain charge neutrality on the vehicle (neutralizer). Ions may be produced either directly by surface contact

ionization[9,12] or indirectly by electron bombardment of a gas[7,13]. Contact ionization is restricted to gases which have an ionization potential lower than the work function of the surface. The electron bombardment thruster can be operated on any gas. Mercury vapor was used in the electron bombardment thruster in this study. This type of thruster will be described in greater detail in the following.

Electron Bombardment Ion Thrusters

A cross section of a typical electron bombardment ion thruster utilizing a refractory cathode is shown in Figure 1. This type of ion thruster produces electrons by means of the thermionic emission process. This is accomplished by electrically heating a refractory metal cathode to a very high temperature. The electrons which are emitted by the cathode are accelerated by an electric field to the surrounding anode structure which is held positive with respect to the cathode by means of an external DC power supply. The cathode and anode are mounted within a cylinder with an opening at one end. This cylinder, which is commonly called a discharge chamber, acts as a containment vessel for the plasma produced in the discharge. A perforated metal plate, known as the screen grid, is mounted on the open end of the chamber. The screen grid establilishes a boundary for the plasma from which the ions can be extracted. An accelerator grid is held in close proximity to the screen grid on electrical insulators. The ion source would typically be maintained at about 2,000 volts positive with the accelerator grid at 2,000 volts negative. The negative accelerator grid prevents electrons in the beam plasma from backstreaming into the source. The two grids have an identical matrix of holes which are aligned to minimize impingement during ion extraction. The propellant is fed into the discharge chamber through

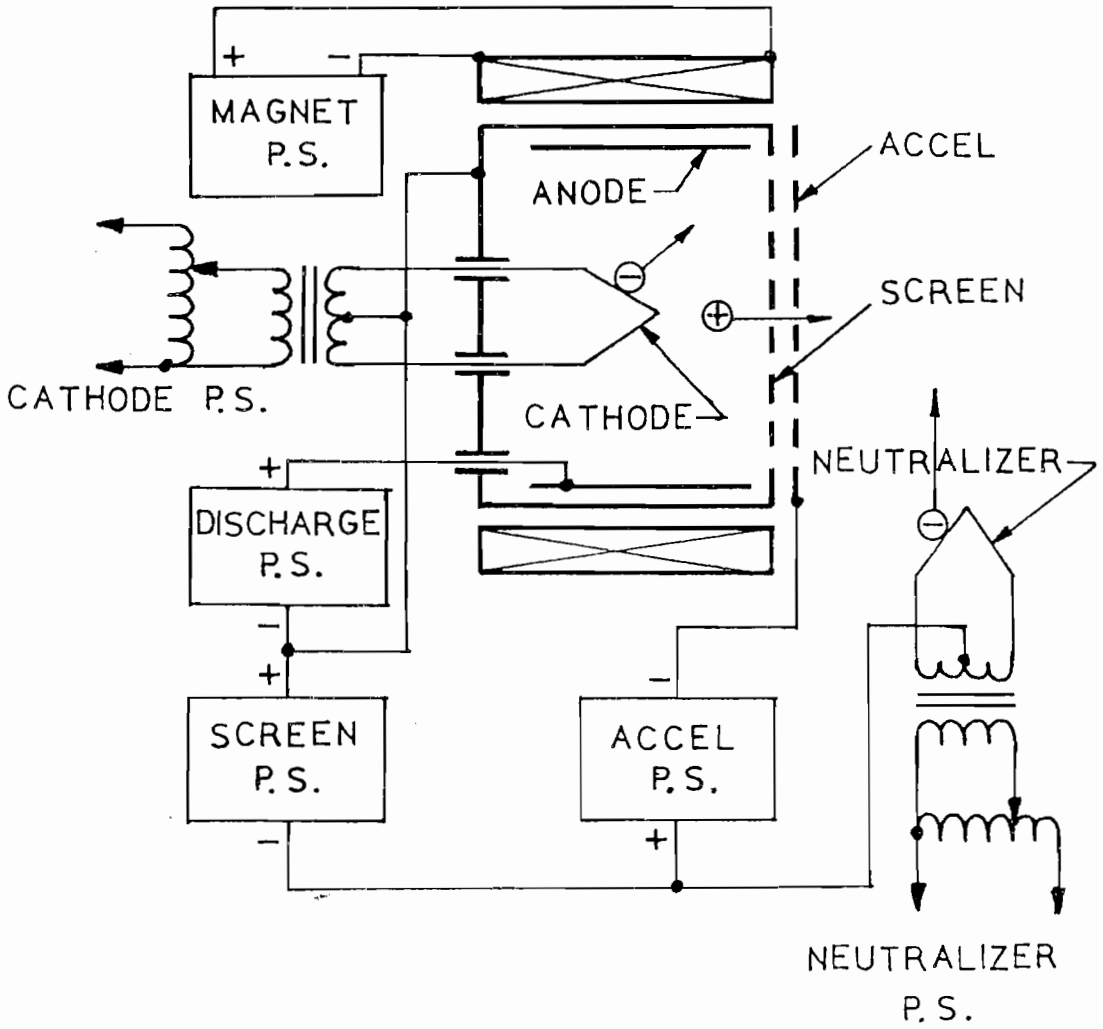

Figure 1 - Cross Section of Electron Bombardment Ion Thruster utilizing refractory cathode.

a manifold which is designed to distribute the gas evenly and in a way which optimizes the fraction which is ionized and extracted. An external magnetic field is applied to the entire discharge chamber to reduce the diffusion of electrons to the anode, ie, to increase their effective residence time in the discharge.

The refractory cathode ion thruster is operated in the following manner. (1) The arc voltage, magnetic field current, and gas flow rate are set to some appropriate values chosen from past experience. (2) The filament current is slowly increased until the discharge commences and then further increased until the desired level of discharge current is achieved. (3) The neutralizer filament power is set at a level which is sufficient to produce an electron emission which can balance the ion beam current. (4) The positive (screen) and negative (accelerator) high voltage power supplies are turned on simultaneously to initiate the ion beam extraction. (5) The flow rate, magnetic field, and arc parameters are further adjusted to produce the desired level of ion beam current.

Ion sources utilizing refractory cathodes start and run easily, use practically any gas, and are relatively simple to build. These features make this type of ion source very popular for land-based uses such as ion implantation, ion milling, and mass spectroscopy. However, refractory cathodes have a lifetime which is too short for most of the space applications of interest; therefore, it has been replaced by a device called the hollow cathode. The hollow cathode ion source is substantially more complicated in design and operation than its refractory cathode counterpart. However, the hollow cathode lifetime is two to three orders of magnitude greater (1,000 to 10,000 hours). The detailed physical

processes involved in the operation of the hollow cathode are not well understood and continue to be an active area of research.

A cross section of an electron bombardment ion thruster utilizing a hollow cathode is shown in Figure 2. The hollow cathode is a refractory metal tube with an electric heater wound on one end. The other end of the tube is connected to a source of gas (vaporizer or tank) and includes some means of regulating the flow rate. The heated end of the tube is usually fitted with an orifice (tip) to restrict the flow and thereby maintain a relatively high pressure within the tube. The interior of the tube is usually coated with a low work function material such as barium oxide in order to improve the thermionic emission. An electrode, referred to as the "keeper," is mounted a short distance from the cathode tip. The keeper electrode is held positive with respect to the tube by means of an external DC power supply. The hollow cathode is mounted within a small cylindrical antechamber which will be called the keeper discharge chamber. The electrons produced in the keeper discharge chamber are drawn through an aperture into the main discharge chamber by the anode which is held at a higher positive voltage than the keeper. The function and design of the main discharge chamber and the extraction grid system are essentially identical to the refractory cathode ion source described previously.

The hollow cathode discharge produces a high density plasma in the keeper discharge region. Some of the electrons in the keeper plasma are drawn through a ring shaped aperture (annulus) into the main discharge region by an electric field. The electric field is present at the aperture because of the difference in the plasma potential between the keeper and main discharge regions. The actual boundary between the two plasma regions may have a tendency to protrude back into the keeper

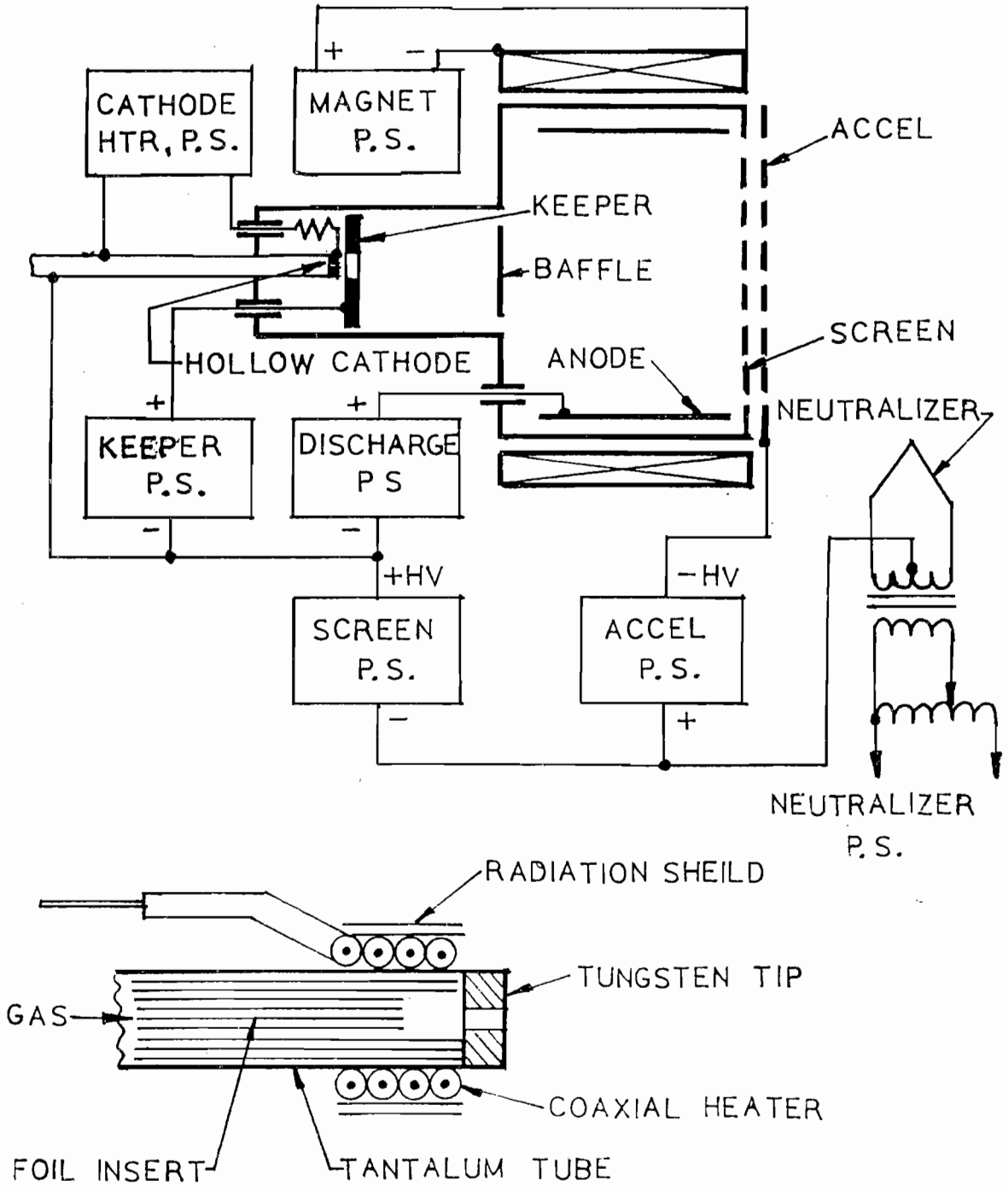

Figure 2 - Cross Section of Hollow Cathode Ion Thruster and Detail of Hollow Cathode Construction.

plasma[14,15]. This type of plasma interface is often referred to as a double sheath. The aperture, in effect, acts as a virtual cathode which supplies high energy electrons to the main discharge.

Preliminary Ion Thruster Experiments

Plasma fluctuations were first observed on a 20-cm mercury ion thruster at Colorado State University (CSU).[1] The thruster was designed and constructed at the Jet Propulsion Laboratory (JPL). These fluctuations were found while using an oscilloscope to measure the ripple present on the arc, keeper, and magnet power supplies. The thruster used in these tests was equipped with a hollow cathode mounted within a magnetic pole piece. The magnetic circuit was designed to produce a field which expands from the cathode pole piece to the edge of the screen grid.

The ripple current on the thruster power supplies was first measured using resistors to simulate the maximum thruster load conditions and subsequently during actual thruster operation. With a resistive load, the ripple current on the arc power supply was about 5% of the DC value and the frequency was 120 hertz, which is typical for a full wave bridge rectifier. However, during thruster operation, the arc current was characterized by the presesence of high frequency fluctuations (on the order of 20 Kilohertz) with a peak to peak amplitude as large as the DC current level.

An oscilloscope was also used to measure the plasma potential fluctuations within the main discharge chamber of the ion thruster by means of an emissive probe. A diagram of the circuit and details of the emissive probe are shown in Figure 3. The probe was made by swaging and spot welding a low voltage light bulb filament onto two tantalum support

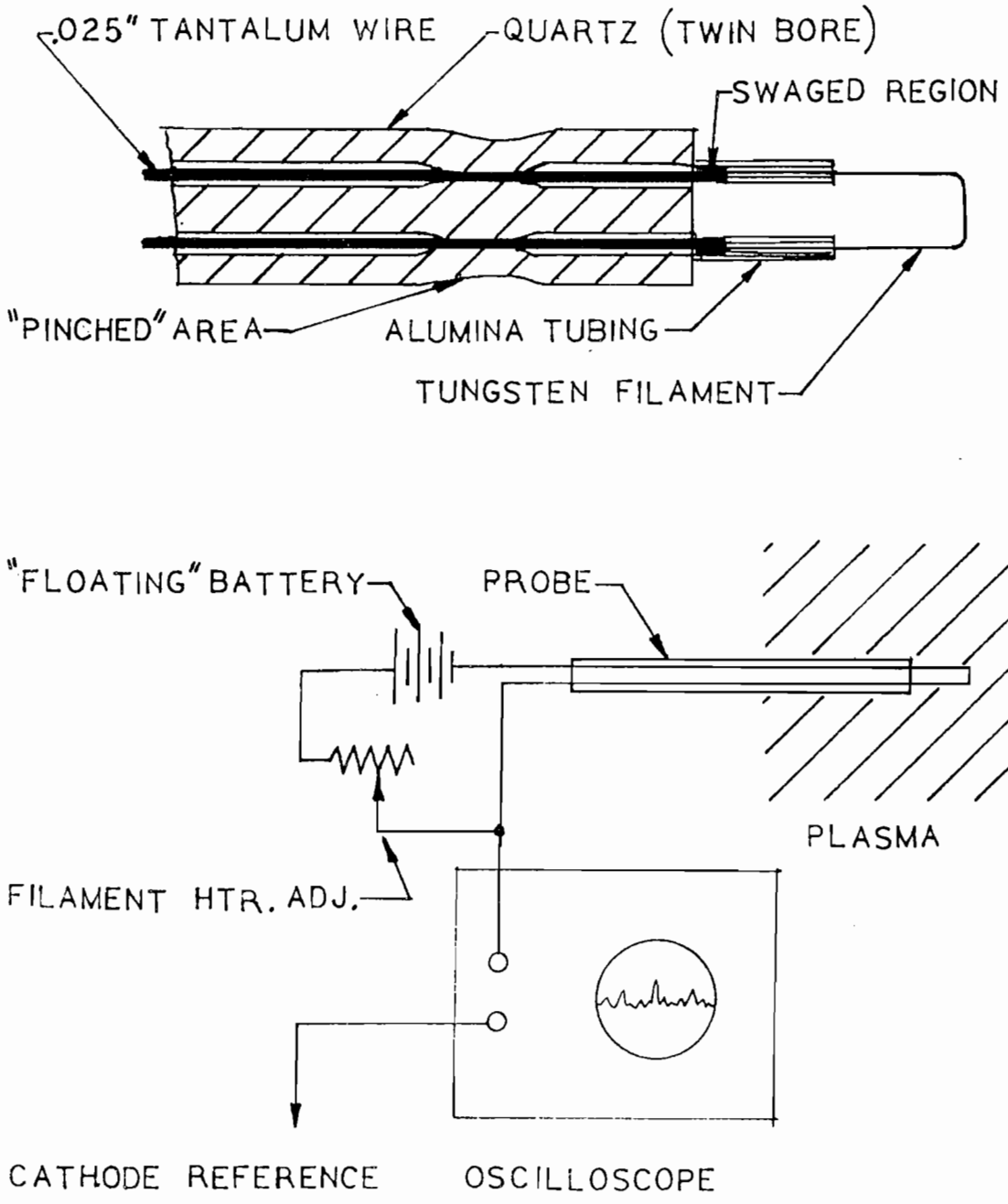

Figure 3 - Details of Emissive Probe Construction and Circuit Diagram for Operating Emissive Probe.

wires. The tantalum wires were run through two short pieces of thin walled alumina thermocouple tubing and into a double bore quartz tube. The thin alumina tubes provide a transition region between the hot filament and the relatively large thermal mass of the quartz tubing. During probe construction, a section of the quartz tube was heated to the plastic state and drawn out to fix the tantalum wires in place. The filament wire was heated with a floating 6 volt battery. The filament current was controlled and limited with a potentiometer.

To operate the probe, the filament current was increased until the relative increase in the average (DC) floating potential was minimal. At that point, the emissive probe was presumably emitting electrons at a sufficient rate to balance the random electron current from the plasma and consequently would follow the fluctuations in the plasma potential. Reference 16 contains a detailed description of emissive probe theory and shows that the frequency response can be well into the megahertz region when proper care is taken to minimize the capacitive coupling to ground.

These emissive probe measurements had no direct provision for determining the frequency spectra, but it was possible to make the following general qualitative observations: (1) The plasma potential fluctuation frequency in the main discharge region was found to increase nearly linearly with increasing magnetic field, (2) the frequency of the fluctuations also increased as the arc current was increased, (3) the detailed characteristics (wave shape and amplitude) were approximately the same as the arc voltage fluctuations, and (4) the frequency decreased when the beam current was not being extracted.

A simple cylindrical Langmuir probe was also placed within the main discharge region. A sawtooth waveform was applied to the probe with respect to the cathode potential. The waveform had a maximum amplitude of +60 volts at a frequency of 2 Kilohertz. The current-voltage characteristics were displayed on the x-y oscilloscope utilizing a 10 ohm shunt resistor to produce a voltage proportional to the probe current. The resulting display indicated the presence of oscillations similar to those found by previous workers[17] with a refractory cathode ion thruster. The size of the noise envelope on the Langmuir probe was about 5 volts when the arc voltage was 30 volts. This figure was approximately the same as the plasma potential fluctuations measured with the emissive probe described previously.

These initial observations prompted a review of the plasma physics literature in order to find a possible physical mechanism which could explain the cause of the fluctuations. The following section contains a survey of the more commonly observed plasma wave mechanisms, with particular emphasis given to those which have been found in ion sources which are similar to the ion thruster geometry and plasma parameter range.

Original Survey of Possible Plasma Fluctuation Mechanisms

The original experimental setup described in the previous section was not equipped to perform an exhaustive plasma wave study. Therefore, a literature survey was conducted in order to give some possible insight into the fluctuation mechanism and some direction to the next series of experiments. A brief summary of the fluctuation characteristics will be given first.

The fluctuation frequency is on the order of 20 Kilohertz and appears to increase linearly with the magnetic field. In addition, the frequency increased with the arc current, and is reduced when the ion beam is shut off. The effect of the magnetic field and the arc current on the frequency may be indirect; ie, by increasing the plasma density or the electron temperature. The observed fluctuation characteristics and the general conditions found in the ion thruster; ie, plasma density, electron temperature, geometry, and magnetic field strength, were used to evaluate the feasibility of the plasma fluctuation mechanisms described in the following section.

The most commonly observed plasma oscillation is the electron plasma frequency, which was predicted and observed by Tonks and Langmuir[18]. The electron plasma frequency is given by,

$$\omega_e = \left[N_e e^2 / M_e \epsilon_o\right]^{1/2} \quad , R S^{-1} \tag{1}$$

where N_e and M_e are the electron density and mass respectively, e is the charge on the electron, and ϵ_o is the permittivity of free space. It should be noted that ω_e is independent of the plasma dimensions and the magnetic field, ie, it is the "natural" resonant frequency of the electrons in a plasma of density N_e. Using Equation (1) and a typical value of the electron density in the ion thruster[19,20,21] of 5×10^{17} electrons m^{-3}, it is found that the electron plasma frequency is about 6.7×10^9 hertz, which is too high to be considered. In a similar manner, the so-called ion plasma frequency can be found by substituting the mass of the ion for that of the electron in Equation (1). For the same density, it is found that the ion plasma frequency for mercury is about 1.1×10^7

hertz. Thus, the electron and ion plasma frequency are too large to be considered.

A plasma fluctuation mechanism commonly found in magnetically confined plasmas is the electron cyclotron frequency[22] (or gyrofrequency) which is given by,

$$\omega_{ce} = \left| eB/M_e \right| \quad , R\,S^{-1} \tag{2}$$

where B is the magnetic flux density, e is the charge on the electron, and M_e is the mass of the electron. This frequency represents the inverse of the time for the electron to make one full revolution perpendicular to the magnetic field. Notice that the frequency is independent of plasma density, the electron temperature, and the plasma dimensions. Using Equation (2) and a typical magnetic flux density for the ion thruster of 25×10^{-4} webers m^{-2} [23] it is found that the electron cyclotron frequency is about 7×10^{7} hertz which is too high to be considered. It is also possible to have a resonance at the ion cyclotron frequency which can be found by substituting the ion mass for the electron mass in Equation (2). For the same magnetic flux density, the ion cyclotron frequency for mercury is about 200 hertz, which is much lower than the observed value.

In addition to the low frequency, the ion cyclotron resonance is not possible within the ion thruster because the radius of the orbit is larger than the dimensions of the thruster. The gyroradius (or Larmour radius) for the ion is given by,

$$R_i = \left[M_i V_+ / eB \right] \quad , M \tag{3}$$

where e is the charge on the ion, V_+ is the velocity of the ion in a

plane perpendicular to the magnetic field B, and M_i is the mass of the ion. If the thermal energy of the ion is equally divided among the three degrees of freedom, the perpendicular velocity (2 degrees of freedom) is equal to,

$$V_+ = \left[2K_bT/M_i\right] \ , MS^{-1} \tag{4}$$

where T_+ is the ion temperature, and k_b is Boltzmann's constant. If the ion temperature is assumed to be equal to the wall temperature of the ion source, typically 600°K, and the magnetic flux density is 25×10^{-4} weber m^{-2}, Equation (4) gives a perpendicular ion velocity for mercury of about 220 m sec^{-1} and Equation (3) gives a Larmour radius of about 18 centimeters. This result is about twice as large as the radius of the ion thruster under investigation; therefore it is not possible to have such a resonance.

Another fluctuation mechanism which was considered was the EXB (the cross product of the electric and magnetic field) drift instability. The EXB drift (also called the guiding center drift) may occur when the static electric field in the plasma has a component which is perpendicular to the applied magnetic field. In this case the ions and electrons drift at the same velocity and in the same direction, mutually perpendicular to both the electric and magnetic field. In the drift frame of reference, the ion and electron motion is identical to the motion in the rest frame when no electric field is present; ie, circular motion at the gyrofrequency, Larmour radius, and direction for the respective particle.

In the case of the ion thruster under consideration, the magnetic field is predominantly axial and the electric field in the main discharge

is radial; therefore, an EXB drift may be expected that would produce a rotation of the plasma as a whole in the Θ-direction. Such a configuration has been shown to produce various types of instabilities[3,24,25] under the proper conditions. However, it was pointed out above that the ion Larmour radius is too large in the ion thruster to permit complete cyclotron orbits. Therefore, the ions will not participate in the Θ-drift and the instability mechanisms described in the cited references would not be applicable. Furthermore, electrostatic ion cyclotron waves and the lower hybrid resonance can be eliminated for the same reason.

Cohen[26] developed a new theory to predict the conditions for the onset of anomalous diffusion resulting from an unstable plasma state in an ion thruster. The theory was based on the earlier work of Kadomtsev and Nedospasov[27]. However, the assumptions were modified to reflect the ion thruster plasma conditions. In particular, the analysis was applicable to the lower pressure regime and magnetic field intensity normally found in the ion thruster; ie, the magnetic field did not effect the motion of the ions. Cohen made the assumption that small perturbations in the number density and plasma potential can exist in the Θ-direction. Under normal, stable conditions these will be damped out. However, he derived an expression which predicts a so-called critical magnetic field at which such perturbations would grow without bounds, ie, the plasma would become unstable. As a result, the large perturbations in the plasma potential in the Θ-direction produce Hall electron currents in the r-direction and consequently enhanced diffusion losses.

Cohen's theory predicts that the frequency of the oscillation will be

$$\omega_c = \left[K_b T_+ (4.36)/2\pi eBR^2\right] \quad , \quad RS^{-1} \tag{5}$$

where k_b is Boltzmann's constant, e is the charge on the electron, T_+ is the ion temperature, B is the magnetic flux density, and R is the radius of the discharge. The coefficient in the brackets was evaluated in Cohen's analysis using various appropriate assumptions about the plasma conditions in the ion thruster. For a 20-cm diameter thruster, with T_+ equal to 600°K (the wall temperature), and B equal to 25×10^{-4} webers m^{-2}; Equation (5) yields a frequency of about 1400 hertz. This calculated frequency is about an order of magnitude lower than the observed frequency. However, an instability may alter some of the conditions under which Equation (5) was derived; therefore, it may only represent the frequency at the onset of the instability.

Cohen also derived an expression for the ion production energy per beam ion (eV/ion) and predicted that the minimum would occur at the so-called critical magnetic field. The resultant expression appeared to agree quite well with observations of refractory cathode ion sources at that time[2,17,26]. (Later, Martin[28] established the validity of Cohen's theory with a series of experiments using a refractory cathode ion source with several different anode radii.) However, the fluctuations in the JPL 20-cm hollow cathode ion thruster were evident at all values of the magnetic field current, ie, the minimum ion production energy per beam ion did not correspond to the onset of the fluctuations[29,30]. Thus, there was apparently something different about the fluctuations observed in the hollow cathode ion thruster.

The last plasma fluctuation mechanism to be considered was the ion acoustic resonance. This has been the subject of an extensive experimental study by Alexeff and Neidigh[31] and others[32-36]. Ion sound waves are longitudinal compression waves which are essentially a balance between the momentum of the ions and a restoring force due to the thermal pressure of the electrons. The ions and electrons are constrained to move together by electrostatic forces. In bounded plasmas, such as the ion thruster, these waves can develop spontaneously[18,31,34] and produce both radial and longitudinal resonant modes of oscillation. Ion acoustic resonances are generally characterized by standing waves in the plasma density and potential. In other words, both of these plasma properties would appear to change in phase with each other throughout the plasma; however, a scan across the resonant cavity would exhibit nodes and antinodes in the amplitude of the oscillation.

The longitudinal ion acoustic resonant frequency is given by

$$F_{is} = (1/\lambda)\left[\gamma_e K_b T_e / M_i\right]^{1/2}, \text{HZ} \qquad (6)$$

where λ is the wavelength, γ_e is the polytropic process exponent for the electrons, k_b is Boltzmann's constant, T_e is the electron temperature, and M_i is the mass of the ion. For a longitudinal mode of resonance, the fundamental frequency corresponds to a wavelength of 2L, where L is the length of the plasma column. The value of γ_e may be 1 or 5/3; ie, the values appropriate to isothermal and isentropic compression processes respectively.[33] γ_e is usually set equal to 1 because the thermal velocity of the electrons is much greater than the ion acoustic velocity; therefore, they have time to equalize their temperature on a time scale

much shorter than the period of the wave; hence, they can be considered isothermal. The value of $\gamma_e = 1$ is also predicted by kinetic theory[34].

If it is assumed that the electron temperature in the main discharge of the JPL 20-cm ion thruster is about 5 electron volts at a discharge voltage of 30 volts, and the chamber length is about 15 centimeters, then Equation (6) predicts a longitudinal ion acoustic frequency of about 5100 hertz. For the fundamental frequency of the radial ion acoustic mode, $(1/\lambda)$ in Equation (6) should be changed to $(2.405/\pi D)$, where the coefficient is the first zeroth order Bessel root and D is the diameter. For the same conditions, the radial ion acoustic frequencies are within a factor of 2 or 3 of the observed value and therefore may be representative of the true mechanism.

To summarize, a review of several commonly observed plasma fluctuation mechanisms has been conducted. The plasma parameters and magnetic field strength present in the ion thruster have been used to determine the frequency and/or the feasibility of each fluctuation mechanism considered. Two of the mechanisms were regarded as promising. The first is a rotating (flute like) instability that was developed by Cohen[26] to explain the onset of anomolous diffusion in refractory cathode ion thrusters above a certain "critical" magnetic field. The second possible mechanism is the ion acoustic resonance. Calculations have shown that both mechanisms would be likely to produce oscillations within an order of magnitude of the observed frequencies. However, both mechanisms appear to have their own shortcomings. The Cohen instability mechanism may not apply because the observed fluctuations exist over the entire operating range of the thruster, and the minimum ion production energy per

beam ion did not correspond to the onset of the fluctuations. The fundamental ion acoustic resonance frequency predicted by theory is a factor of two or three times lower than the observed fluctuation frequency. However, higher order modes are possible, or there may be an entirely different fluctuation mechanism applicable in this case.

Follow-Up Ion Thruster Experiments at JPL

Additional tests were performed on the JPL 20-cm ion thruster (unpublished) at JPL as a follow-up of the original observations described above. The tests were conducted in a 2.13m diameter by 4.57m long vacuum facility which was equipped with a liquid nitrogen liner and a frozen mercury target. The purpose of these tests was to document some of the effects described qualitatively above, and to measure the speed and direction of the plasma potential fluctuations in the main discharge. The later group of experiments was aimed at discriminating between the two more probable fluctuation mechanisms described in the last section.

The AC component of the arc current was observed by means of a Tektronics Model P6042 clamp-on current probe. This probe has a frequency response of up to 30 megahertz. The probe was electrically isolated from the main discharge power supply lead it was clamped onto; therefore, the output could be fed directly into a grounded oscilloscope when the ion thruster was at high voltage. A typical picture of the arc current fluctuations is shown in Figure 4A. A crude estimate of the fluctuation frequency was made by adding up the number of cycles on each trace and dividing by the time base. This simple method was used to produce the data shown in Figure 4B which is a plot of the fluctuation frequency as a function of the magnetic field current over a range from 0.45 to 0.90 amperes. The error bars on the figure represent the range of

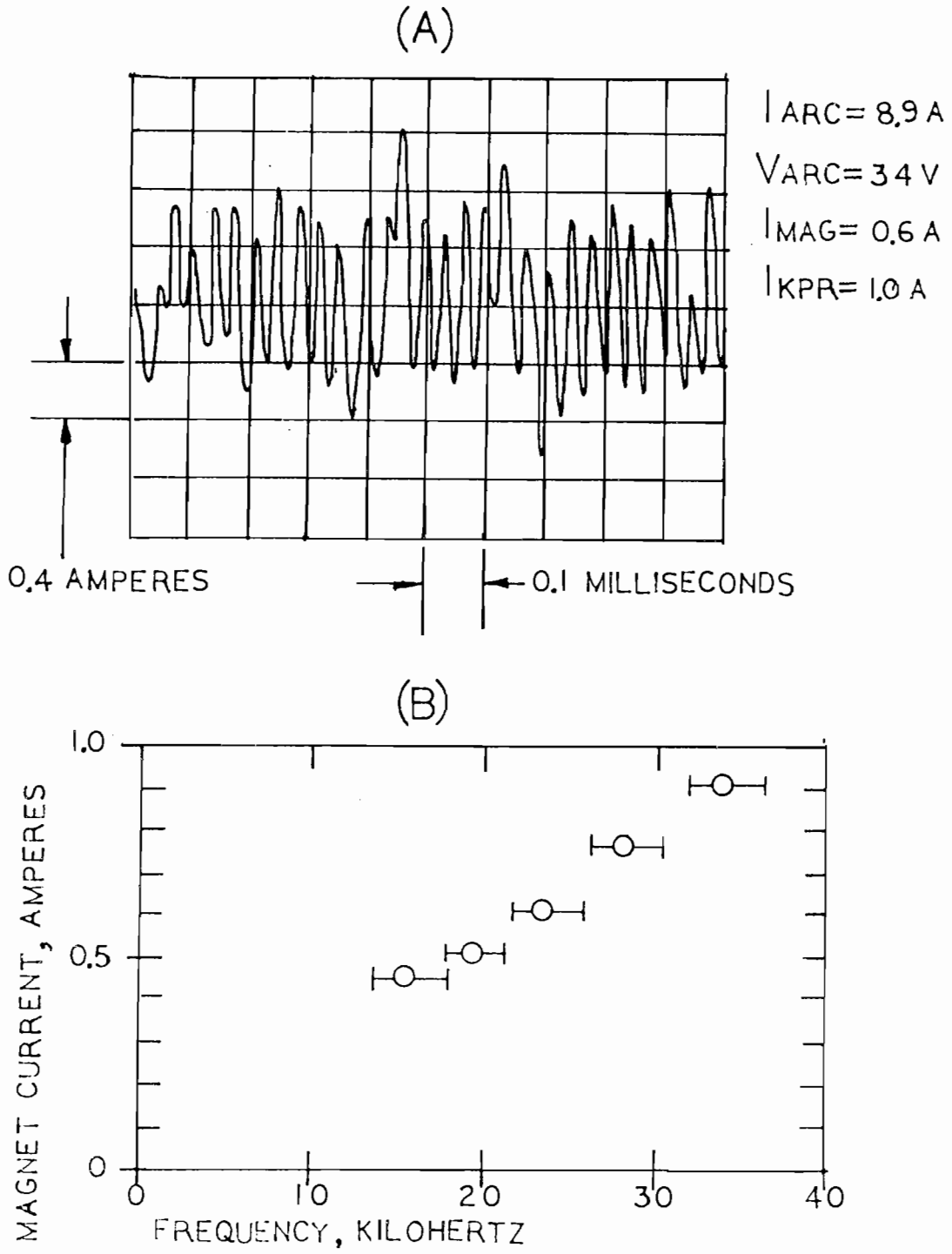

Figure 4 - Arc Current Fluctuations in Hollow Cathode Ion Thruster: (A) Oscilloscope Trace using clamp-on current probe, (B) Fluctuation Frequency as a Function of Magnet Current.

frequencies which is observed on a cycle-to-cycle basis from the original oscilloscope photograph. The normal operating magnet current for this thruster was 0.65 amperes, where the ion production energy per beam ion was at a minimum.[29,30] The arc current and voltage were maintained at 8.2 amperes and 35 volts respectively during this test. Note that the magnet current and the frequency are related linearly over the range investigated.

When the magnet current was reduced below 0.45 amperes, the ion thruster changed mode and went into a low frequency (approximately 60 hertz) large amplitude oscillation. Figure 5 shows the AC component of the discharge current at a magnet current of 0.4 amperes. Notice that the amplitude of the fluctuations has increased by a factor of four over the previous trace shown in Figure 4a. In addition, the discharge would go off when the magnetic field current was reduced below 0.3 amperes. This unstable behavior has also been observed in other studies with this thruster.[29,30]

Figure 6 shows the relationship between the arc current and the fluctuation frequency. These data were taken at a magnetic field current of 0.75 amperes and an arc voltage of 35 volts. This figure shows that the increase in frequency was almost linearly related to the arc current.

Figure 7 shows the effect of ion beam extraction on the frequency. The figure contains two oscilloscope photographs of arc current fluctuations taken at identical discharge parameters. However, the high voltage was off during the top trace and on during the lower trace. The discharge current and voltage were 8.2 amperes and 35 volts respectively and the magnet current was at 0.75 amperes. The ion thruster produced a beam of 850 milliamperes with the high voltage on. Note that the

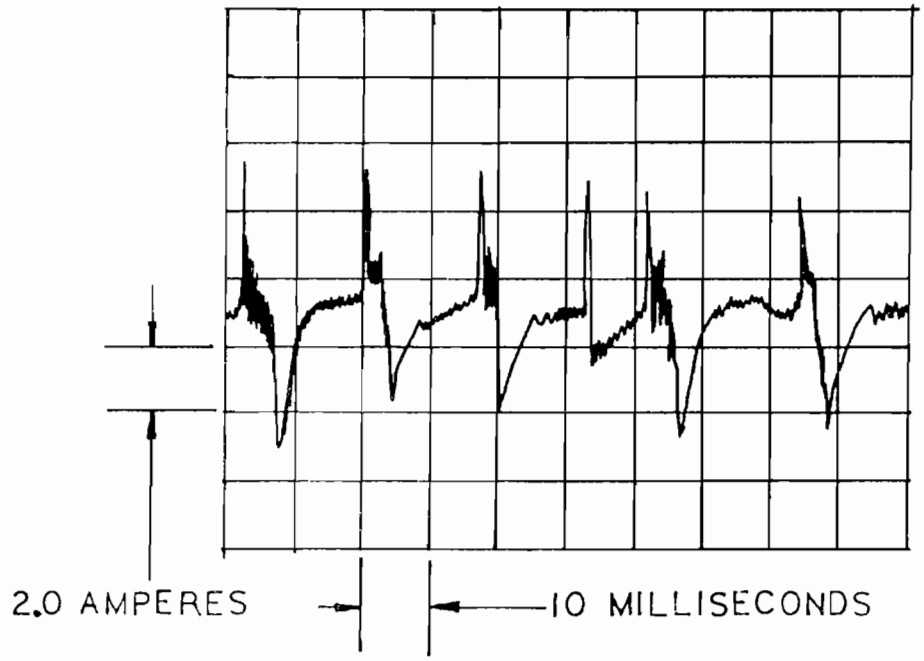

Figure 5 - Arc Current Fluctuations During Highly Unstable Operation at Magnet Current of 0.4 Amperes.

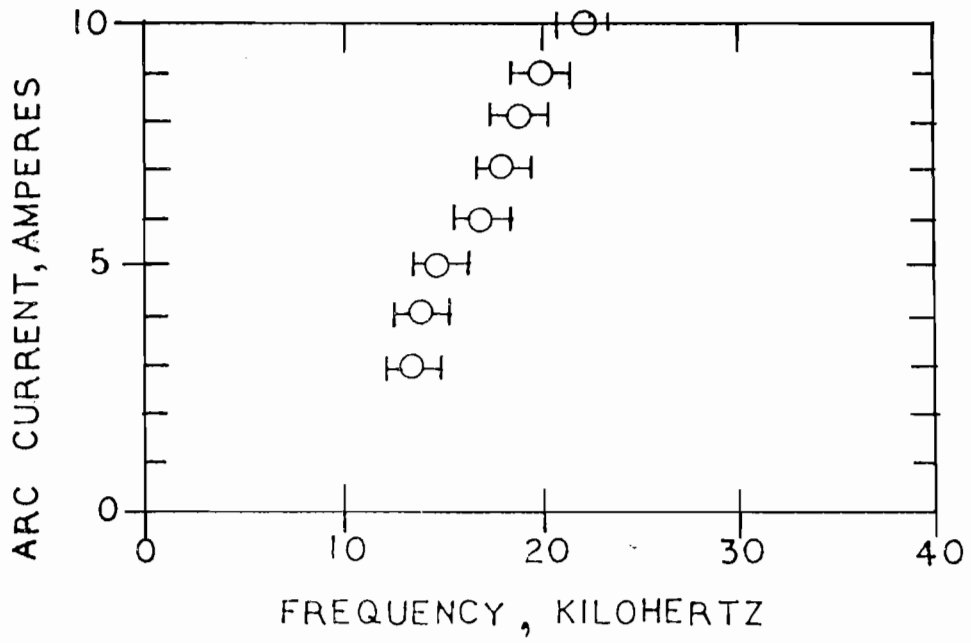

Figure 6 - Fluctuation frequency as a function of the arc current.

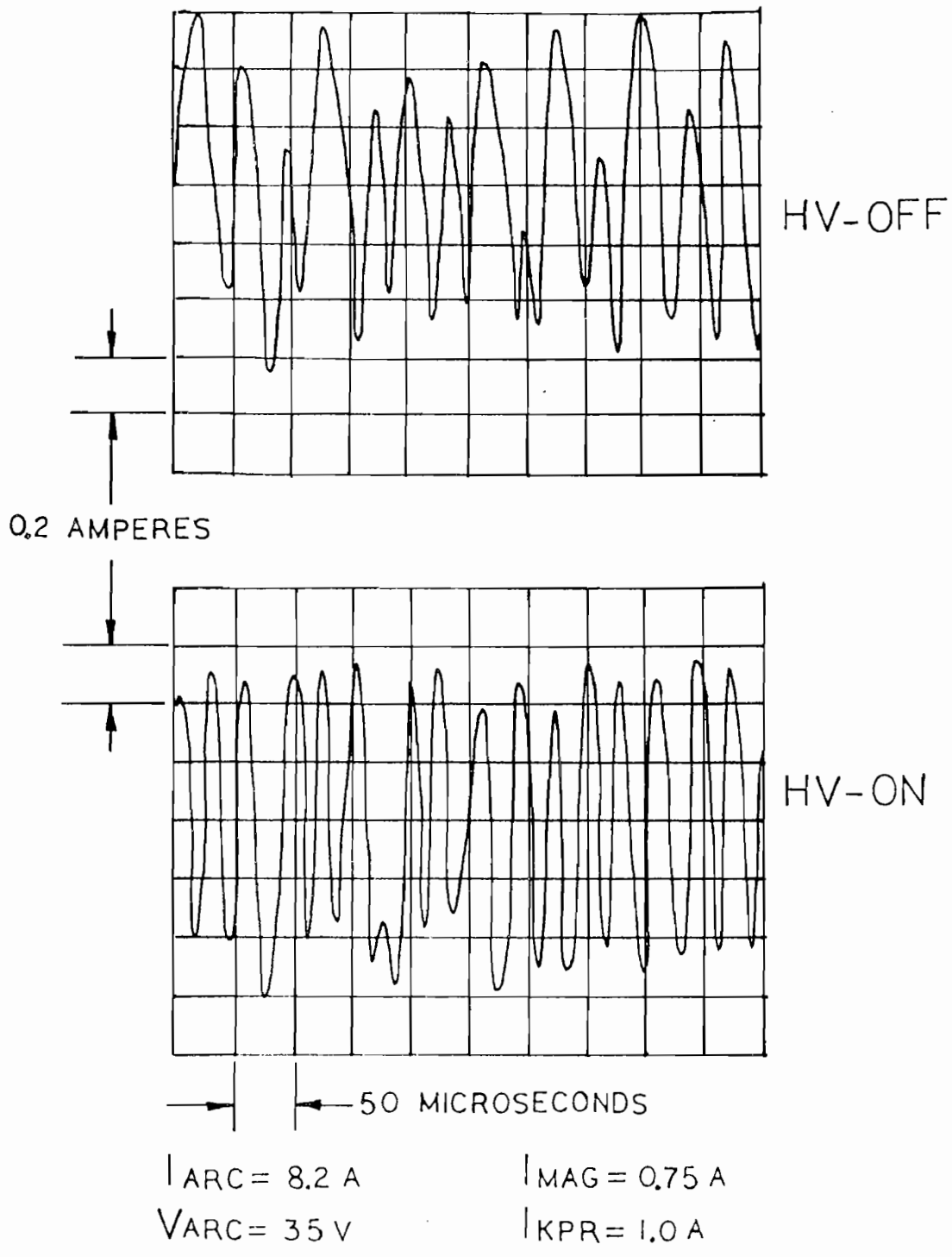

Figure 7 - Effect of high voltage ion beam extraction on the arc current fluctuations, top - HV off, bottom - HV on.

frequency increased from about 30 Kilohertz to 36 Kilohertz when the high voltage was turned on, but the general shape and amplitude of the fluctuations did not appear to change.

It was also noticed during this series of tests at JPL that the arc current fluctuations appeared to be a smaller fraction of the DC current level than the previous tests at CSU indicated. There were two reasons that were proposed for this discrepancy: (1) The shunt used to monitor the arc current at CSU was not compensated for internal inductance; therefore, the voltage across the shunt was increased by the induced voltage. This would give the appearance of being a larger arc current fluctuation when it was displayed on the scope. (2) The filter in the JPL discharge power supply had more inductance than the supply used at CSU; ie, a larger power supply inductance should reduce the arc current fluctuations substantially.

An experiment was also performed to determine the speed and direction of the potential fluctuations in the main discharge plasma. Figure 8A shows the details of the experimental setup. Four emissive probes were located within the main discharge chamber. One probe was used as a reference while the remaining three probes were placed at various positions away from the reference probe in the r,Θ, and z-directions respectively. The emissive probes used in this experiment were identical to those described earlier. The high voltage was off during this experiment; therefore, the floating probe potential could be fed directly into an oscilloscope.

The following procedure was followed in these tests. (1) The reference probe and one of the other probes, for example a probe in a

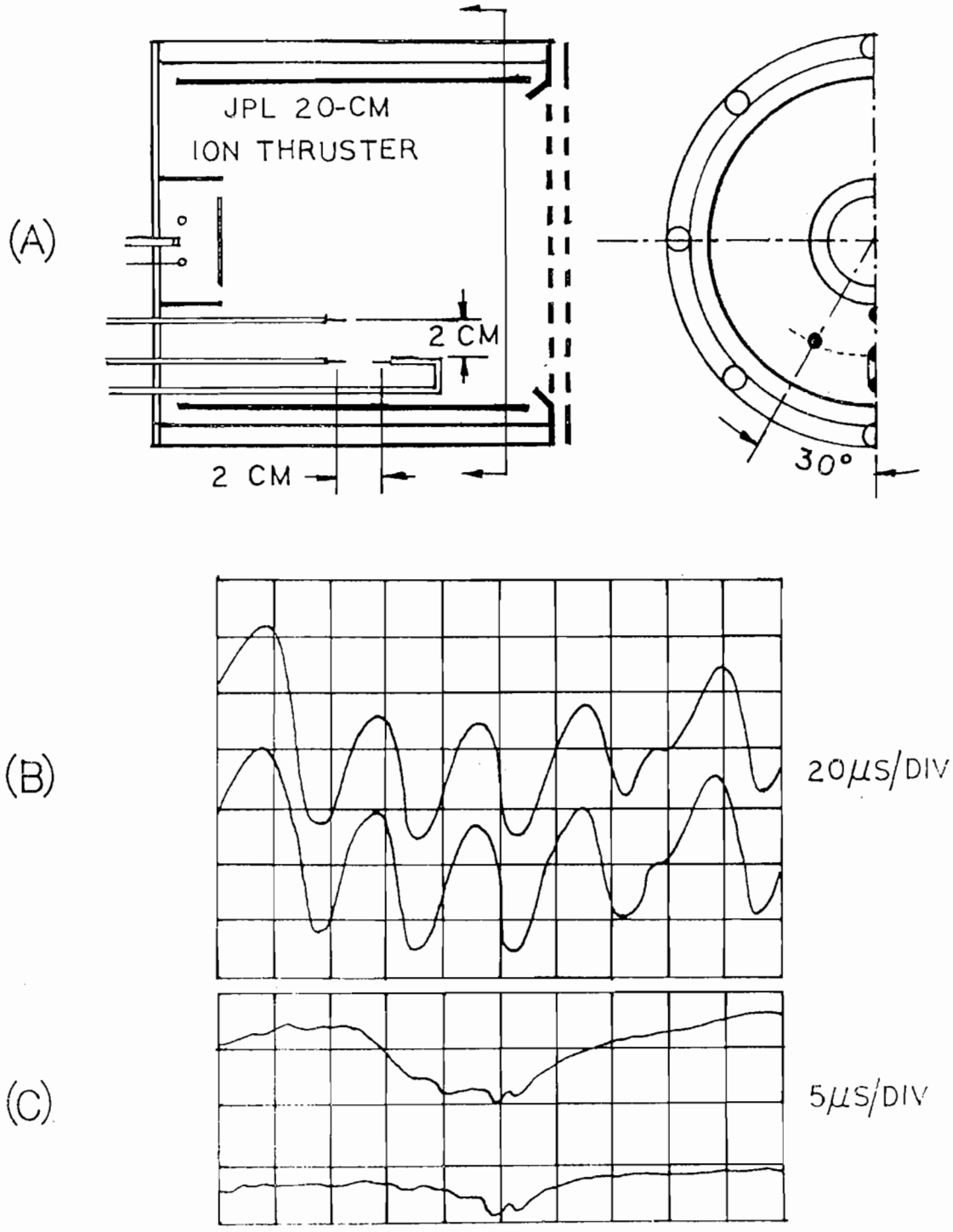

Figure 8 - Ion thruster emissive probe measurements, (A) Probe locations in thruster, (B) and (C), Variation with azimuthal angle of 30^{0}, 20 and 5 microseconds per division respectively.

different Θ-position, was heated to the proper emission level with their own respective floating (battery) power supplies. (2) As described earlier, the filament current was increased until the relative increase in the floating potential was minimal. The probe was then assumed to be at or close to the plasma potential. (3) The floating potential from each probe was fed into a Tektronics Model 555 Dual beam oscilloscope. (4) The AC plasma potential fluctuations were then compared at the same instant in time in different positions within the main discharge plasma.

Figure 8B shows a typical oscilloscope trace which was taken with the probes at two different Θ-positions, but at the same r and z-position. The probes were about 30 degrees apart at a radius of 5 centimeters from the central axis of the thruster. The time base used in Figure 8B was 20 x 10^{-6} seconds per division; therefore, the average period for the fluctuations was about 40 x 10^{-6} seconds per cycle. In this case, if the potential fluctuations were moving through a complete cycle (Θ-rotation of 360°) in a time of 40 microseconds, there would have been a phase shift of about 3 x 10^{-6} seconds (30°) between the two probe traces. Figure 8C contains a pair of traces taken under the same conditions at a time base of 5 x 10^{-6} seconds per division. It was evident from Figure 8C that, within the time resolution of the scope, there was no phase shift between the two probe traces. Therefore, it was concluded that the fluctuations were not caused by a disturbance rotating in the Θ-direction. Similar tests produced the same results in the r and z-directions. In other words, there was no evidence of wave motion in the main discharge plasma; ie, the plasma potential fluctuations appeared to be at the same phase in every position.

Standing waves can occur in a bounded plasma if the wave is reflected from the boundaries. The fundamental mode of a standing wave (radial or longitudinal) will appear to be "in phase" at all locations within the plasma. In the ideal case, the amplitude will vary symetrically around the axis for the radial case, or half the length in the longitudinal case. However, in the case of the ion thruster, the situation is complicated by gradients in the plasma density, specie temperature, plasma potential, and the magnetic field. Consequently, it was not clear how this would affect the amplitude distribution of a standing wave in an ion thruster. Therefore, with the limited plasma potential measurements available from the ion thruster, it was thought that the constant phase characteristics may be evidence of standing waves.

To summarize; the follow-up experiments at JPL confirmed the earlier observations at CSU. There was some difference in the magnitude of the observed current fluctuations which were assumed to be caused by measurement errors at CSU and differences in the arc power supply filters. In addition, it was not possible to detect any discernable wave motion in the main discharge plasma, ie, the plasma potential fluctuations appeared to be in phase at every location tested. This behavior was thought to be indicative of standing waves.

III. BELL-JAR EXPERIMENTS

The results of the experiments described in the last chapter gave an indication that ion acoustic waves may be causing the fluctuations. First, the frequency of the fluctuations was in the proper range for ion acoustic waves, and secondly, the limited plasma potential measurements taken in the main discharge displayed possible standing wave characteristics. This type of behavior has been associated with ion acoustic waves in the past.[33,34] Furthermore, it was known that electron currents could induce ion acoustic waves if the electron drift exceeded a certain critical velocity.[34,36-38] This had been considered as a possible mechanism for turbulence in ion thrusters.[39] Additional evidence of current driven ion acoustic instabilities came after the follow-up experiments described in the last section.[40-42] The standing wave behavior was originally not understood because experiments had shown that ion acoustic waves were not reflected at the boundaries.[32] However, it is now known[43] that the waves can be reflected by a boundary when the wavelength is of the order or longer than the density gradient scale length, $N/(dN/dx)$. Waves with shorter wavelengths are not reflected. There is also some evidence that there are feedback mechanisms which generate backward waves.[33]

The frequency of a longitudinal ion acoustic resonance, given in Equation (6), indicates that it should be possible to predict the resonance frequency by using the measured values of electron temperature

and chamber length. The predicted frequency could then be compared to the measured value. Moreover, the electron temperature should change as a function of the magnetic field current and arc current in a way which produces the frequency changes observed in the last section (Figures 4B and 6). It was concluded that a series of electron temperature measurements would easily prove or disprove whether an ion acoustic resonance in the main discharge was responsible for the fluctuations. This was the original motivation behind the experiments described in this section.

Design of Bell-Jar Test Setup

It was noted in the last chapter that the frequency of the plasma fluctuations was slightly higher when the ion beam was being extracted and that the general character of the fluctuations (wave shape and amplitude) did not change, providing the discharge conditions remained constant. From this observation, it was concluded that experiments could be performed in a bell-jar vacuum facility without extracting the ion beam from the ion source. In addition, a bell-jar experimental setup was considered to be easier and less expensive to operate and more flexible in terms of instrumentation than the large ion thruster test facility. Therefore, a decision was made to perform the next series of tests within a bell-jar.

The expanding magnetic field configuration in the ion thruster was recognized as a complicating factor in the interpretation of data and the theoretical analysis. For this reason, it was decided that future experiments should be performed with the ion source with a uniform axial magnetic field. This was accomplished by constructing an ion source with

non-magnetic materials and placing it within a set of properly spaced magnetic field coils. The details of the first generation bell-jar test setup is shown in Figure 9. In this case, the number of windings per coil and the spacing were adjusted to produce a uniform field (measured within 5%) throughout the entire ion source. The spacing between the field coils and the ion source and the radiation shielding on the ion source minimized the heat transfer from the ion source to the coils. The magnetic field produced by this arrangement of coils was equal to 6.4×10^{-4} weber meter^{-2} ampere.$^{-1}$ After a few initial tests with this setup, it became apparent that the thermal environment of the ion source could affect the characteristics of the instability considerably. It was found that the ion source took several hours to come to thermal equilibrium where repeatable fluctuation characteristics could be measured. In addition, the fluctuations were apparently affected by refill cycling in the liquid nitrogen cold plate. These thermal effects were essentially eliminated by the following measures: (1) The body of the ion source was externally heated and controlled to a temperature of 500°C, which was higher than the normal equilibrium value. (2) The cold plate temperature was carefully monitored and used to set the liquid nitrogen fill controller at a point which maintained a consistent cold plate temperature.

There was some concern about the flow distribution in the ion thruster (which is normally fed through one side of the source) affecting the symmetry of the proposed electron temperature measurements. Therefore, the new ion source was equipped with a multi-baffled rear flow distributor. In addition, there was also some concern about identifying an appropriate characteristic length for the resonance; ie, should the screen to backplate length or the screen to baffle length be used? This

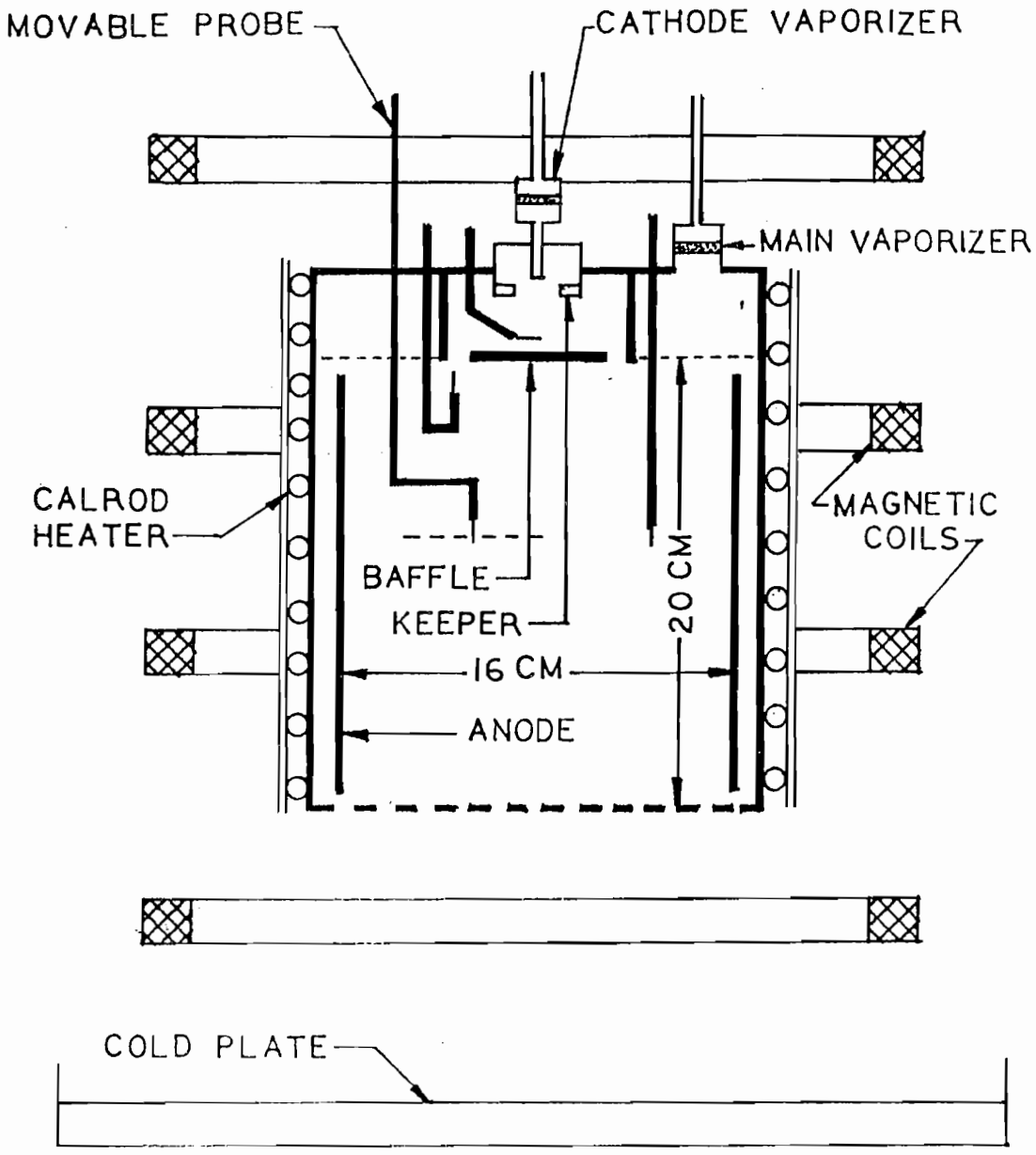

Figure 9 - Cross section of bell-jar test setup.

was resolved by moving the backplate into the same plane as the baffle plate. The keeper discharge chamber and baffle aperture geometry were identical to those for the ion thruster. However, the anode diameter was reduced to 16 centimeters and the main discharge chamber length was increased to 20 centimeters.

Figure 9 also shows the location of several probes on the ion source. One of the probes could be swept radially by remote control across the discharge chamber. Most of the probes used were emissive probes, similar to those described earlier. However, they were now set up to operate in a way which would eliminate the error associated with the normal voltage drop across the filament. This was done by heating the filament with a half wave rectified (60 hertz) signal which was isolated from the line with a standard filament transformer. The potential of the emissive probe was monitored on an oscilloscope with an input impedance greater than one megohm. The time base trigger on the scope was set to commence monitoring the potential during the half-cycle when the filament heating power was off; ie, the voltage across the probe was zero. The emissive probes were also used as standard Langmuir probes, ie, with the heating power off.

The ion source used in the bell-jar tests was supported above a 0.41 meter diameter liquid nitrogen cold plate which was contained within a 0.45 meter diameter by 0.75 meter long bell-jar. The bell jar was supported on a 0.10 meter high collar which provided feedthroughs for wiring, mercury, and liquid nitrogen for the cold plate. The system was pumped by means of a 0.15 meter diameter diffusion pump equipped with a liquid nitrogen chevron. The ion source was powered with Trygon-mercury series regulated power supplies. The main and cathode vaporizers were temperature controlled with proportional controllers. The cathode

vaporizer had the option of using the arc voltage as the control parameter; ie, the arc voltage could be controlled in this manner.

The bell-jar experimental setup was also equipped with a Hewlett Packard Model 310 frequency spectrum analyzer. The spectrum analyzer is essentially an AC voltmeter which can be tuned to measure a specific band of frequencies in the same way as a radio may be tuned to receive a specific broadcast station. The spectrum analyzer tuner is designed to pass all (gain equal to one) of the so-called center frequency component and to increasingly attenuate frequency components above and below the center frequency. The attenuation slope (db/Hz) depends upon the band pass selected. The band pass is conventionally defined as the difference between the upper and lower cutoff frequencies, ie, where the gain has decreased to a value of 0.707.

The frequency spectrum is produced by scanning through a range of frequencies with the tuner and plotting the resultant signal strength amplitude as a function of frequency. The resolution of the frequency spectrum analyzer increases as the band pass is decreased but the signal strength (the integrated value of the passed frequency components) is reduced. The Hewlett Packard Model 310 was equipped with a motor drive to provide a constant scanning speed and a linear voltage output which was proportional to the center frequency. The tuned signal amplitude and voltage corresponding to the center frequency were used to plot the frequency spectrum on an x-y recorder.

Bell-Jar General Operating Procedure

The bell-jar experiments described in the next section were conducted in the following manner. The body heater, described earlier, was used to preheat and maintain the ion source at a temperature of 500°C.

This eliminated changes in the discharge characteristics and fluctuations normally present during warm-up due to the vaporization of condensed mercury present on the walls of the ion source. The cathode heater was maintained at about 30 watts during ion source operation to keep the cathode characteristics consistent. In addition, the liquid nitrogen cold plate temperature was monitored with a thermocouple to check for anomalies in the LN_2 feed system. After making the above provisions for thermal control it was found that reasonably consistent data could be taken within 15 minutes after starting the ion source.

The ion source was started in the following manner. The cathode heater was turned up to about 50 watts and the main discharge and keeper discharge power supplies were set at 50 volts and 30 volts respectively. The magnet was set at 2.0 amperes. The keeper start supply (165 volts) was turned on to provide the initial breakdown conditions at the cathode. The keeper start supply was attached to the keeper electrode through a 7.5 kilohm resistor and isolated from the keeper power supply with a diode. Finally the cathode vaporizer was manually set to maximum power (about 15 watts). Thus, with these preparations, the flow of mercury vapor would increase until the conditions for breakdown were reached.

After breakdown commenced, when the keeper discharge current was approximately 20 milliamperes, the diode was forward biased and the high current keeper power supply would come into play. The main discharge would normally come on with the keeper discharge. After starting, the keeper and main discharge were set at 1 and 5 amperes respectively and the cathode heater was turned down to 30 watts. At this point, the vaporizer heater was set in the control mode which maintained the arc voltage (main discharge) at a predetermined value.

Usually measurements were taken at a time interval of about 30 minutes after startup of the ion source. The frequency spectra of the main discharge voltage and the cathode vaporizer temperature were monitored during this warm-up period as a way of checking for consistent operation. Measurements were taken only after the above parameters were essentially constant over a ten minute period.

First Series of Bell-Jar Experiments

The general starting and operating characteristics of the new bell-jar ion source were found to be essentially the same as the 20-cm ion thruster in spite of the differences in the geometry and the propellant feed system. In addition, there appeared to be no significant difference in the general shape and amplitude of the arc current fluctuations observed on the oscilloscope. However, in major contrast to the previous observations, it was found that the magnetic field had very little effect upon the fluctuation frequency.

Figure 10 contains a series of arc voltage frequency spectra that were made at different magnet current levels. The range of magnetic field used in this figure is comparable to the range covered with the ion thruster in Figure 4B. The arc current and voltage were held at 5 amperes and 25.5 volts respectively, and the spectra were taken at a bandwidth of 200 hertz. Two observations can be made regarding this figure. (1) There was no clear relationship between the magnetic field level and the fluctuation frequency. The frequency of the major peak in the spectrum was found to be about 14 Kilohertz $\pm$ 1 Kilohertz over the entire range of magnet currents used. (2) The amplitude of the spectrum decreased with increasing magnetic field. Both of these features were different than the previous observations with the ion thruster.

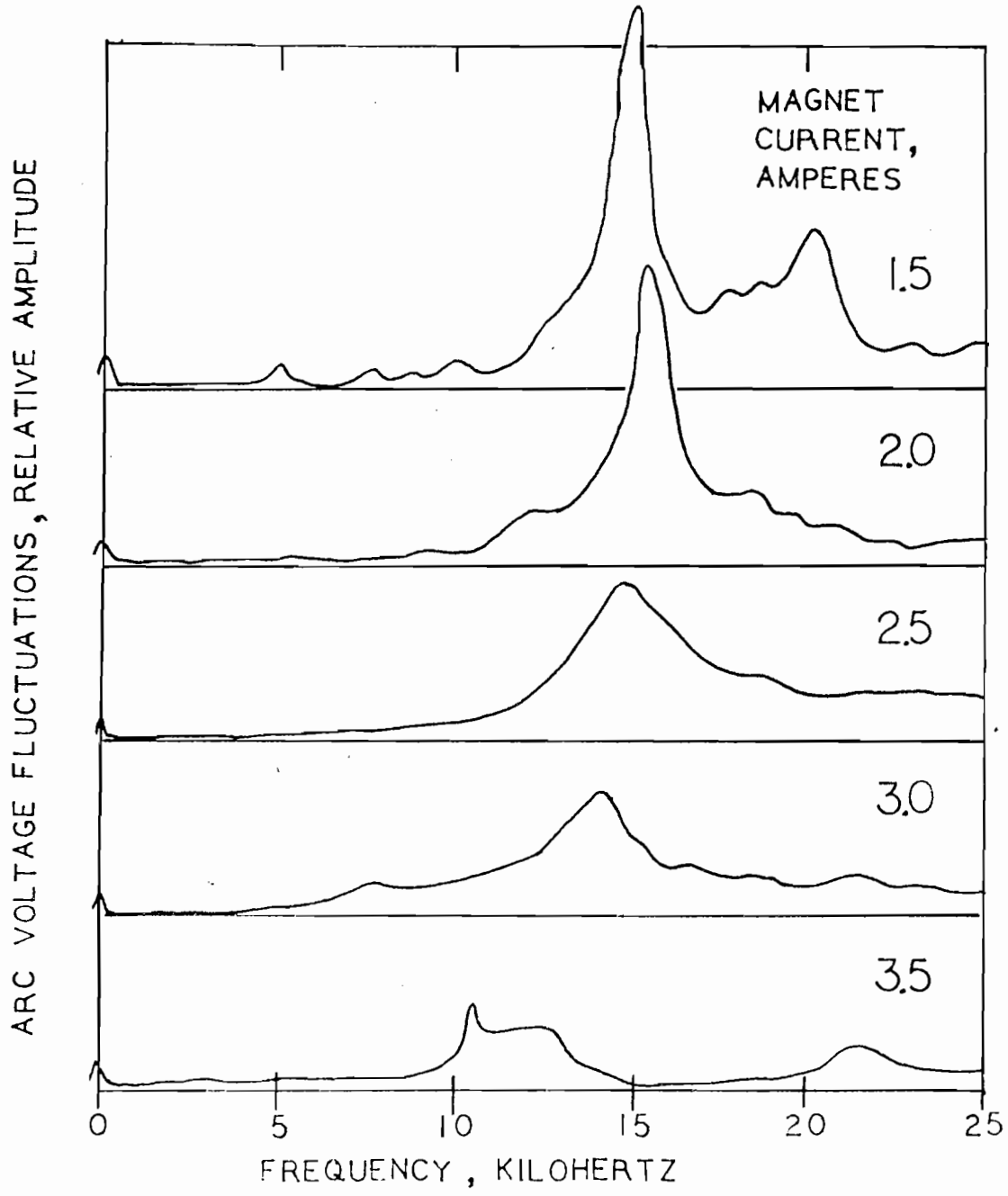

Figure 10 - Frequency spectra of arc voltage fluctuations as a function of the magnet current for the bell-jar ion source.

A second experiment was performed to determine the frequency spectra of the arc voltage fluctuations as a function of the arc current. The arc voltage and magnet current were held at 25 volts and 1.4 amperes respectively during this test. In this case, the shape of the frequency spectra did not change appreciably with the changes in arc current.

Figure 11A contains a plot of the principal frequency (major peak) as a function of arc current. Note that the frequency increases almost linearly with the arc current. The relationship between the arc current and the fluctuation frequency is essentially the same as the ion thruster data shown in Figure 6. Figure 11B is a plot of the relative amplitude of the principal frequency (major peak) as a function of arc current. Note that the amplitude of the fluctuations is approximately linearly related to the arc current.

The previous ion thruster tests at JPL were conducted with the arc voltage controlled to approximately 35 volts, which was the standard operating point. However, with the bell-jar experiments, it was discovered that the arc voltage had a profound effect on the frequency spectra. Figure 12 contains a series of arc voltage frequency spectra which were taken as a function of arc voltage. The arc current and magnet current were held at 5 and 1.4 amperes respectively. The spectra indicate that when the arc voltage was increased, (1) the frequency (of the major peak) increased, (2) the amplitude decreased, and (3) the general shape of the spectra changed considerably. This change in the frequency with arc voltage is responsible for the frequency difference described in the last paragraph; ie, the lower arc voltage would be expected to be associated with lower frequency fluctuations given the arc voltage-frequency relationship just described.

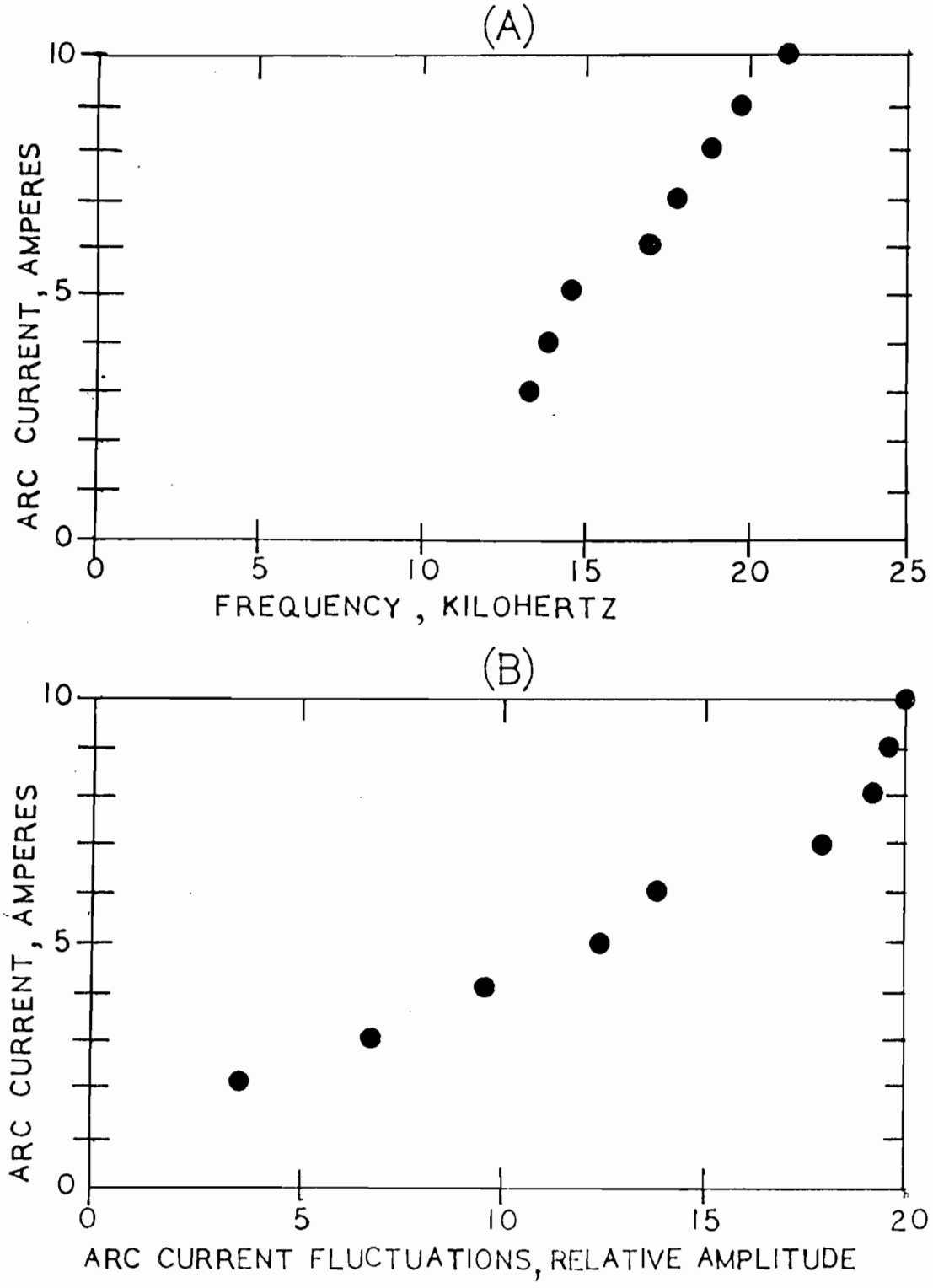

Figure 11 - Effect of the arc current on arc current fluctuation (A) frequency, and (B) amplitude.

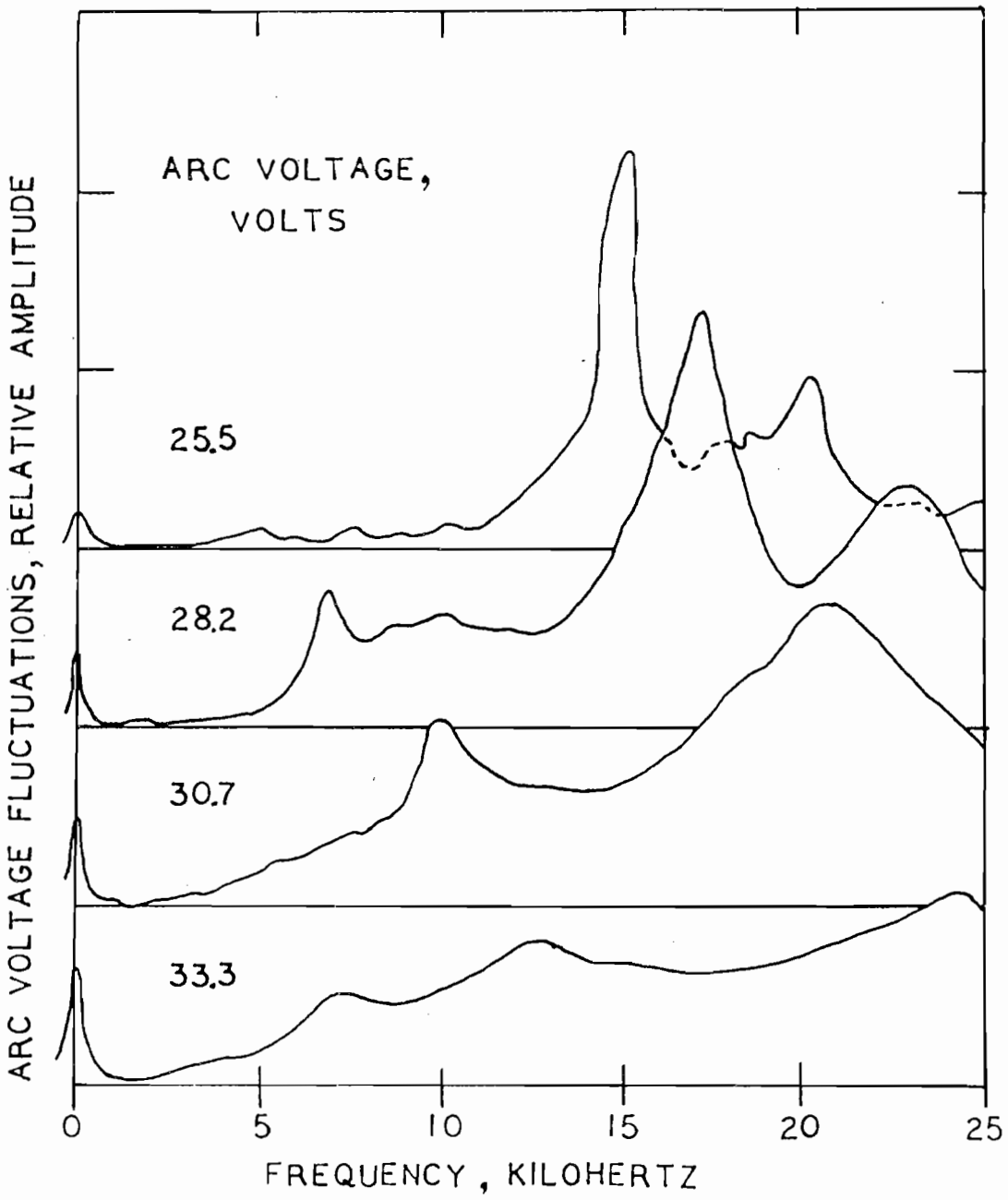

Figure 12 - Frequency spectra of arc voltage fluctuations as a function of the arc voltage.

A simple experiment was performed to determine the relationship between the plasma fluctuations and the arc power supply filter. Figure 13 contains 2 sets of oscilloscope traces which were taken at the same discharge operating point. The traces were made by monitoring the voltage across the discharge and the arc current simultaneously using the dual beam scope and the clamp-on current probe described earlier. The set of traces on the left were taken with the standard power supply (Trygon Mercury Series Model 60-15). The voltage and current measured at the terminals of the ion source were 25.5 volts and 5.0 amperes respectively. It should be noted that the peak to peak value of the arc current fluctuations was roughly about half of the DC level, and the peak to peak value of the arc voltage fluctuations was about 8 volts.

The right side of Figure 13 contains a pair of traces which were taken with the same power supply and the same operating point but with the addition of a 40 millihenry choke in the arc circuit. The figure shows that the arc current fluctuations can be reduced considerably with a choke. However, it should be noted that the arc voltage fluctuations have more than doubled in size at the same time. Thus, it can be concluded that a filter can change the relative amplitude of the voltage or current but it cannot eliminate the fluctuations. In addition, frequency spectra have shown that the frequency is not affected in any substantial way by additional power supply filtering. Figure 13 also shows that the arc current and voltage fluctuations are 180° out of phase. In other words, the AC components are displaying a negative resistance characteristic. This is also a feature of electronic oscillators and was suspected of having some bearing on the cause of the fluctuations.

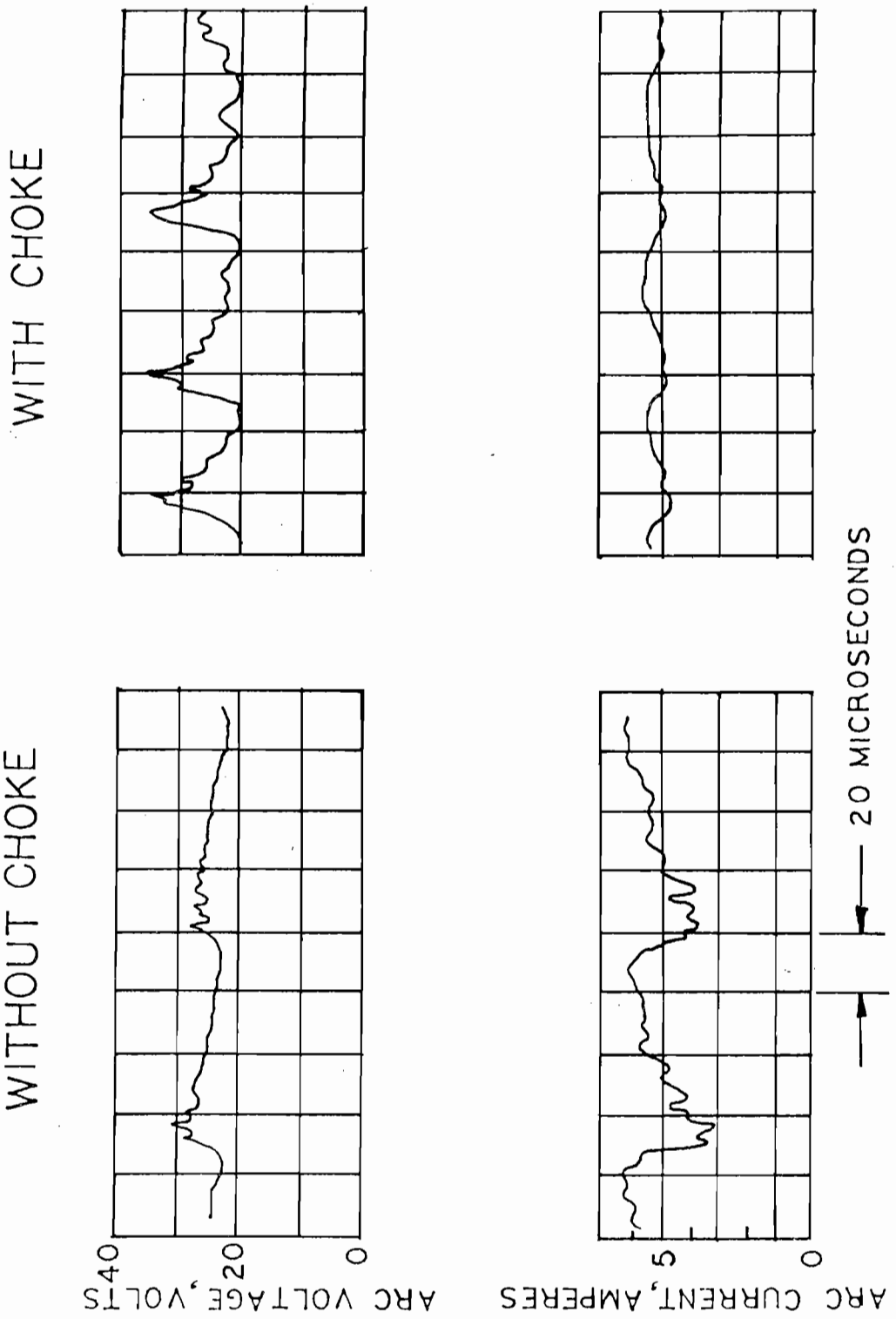

Figure 13 - The effect of a 40 millihenry choke in series with the arc power supply on the arc current and voltage fluctuation characteristics.

Emissive probes were located in several positions within the ion source. The previous measurements in the ion thruster were limited to the main discharge chamber. However, the new bell-jar experimental set was equipped with a probe within the keeper discharge region, and another probe which was located just outside of the baffle aperture (see Figure 9) in the main discharge. Figure 14 shows a comparison of the plasma potential fluctuations take at the same time in these two locations with the arc current and voltage set at 5.0 amperes and 25.5 volts respectively. First, it should be noted that the plasma potential fluctuations in the main discharge are almost identical to the arc voltage fluctuations (see Figure 13 for a comparison) in terms of the amplitude and the fine features of the wave shape. Secondly, Figure 14 shows that the plasma potential fluctuations in the two regions are approximately 180° out of phase. In particular, it should be noted that the potential difference between the two regions varies over a very wide range. In this case, the voltage increase through the baffle aperture was oscillating from a low value of about 7 volts up to a maximum of about 21 volts. Finally, a comparison between Figures 13 and 14 shows that the arc current is 180° out of phase with respect to the plasma potential fluctuations within the baffle aperture region. Therefore, it can be said that the baffle aperture plasma region is responsible for most of the negative resistance characteristics which have been observed on the arc (see Figure 13). This feature was thought to be a possible manifestation of the anomoulous electrical conductivity (runaway electrons) which was proposed by Wells[44] to explain the characteristics of plasma in the baffle aperture region of a hollow cathode ion thruster.

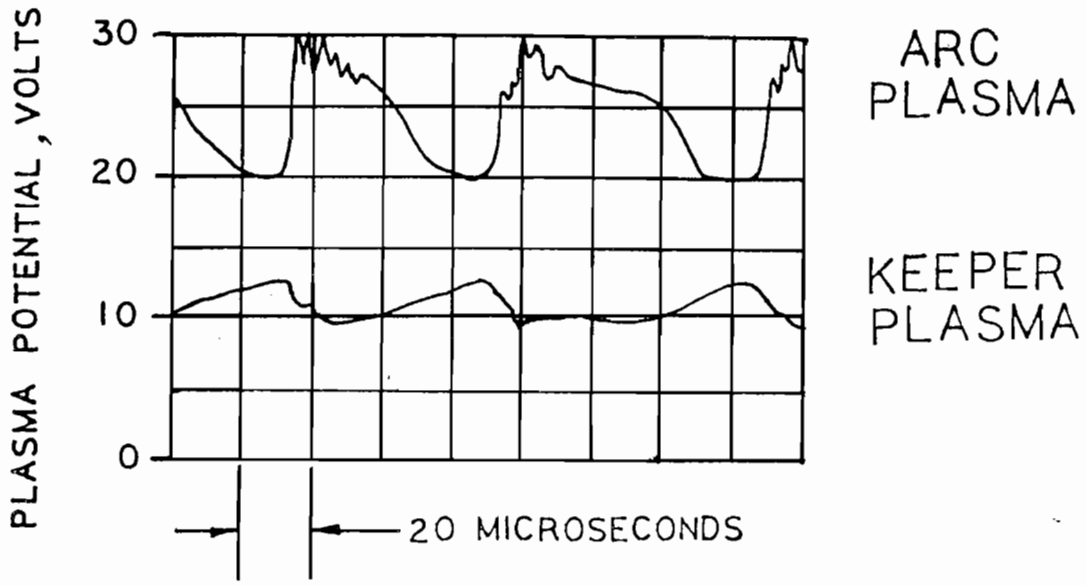

Figure 14 - The relationship between the plasma potential fluctuations in the arc and keeper plasma.

The emissive probes in the bell-jar ion source were also used as standard Langmuir probes, ie, with the filament heater power off. Langmuir probe characteristics were taken as a function of radius within the main discharge region, at one point within the Keeper discharge region, and immediately downstream from the baffle aperture (the "slot" region). These measurements were made as a function of the arc voltage, arc current, and the magnetic field current. The Langmuir I-V characteristics were displayed on an x-y recorder using the circuit shown in Figure 15. The Langmuir probe voltage was swept by means of a ten turn potentiometer which acted as a variable voltage divider. The output of the pot was fed into the base of an NPN power transistor. With this method it was possible to use a very accurate high resistance potentiometer to produce a smooth increase in voltage with the power transistor carrying the majority of the current.

The Langmuir probe characteristics in the main discharge plasma contain a so-called primary electron component which must be removed in order to find the true Maxwellian electron temperature. This was accomplished by using a computer probe data reduction routine developed at CSU by Beattie.[45] The I-V characteristics were converted to digital form on a digitizer and fed into the computer routine. The remaining part of this section will be used to describe the results of the Langmuir probe analysis. The data review will cover the effects of the previously discussed ion source parameters on the Maxwellian electron temperature. The electron temperature measurements will then be used to calculate the appropriate ion acoustic resonance frequency for the main discharge chamber.

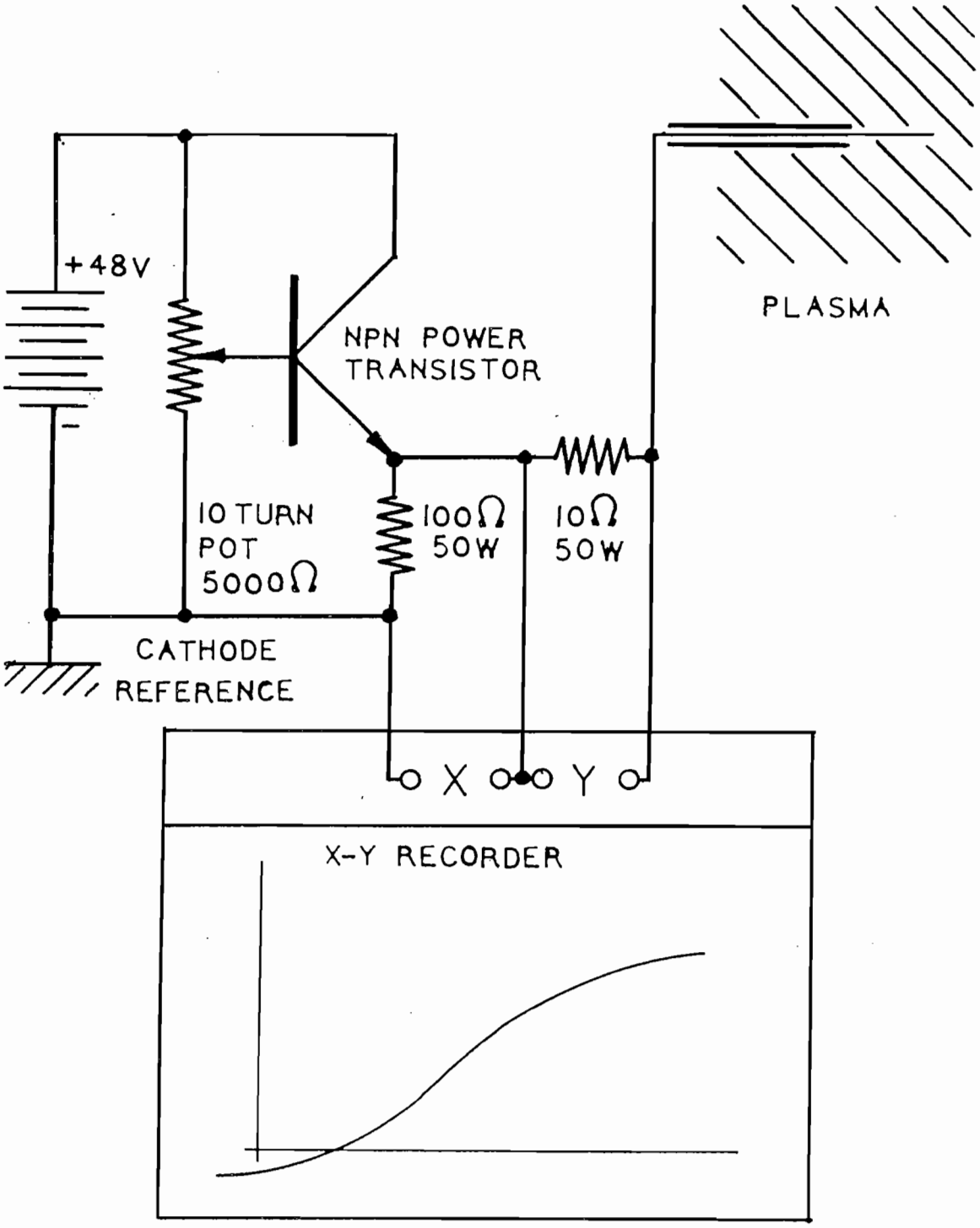

Figure 15 - Langmuir probe circuit diagram.

Figure 16 shows a plot of Maxwellian electron temperature as a function of the magnetic field current from the central axis to within 0.5 centimeters of the anode. These data were taken at an arc current current and voltage of 5.0 amperes and 25.5 volts respectively. Note that there is a general trend of decreasing Maxwellian electron temperature as the magnetic field is increased. In addition, there is a peak in most of the curves which roughly corresponds to the opening in the baffle aperture. The electron temperature decreases by about 50% when the magnet current is increased from 1.5 to 3.5 amperes. A change of electron temperature of that magnitude should reduce the fluctuation frequency by about 30% if there is an ion acoustic resonance in the main discharge. However, it was shown (Figure 10) that with the bell-jar source the fluctuation frequency remains approximately constant when the magnetic field current is varied over the same range.

The Maxwellian electron temperature is shown as a function of arc current in Figure 17 for the same region described in the last paragraph. In this case, the arc voltage was controlled to 25.5 volts and the magnet current was set at 1.5 amperes. The arc current level ranged from 5.0 to 10.0 amperes. It can be seen from the figure that the Maxwellian electron temperature increased by about 30% when the arc current was increased from 5.0 to 10.0 amperes. Using the hypothesis that the fluctuations are caused by an ion acoustic resonance in the main discharge, one would expect about 14% increase in the fluctuation frequency for a 30% increase in electron temperature. However, Figure 11 indicates that the fluctuation frequency increased by about 40% over this range of arc currents tested.

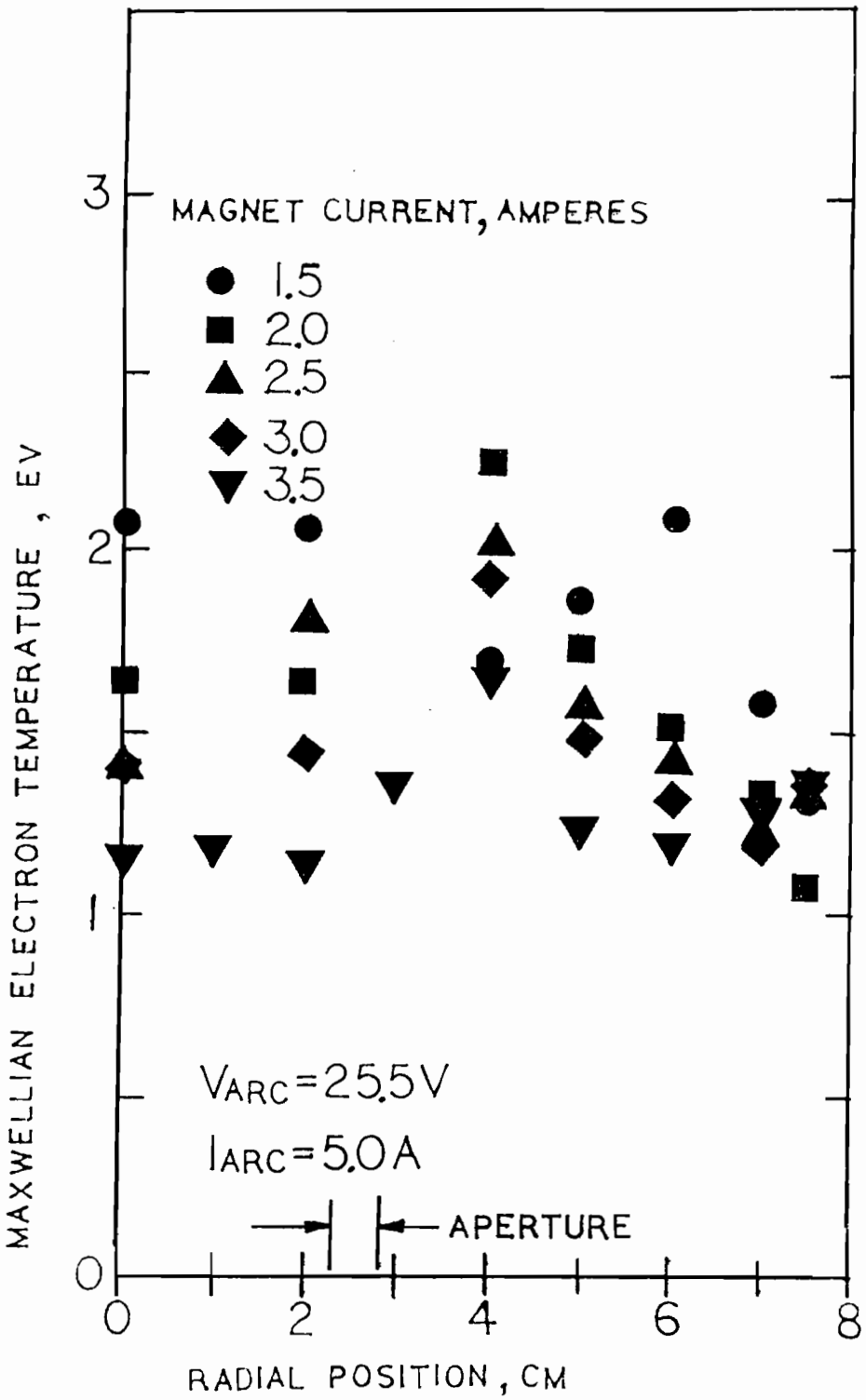

Figure 16 - Maxwellian electron temperature as a function of radial position in the main discharge for several magnet currents.

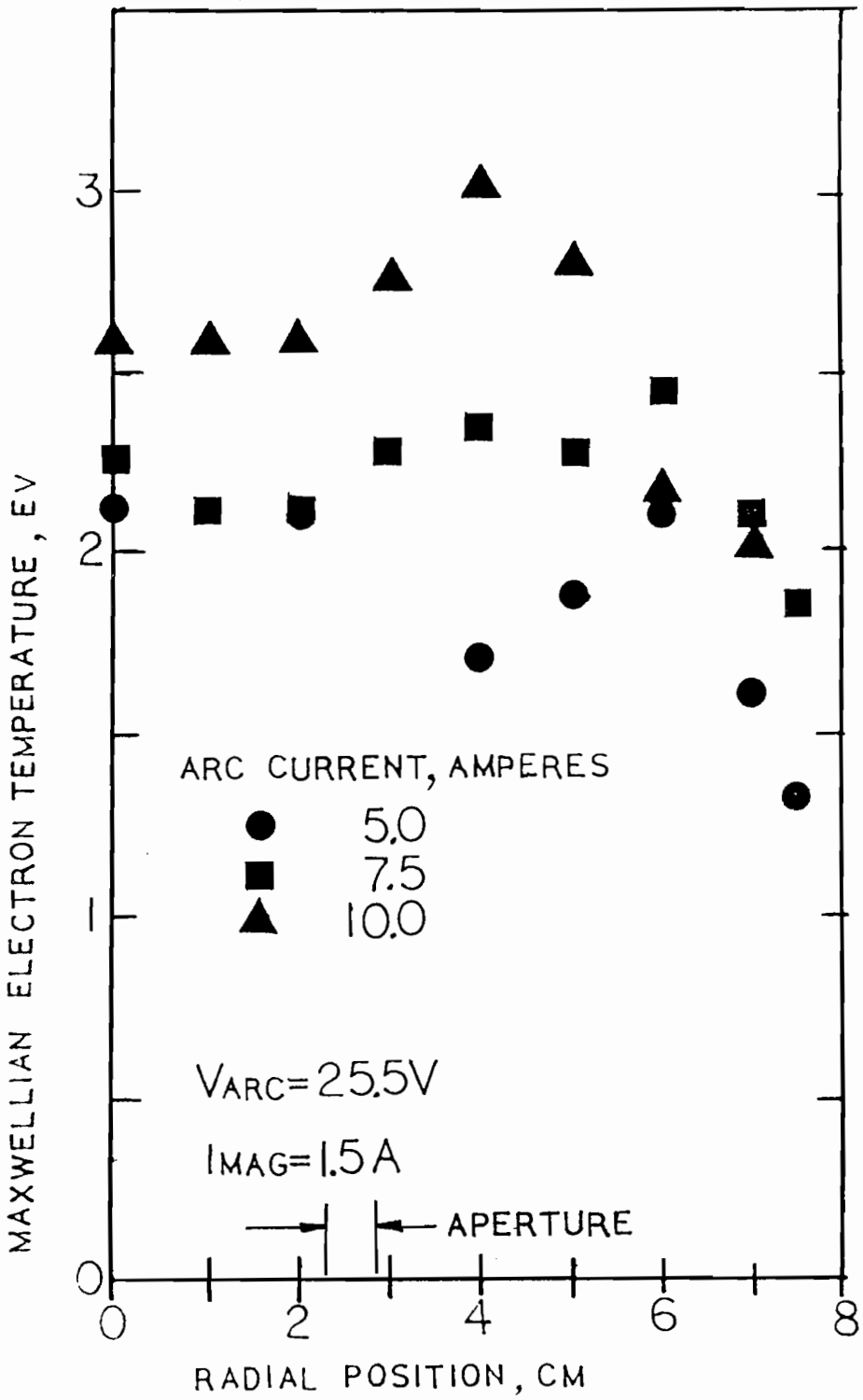

Figure 17 - Maxwellian electron temperature as a function of radial position in the main discharge for several values of arc current.

Figure 18 shows a plot of the Maxwellian electron temperature as a function of the arc voltage at a fixed arc and magnet current of 5.0 and 1.5 amperes respectively. The probe data was taken over the same range of positions in the main discharge chamber as the two previously described sets of data. Notice that the increase of the Maxwellian electron temperature is less than 20% when the arc voltage is charged from 25.5 to 33.3 volts. This should result in a frequency increase of about 10% if the main discharge ion acoustic resonance hypothesis were applicable. However, the frequency spectra covering the same range of arc voltage (Figure 12) indicate that the frequency (major peak) increases by almost 100%.

The Maxwellian electron temperature measurements described in the previous paragraphs ranged from about 1 to 3 electron volts in the main discharge chamber of the bell-jar ion source. The length of the main discharge chamber is 20 centimeters. Therefore, using Equation (6), the ion acoustic resonant frequency should range from about 1700 to 3000 hertz. This is an order of magnitude lower than the measured fluctuation frequency.

To summarize, the hypothesis that an ion acoustic resonance is present in the main discharge is dismissed for the following reasons. (1) The changes in the Maxwellian electron temperature in the main discharge region resulting from changes in the magnet current, arc current and arc voltage did not produce the expected relative change in the fluctuation frequency. (2) The ion acoustic frequency calculated using the Maxwellian electron temperature measured in the main discharge is an order of magnitude less than the measured fluctuation frequency.

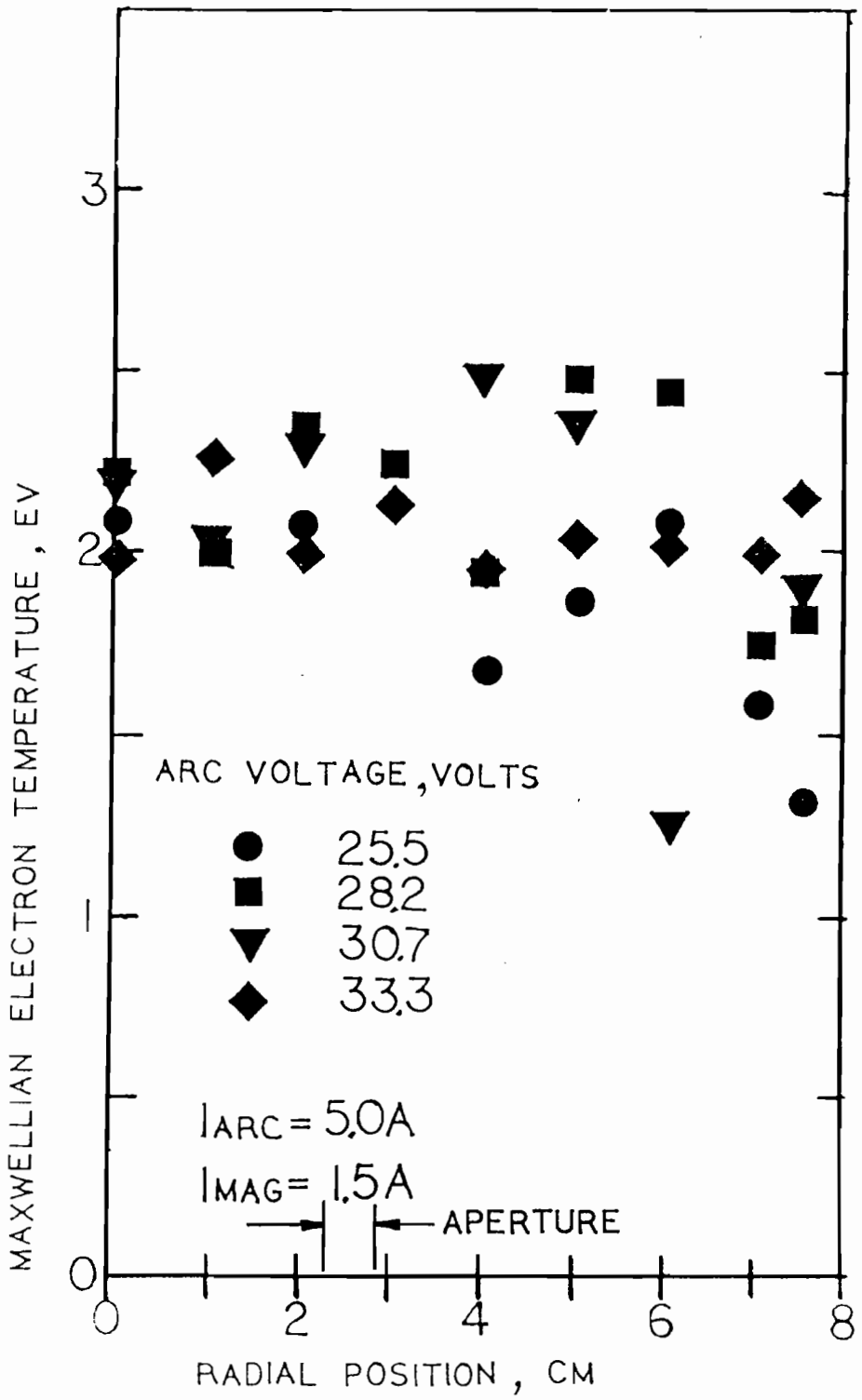

Figure 18 - Maxwellian electron temperature as a function of radial position in the main discharge for several values of arc voltage.

An unusual feature of the plasma fluctuations was the fact that the frequency changed considerably with the magnet current in the ion thruster but did not change with the bell-jar ion source. This implies that the geometry of the magnetic field has a large influence over the fluctuation frequency but that it does not have a direct role, for example, like the electron cyclotron resonance. Therefore, one might suspect that the magnetic field may be acting in a secondary manner, for example, by changing the density or plasma potential distribution.

It was also noted that the plasma in the baffle aperture region displayed negative resistance characteristics. Therefore, it might be surmized that the "double sheath" region is unstable and thereby modulating the electron current going into the main discharge. This would also help explain the effect of the magnetic field which, in the case of the ion thruster, can exhibit a profound influence over the plasma conductivity in the aperture region.[44,46,47]

Finally, it was found, with the limited Langmuir probe data taken in the keeper plasma region, that an ion acoustic resonance in the Keeper region may be the cause of the plasma fluctuations. For example, a typical electron temperature in the keeper discharge region was found to be about 1.5 electronvolts. Using Equation (6) and a keeper discharge chamber length of 3.8 centimeters, the ion acoustic resonance frequency is about 11,000 hertz, which is of the same order as the observed fluctuation frequency. The electron temperature measurement in the keeper discharge region was taken on the central axis about one centimeter behind the baffle. More detailed plasma measurements[44] taken in the keeper discharge region of an ion thruster indicate that the electron temperature is a factor of two to three times larger at the baffle aperture than at the

central axis of the keeper discharge. If this feature is also applicable in the case of the bell-jar ion source, then the predicted ion acoustic frequency would be in the range of 15,500 to 19,000 hertz. These predicted values are comparable to the observed fluctuation frequency.

In conclusion, the results of the first series of bell-jar experiments suggest that an ion acoustic resonance in the main discharge chamber is unlikely. However, these experimental results indicated that the baffle aperture and keeper regions may be a logical place to look for the cause of the plasma instabilities. In fact, calculations indicate that an ion acoustic resonance in the keeper discharge chamber would have a frequency which is comparable to the observed fluctuation frequency. These results provided the motivation for a second series of experiments which concentrated on the keeper discharge and baffle aperture regions. This second series of bell-jar experiments will be described in the next section.

It should be mentioned that during the same period Serafini[48-50] identified a similar type of plasma fluctuation in the 8 cm and 30 cm mercury ion thrusters at NASA Lewis Research Center. Correlation techniques were applied to identify the relationship between the noise observed on the various thruster power supplies. The experiments indicate that the beam current fluctuations are related strongly to the discharge current fluctuations in the 30 cm thruster but are weakly related in the 8 cm thruster. In general, the relationship between the various sources of thruster noise were found to be very complex. The 30 cm thruster used in these studies was equipped with a so-called magnetic baffle which produces a magnetic field across the baffle aperture. Frequency spectra indicate that the plasma fluctuation frequency increased with the magnetic

baffle current. Similar plasma fluctuation mechanisms were proposed; however, no direct plasma measurements were made to support these theories.

Second Series of Bell-Jar Experiments

A second series of experiments were conducted in the bell-jar test setup described in the preceeding section. These experiments focused primarily on the baffle aperture and keeper plasma regions. The experimental results will be presented in the following manner: (1) Examples of the average plasma properties in the keeper plasma region will be shown. (2) Frequency spectra will be presented which show the relationship between the frequency and the length and diameter of the keeper discharge chamber. (3) Oscillographs will be given which show the dynamics of various plasma parameters as a function of position and the relationship to the arc current and voltage.

Plasma Properties in the Keeper Discharge Region

A series of Langmuir probe measurements were made in the keeper plasma region. The main purpose for these measurements was to determine the electron temperature in order to calculate the ion acoustic resonance frequency appropriate for that region. These calculated frequency values could then be compared to the measured values of the plasma fluctuation frequency. The Langmuir probe data also provide information on the plasma potential and electron density. The plasma potential measurement can be used to show the length of the transition zone in the aperture region. The electron density distribution may also have an effect on the proposed resonance mechanism, i.e., wave reflection in a region where the density is increasing.

The Langmuir probe measurements were conducted with the large keeper discharge chamber diameter only. The probe could be moved along the length of the keeper discharge chamber and swept radially. The probe I-V data were replotted on semi-log paper and the electron temperature was determined from the slope of the electron repelling part of the I-V characteristics.

Figure 19A shows a plot of the electron temperature as a function of radius for two different values of arc current. The total emission current from the cathode (anode + keeper current) was held constant, and the arc voltage was 30 volts. The chamber length and diameter were 7.0 and 8.9 centimeters, respectively. The probe was located in the keeper plasma region, one centimeter from the plane of the baffle. This figure shows that the electron temperature increases with increasing radius, and reaches a maximum at the radius of the baffle aperture. It is also shown that the electron temperature maximum is higher at the higher arc current. However, both sets of data merge towards a common electron temperature at the center. Figure 19B shows that the electron temperature remained approximately constant along the central axis of the keeper discharge chamber. The fluctuation frequency for the two runs shown in Figure 19 were 9.2 kilohertz for the 7 ampere arc current, and 6.9 kilohertz for the 5 ampere arc current, respectively.

The Langmuir probe measurements described in the last paragraph also indicated a rise in the plasma potential from about 8 volts at the center to 11.8 volts at the aperture. The plasma potential appeared to be approximately equal for the two runs. There was a slight depression of the plasma potential observed at the center near the baffle. The

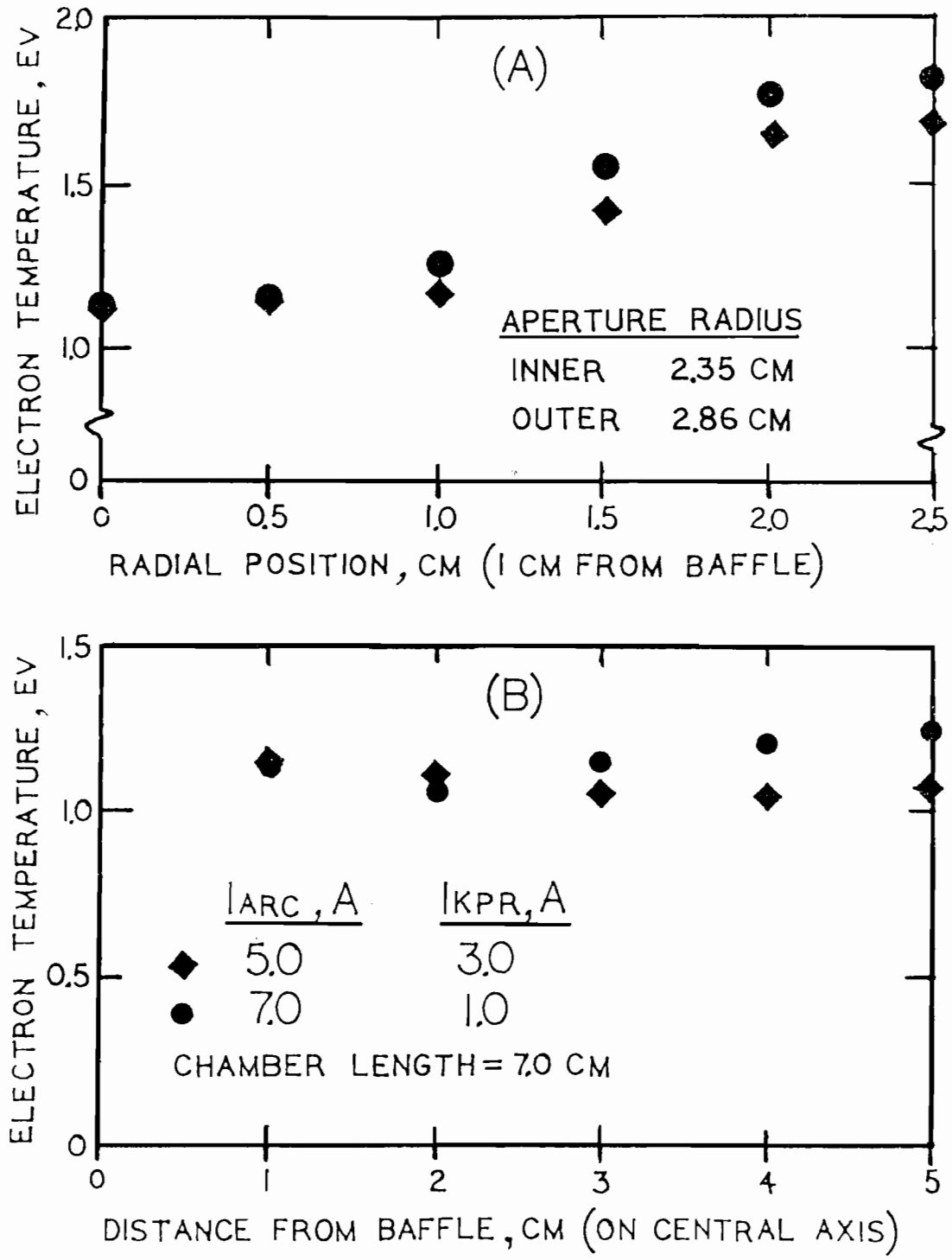

Figure 19 - Electron temperature distribution in keeper plasma region (A) radial, (B) axial.

plasma potential increased from that point up to a value of about 9 volts in front of the keeper electrode. These features are seen in Figure 20.

The electron density for these two runs had a typical gaussian distribution with respect to the radius, with the 7 ampere arc current case being slightly higher throughout. The electron density along the central axis increased substantially for both cases as the cathode region was approached. Regions of increasing plasma density have been shown[51] to be capable of reflecting ion acoustic waves; therefore, in some cases, this condition may be the reason why the ion acoustic resonance can sustain itself. These data are shown in Figure 21.

Electron temperature measurements were also taken at different arc currents, keeper chamber lengths, and keeper currents. However, there were problems with some of these measurements. It was found, under certain conditions, that the mere presence of the Langmuir probe itself could cause a shift in the fluctuation frequency, or what appeared to be an entire mode change; i.e., fundamental to first harmonic frequency. This problem was resolved by assuming the Langmuir probe measurements were substantially correct, in spite of the frequency or mode change. In other words, it was assumed that the probes may have disturbed the motion and/or the boundary conditions and hence the frequency of the fluctuations but did not change the bulk plasma properties. It was also assumed that the frequency spectra were valid only when the Langmuir probes were removed from the keeper plasma region. In this way, it was possible to compare plasma properties with frequency spectra taken under the same conditions; i.e., arc current, arc voltage, keeper chamber length, etc. This method will be used in the next chapter to compare the theoretically predicted frequency with the measured frequency.

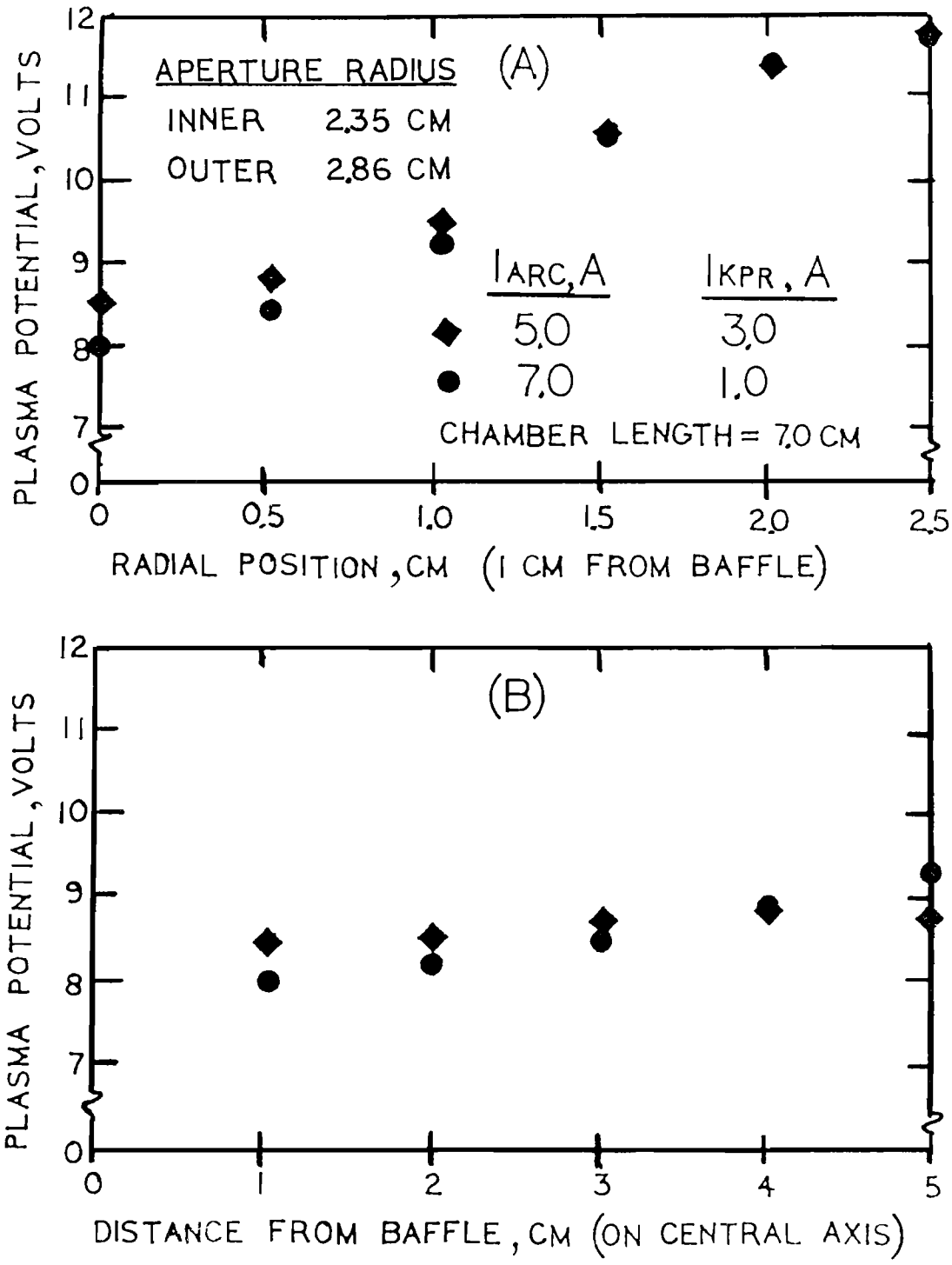

Figure 20 - Plasma potential distribution in the keeper plasma region (A) radial, (B) axial.

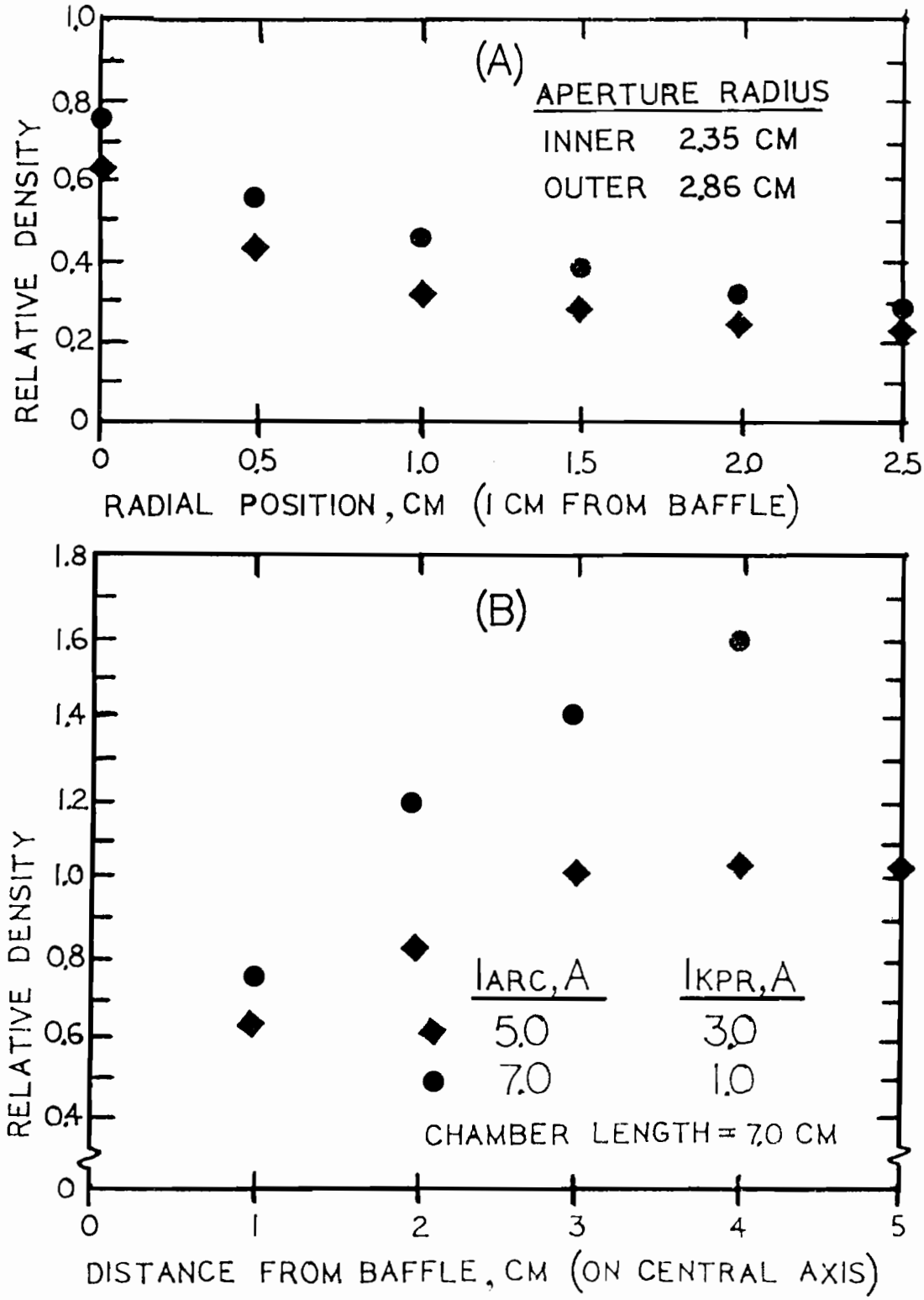

Figure 21 - Electron density distribution in the keeper plasma region (A) radial, (B) axial.

Finally, it should be noted that the measured electron temperatures in the keeper plasma region are in a regime where the calculated value of the longitudinal ion acoustic resonance frequency (Equation 6) is approximately the same as the measured fluctuation frequency.

Effect of Keeper Chamber Geometry on Fluctuation Frequency

The bell-jar ion source was modified to permit the length and diameter of the keeper discharge chamber to be changed. Figure 22 shows details of the keeper discharge chamber used. The length of the chamber could be changed from 0 to 9 centimeters by remote control. There were two different keeper discharge chamber diameters used, which had to be changed manually. The back of the keeper discharge chamber was in the same plane as the keeper electrode ring in both diameter configurations.

Figure 23 shows a typical series of frequency spectra taken as a function of keeper discharge length. This particular group of spectra were taken at a discharge voltage and current of 30 volts and 5 amperes, respectively. Note that there is a dramatic increase in the frequency (first major peak) as the length of the keeper discharge chamber is decreased. In addition, there are other peaks in the spectrum which are approximately multiples of the first major peak frequency.

A plot of the frequency as a function of keeper discharge chamber length is given in Figure 24 for two different keeper discharge chamber diameters. These data were taken at a discharge voltage and current of 35 volts and 5 amperes, respectively. The keeper voltage decreased slightly as the chamber length was increased, but the flow rate through the cathode (as determined from the cathode vaporizer temperature) appeared to remain constant. Notice again that there is a dramatic increase in the fluctuation frequency as the keeper discharge chamber length is decreased.

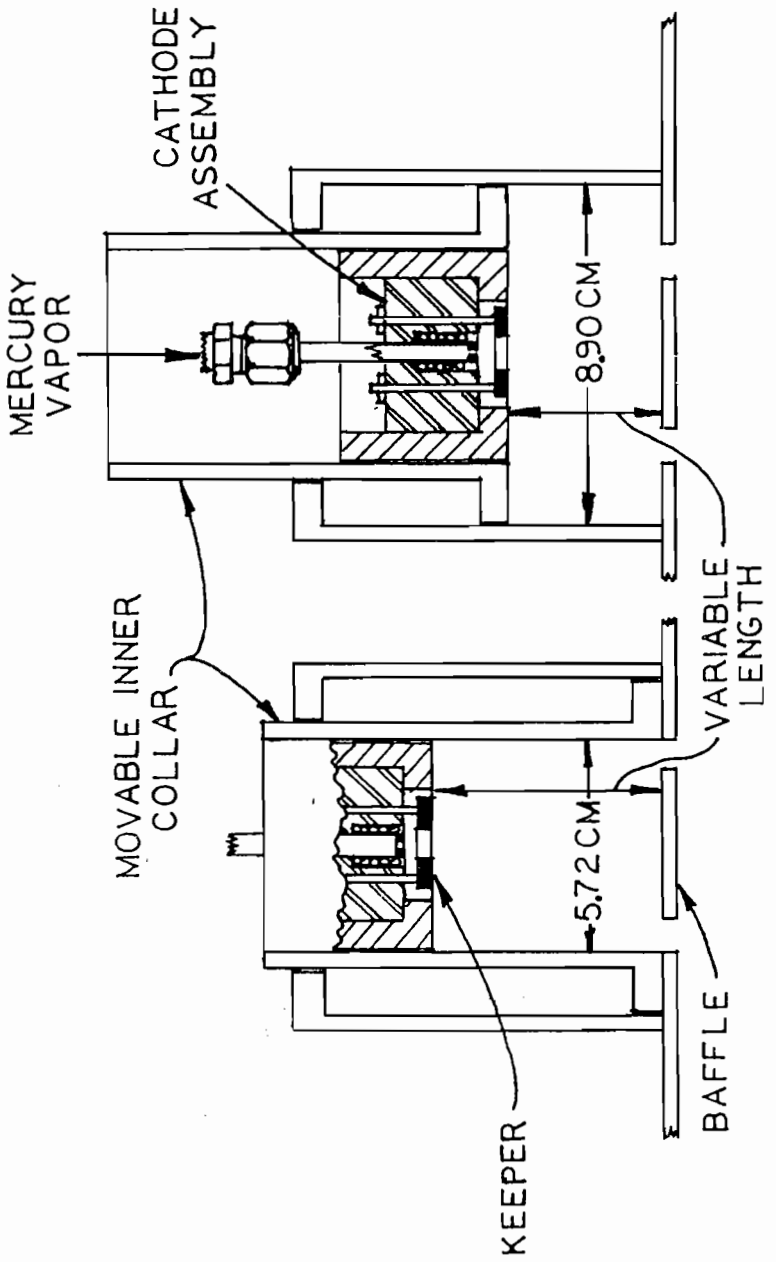

Figure 22 - Variable keeper length assembly cross section, shown for two diameters used.

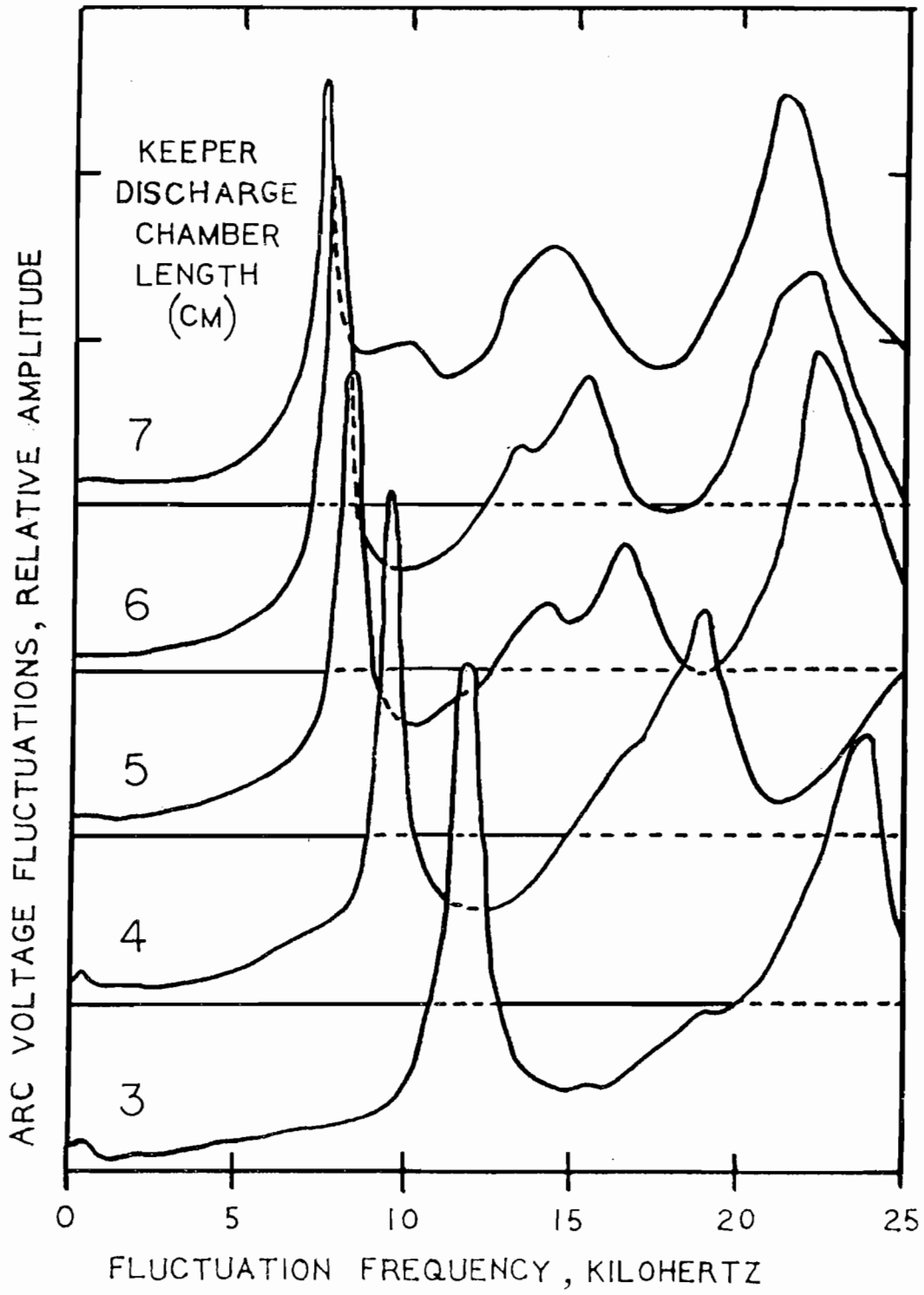

Figure 23 - Frequency spectra of arc voltage fluctuations as a function of keeper discharge chamber length.

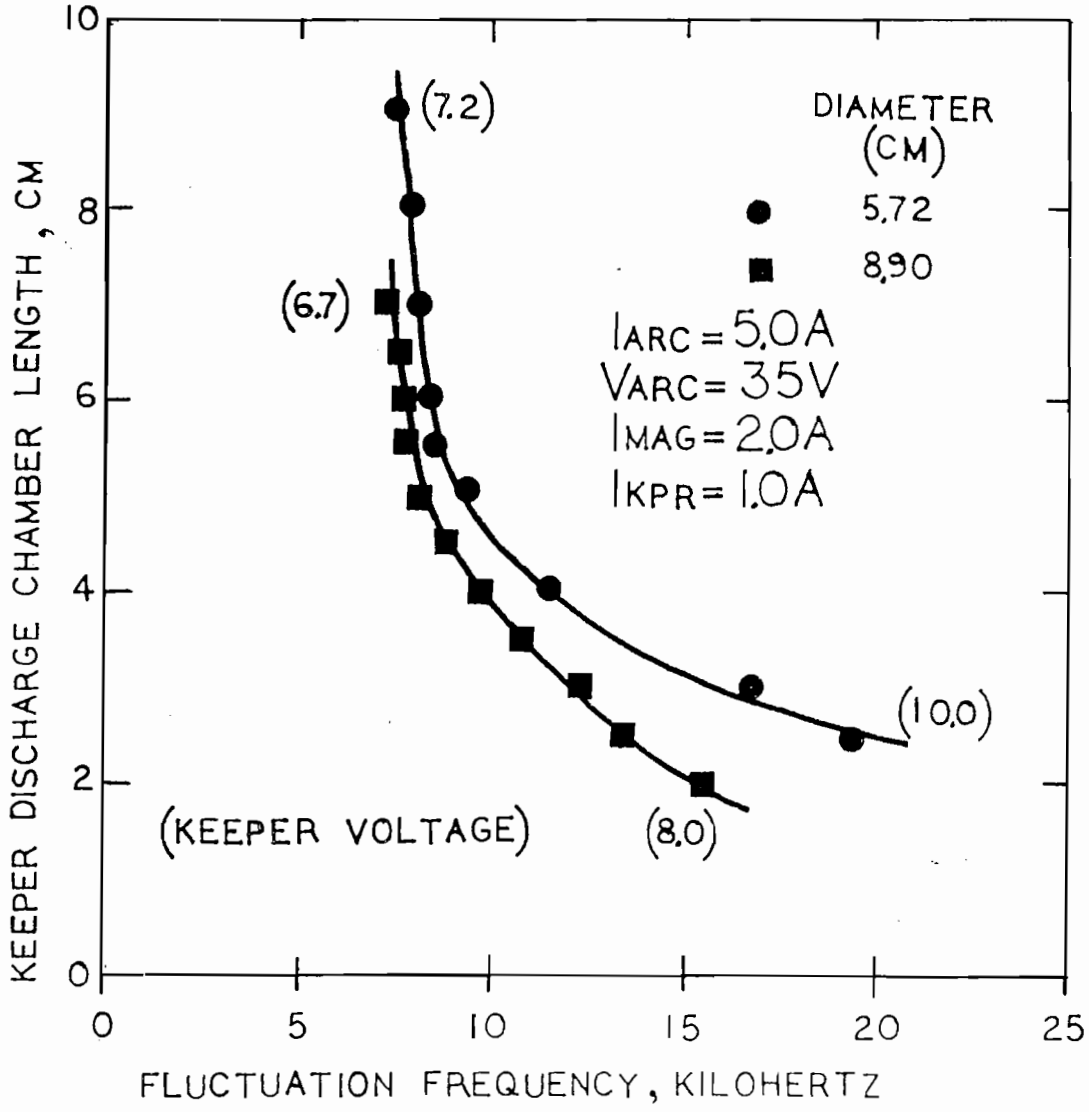

Figure 24 - Plot of arc voltage fluctuation frequency (major peak) as a function of keeper discharge chamber length for two diameters.

In addition, it can be seen that the relative change in the fluctuation frequency with chamber length is greater in the keeper discharge chamber with the smaller diameter.

Dynamics of Plasma Fluctuations

A series of probe measurements were taken in the bell-jar ion source to determine the spacial and temporal relationship between the plasma potential, the electron density and the arc current and voltage fluctuations. Dynamic plasma potential measurements were taken with emissive probes as previously described in Chapter II. Electron density fluctuations were also monitored in a somewhat crude fashion by measuring the current with respect to time collected on a Langmuir probe which was biased to a voltage substantially greater than the plasma potential, i.e., in the electron saturation region.

The plasma potential measurements were assumed to be very accurate providing sufficient heater power was supplied to the emitting surface to produce an electron current greater than the random electron current from the plasma. This was mostly a case of watching the probe response as the heater power is increased; i.e., the observed potential fluctuations on the oscilloscope cease to change with further increases in emitter power. However, the electron density fluctuation measurements have two sources of error. First, the saturation electron current to the probe is approximately equal to;

$$I = \left(N_e A/4\right)\left[8K_b T_e/\pi M_e\right]^{1/2}, \ A \tag{7}$$

where N_e, T_e, and M_e are the electron density, temperature and mass respectively, A is the probe area, and k_b is Boltzmann's constant. Equation (7) shows that the current is a function of both the electron

density and the square root of the electron temperature. Consequently, if the electron temperature changes with time, then the probe current will not be directly proportional to the electron density. A second source of error occurs if the plasma potential varies with time. Equation (7) is written with the assumption that the probe bias voltage is larger than the plasma potential and that the voltage difference is constant. Variations in the plasma potential would change the probe current and hence its proportionality with the electron density. However, in spite of these errors, it is believed that the measured probe current is substantially representative of the electron density fluctuations.

Using the techniques described above, data were taken using a dual beam oscilloscope which permitted observations of the phase relationship between the various parameters.

Figure 25 shows the electron density at various points in the ion thruster and the arc current. The density fluctuations are shown at the center and aperture of the keeper plasma region and in the main discharge adjacent to the anode. The following points can be made about Figure 25. (1) The arc current follows the electron density near the anode quite accurately, although the peaks are not as sharp. (2) The electron density fluctuations at the aperture are almost identical to the arc current fluctuations with the exception that the arc current has a larger negative overshoot after the pulse. (3) The electron density at the center of the keeper plasma region reaches a maximum slightly after the maximum at the aperture region. The electron density decays slowly from the maximum until the onset of the next pulse. The slow decay at the center region occurs while the density at the aperture has dropped to a lower value and remains essentially constant.

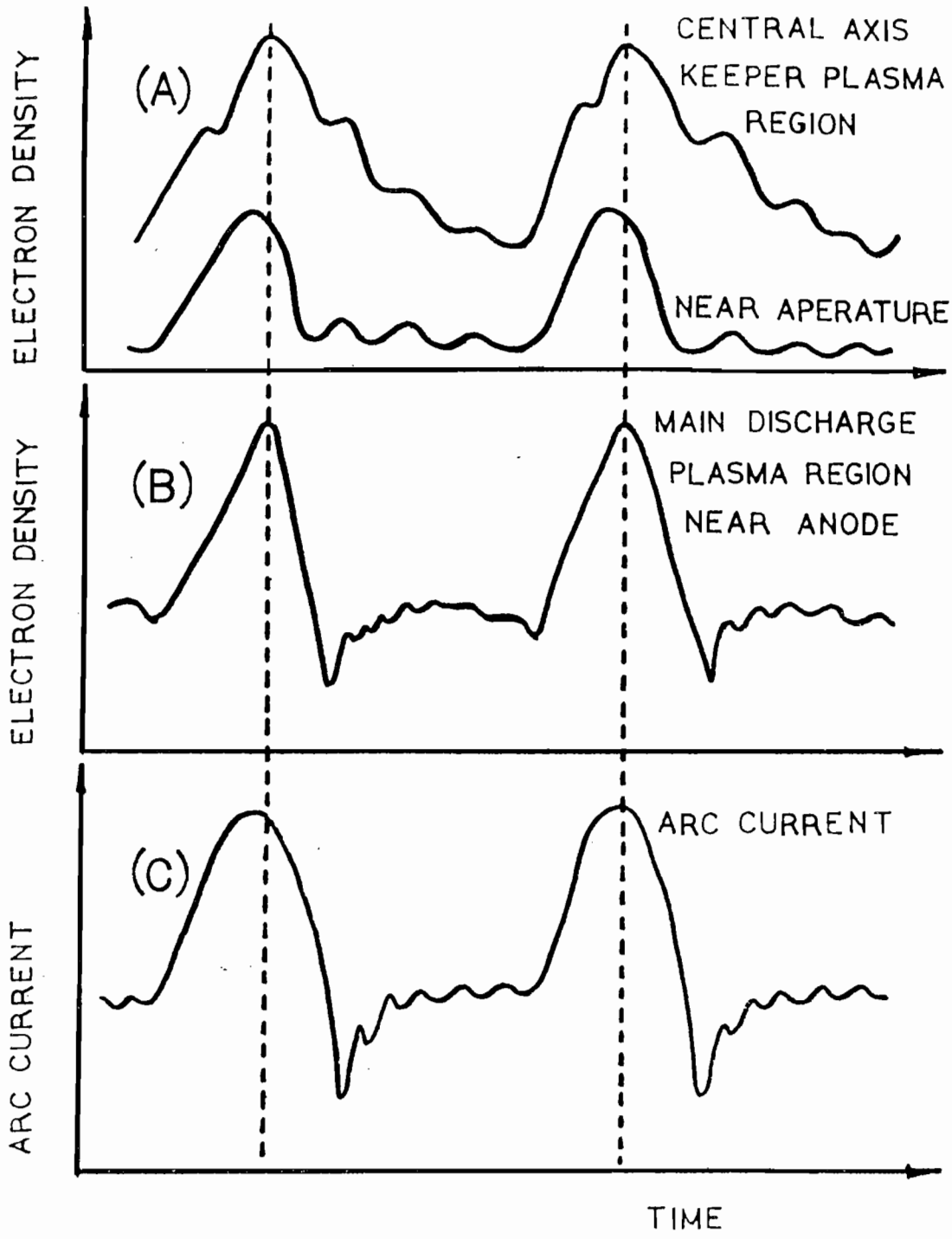

Figure 25 - Dynamic relationship between electron density fluctuations in the keeper plasma region (A) the main discharge, (B) and the arc current (C) respectively.

These observations indicate that there is a strong relationship between the electron density fluctuations in the keeper plasma region and the arc current. This suggests that the keeper plasma region may be modulating the fluctuations throughout the ion thruster. In addition, it should be noted that the coupling between the electron density and arc current is virtually instantaneous compared to the period of the fluctuation.

Figure 26 shows the temporal behavior of the plasma potential at two locations within the keeper plasma region and the relationship with the electron density on axis one centimeter from the baffle. In this case the plasma potential measurements were taken along the axis one centimeter from the baffle and one centimeter from the cathode respectively with the length of the chamber set at seven centimeters. The difference between the two oscilloscope traces has been manually derived from these data and is also shown on the figure. This plasma potential difference is proportional to the electric field along the axis of the keeper plasma region. A set of dashed lines have been placed on the figure which show that the maximum in the electron density along the axis corresponds to the point when the electric field is reversing polarity from positive to negative.

The following points can be made about Figure 26: (1) The electric field along the axis of the keeper plasma actually reverses itself; i.e., the plasma potential near the baffle is more negative than the plasma potential at the cathode end. In fact, the electric field is reversed or near zero for about 75% of the time. During the remaining 25%, the electric field is such as to attract electrons from the cathode to the baffle region. (2) The electron density reaches a maximum slightly after

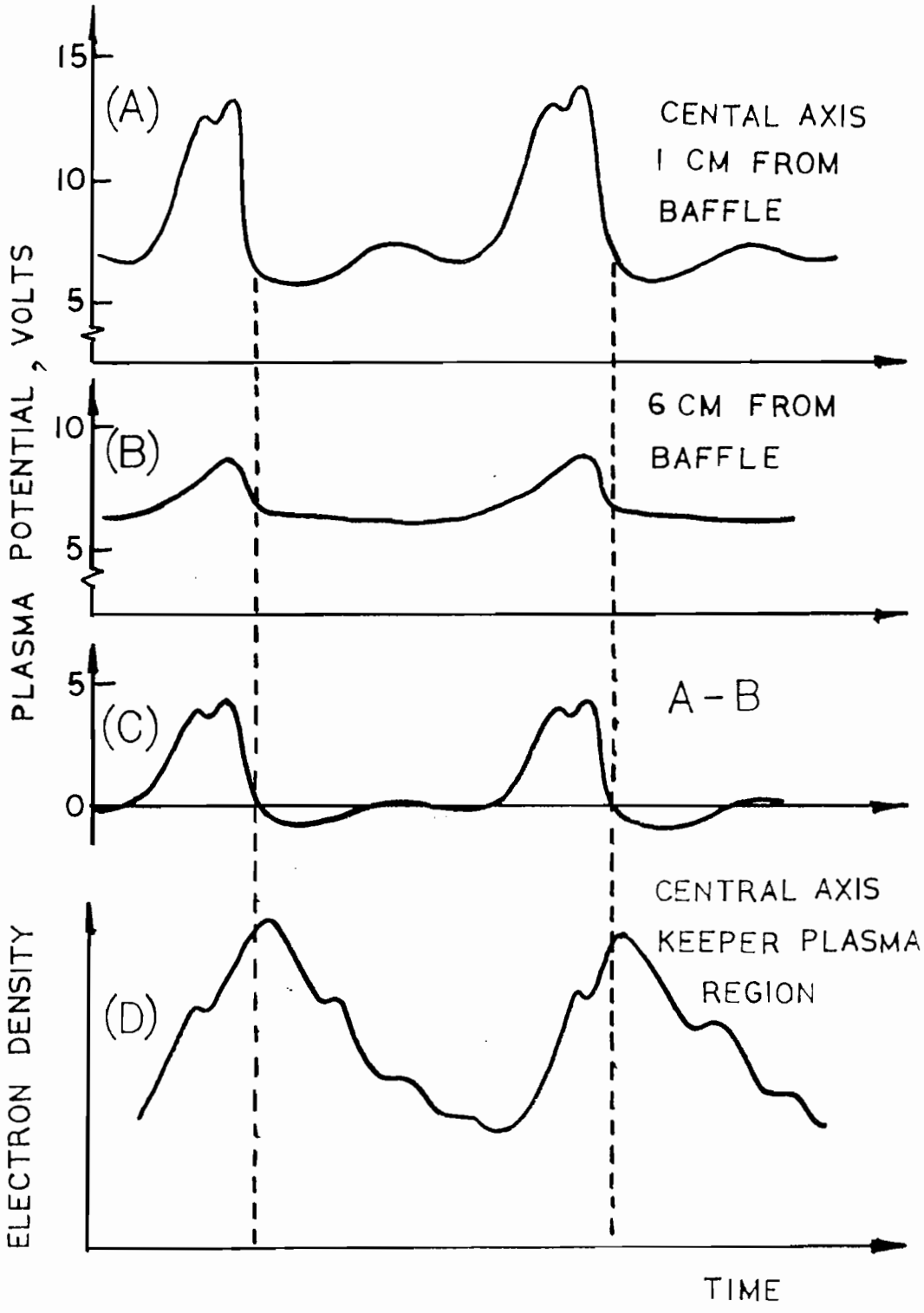

Figure 26 - Dynamic relationship between plasma potential and electron density in keeper plasma region including plasma potential difference along axis.

the electric field reaches a positive maximum. This roughly corresponds to the point in time when the field reverses polarity. This makes some sense, because one would expect the electron density to build up as long as the electric field is positive. (3) The potential increases from about 6.5 to 9.0 volts in front of the cathode during the period of positive electric field. The hollow cathode is generally operated in a space charge limited mode; therefore, a minor increase in the plasma potential can cause the emission current to increase dramatically; i.e., about 60% in this case. In addition, such an increase in potential may lower the work function of the cathode by the Schottky effect. Consequently, more electrons are emitted from the cathode and a larger current can be drawn before the emission limit is reached. It should be noted that in the space charge limited case the low energy component of the emitted electrons are repelled back to the emitting surface.

The data in Figure 26 shows that a large electron current is drawn from the cathode during the relatively short period of time when the electric field is positive. This is apparently followed by a buildup of electron space charge near the baffle region which temporarily causes a reversal in the electric field. This essentially stops the flow of electrons from the cathode to the baffle along the axis. The electron density along the axis drops slowly after it reaches its maximum; therefore, it might be surmised that the electrons diffuse radially and move towards the cathode during this period.

Figure 27 shows the relationship between the electric field along the axis of the keeper plasma and the arc current and voltage respectively. Like the electron density, the arc current reaches a maximum just about when the elecric field reverses polarity. In addition, the minimum arc

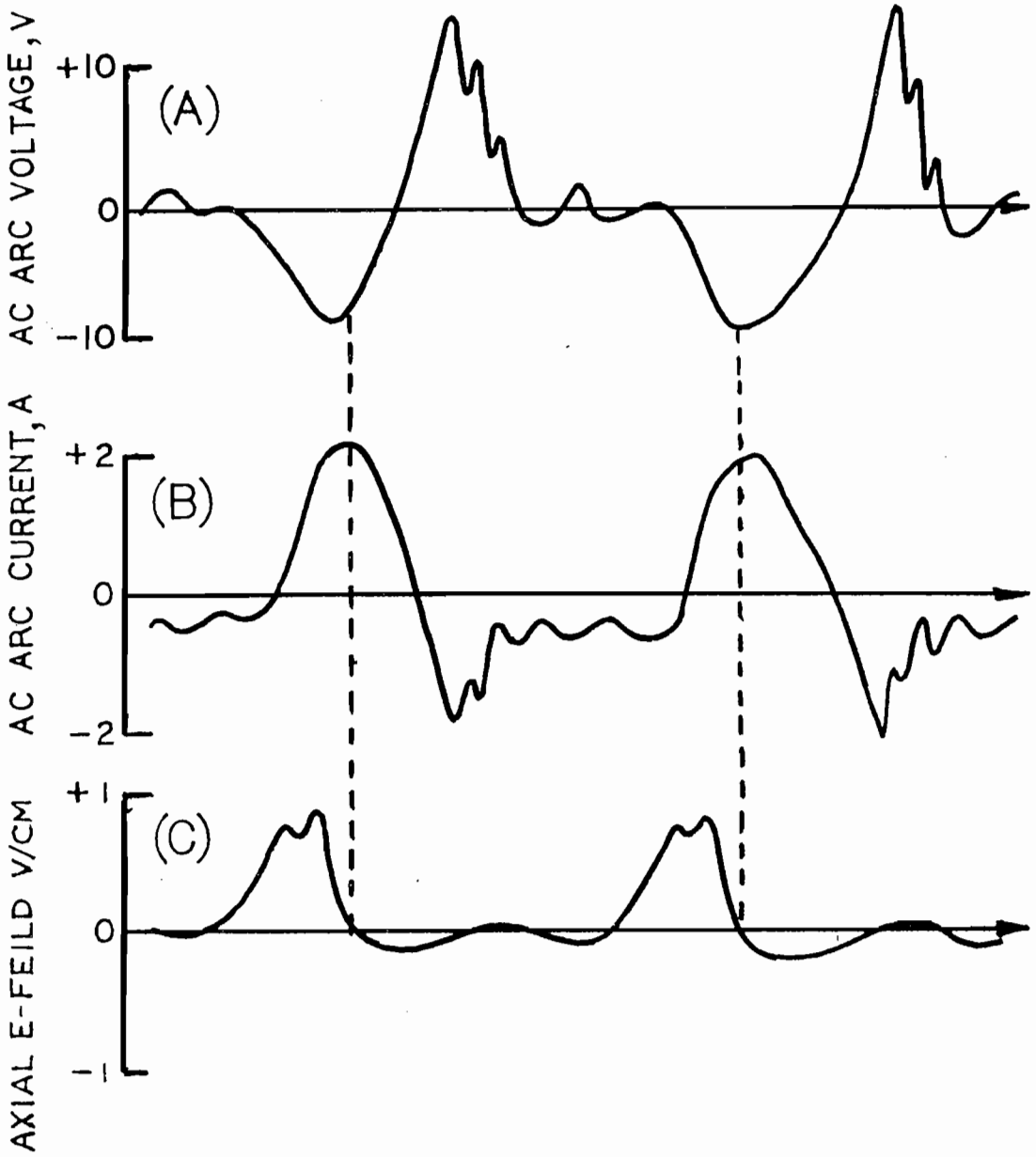

Figure 27 - Dynamic relationship between the arc current, arc voltage, and axial electric field in keeper plasma region.

current occurs approximately when the reverse process takes place. These points are shown on the figure with dashed lines. Finally, the most striking feature of Figure 27 is the fact that the arc current and arc voltage fluctuations are 180° out-of-phase with respect to each other.

From the features just described, it is believed that the hollow cathode ion thruster discharge may be acting like a simple triode, where the space charge fields within the keeper plasma region act as a control grid for the electron current extracted through the aperture. The current regulator in the power supply is not designed to respond to rapid changes such as these fluctuations. Consequently, the power supply appears to be a constant voltage source with a constant series resistor; i.e., the current regulator. In this case, an increase in the arc current would be expected to be accompanied by a proportional decrease in arc voltage; i.e., 180° out-of-phase.

Summary and Statement of the Problem

To summarize, the fluctuation frequency increases with decreasing keeper discharge chamber length and the electron temperature is at a level such that the calculated value of the longitudinal ion acoustic resonant frequency is of the same order as the observed fluctuation frequency. In addition, the arc current fluctuations are coupled to the electron density in the keeper region which is apparently controlled by space charge electric fields within that region. Consequently, it appears that the keeper plasma region is subjected to a rapid increase ("pulse") in the electric field followed by a period of relaxation before the next "pulse." The question is - what causes the pulse in the first place?

The status immediately before the "pulse" is the following: (1) The arc current and arc voltage are essentially constant (presumably close to

their DC average values). (2) The electric field along the axis is approximately constant and near zero. (3) The electron density at the aperture is at some low but approximately constant value. (4) The electron density at the center of the keeper plasma region is dropping slowly at a constant rate.

Thus, the only apparent change in the plasma characteristics before the "pulse" is the decreasing density at the center of the keeper plasma region. Then, for some unknown reason, the plasma potential suddenly rises causing an increase in emission current, etc. It is also assumed that the time between "pulses" is inversely related to the length of the keeper plasma region and that the dynamics are somehow related to the ion acoustic wave motion. With these characteristics in mind, it is now possible to propose a hypothesis which accounts for these fluctuations. This is the subject of the next chapter.

IV. PROPOSED FLUCTUATION MECHANISM

A mechanism will be proposed in this chapter to account for the plasma fluctuations commonly observed in ion thrusters equipped with hollow cathodes. The development of this theory will be divided into four parts. First, a general overview will be presented which will describe the plasma fluctuation mechanism and its affect on the plasma dynamics as a whole in the thruster. Second, the dispersion equation for the region of interest in the ion thruster plasma will be developed and the conditions required for instability will be given. Third, an expression will be derived for the fluctuation frequency based on the proposed mechanism. Finally, the theoretically predicted frequency will be compared with the experimentally measured values.

Background

It has been shown in Chapter III that the plasma potential fluctuations in the main discharge and the keeper plasma region are approximately 180° out of phase with respect to each other. It is also known[44,52] that the transition between these two plasma regions usually takes place near the baffle aperture. It has been found that a major part of this transition occurs over a distance of approximately one centimeter. Consequently, the plasma fluctuations have a dramatic effect on the potential difference across the transition plasma region, which changes from a few volts up to about 30 volts during a single fluctuation cycle.

Some of the electrons in the keeper plasma region are accelerated through the transition region into the main discharge chamber. At the same time, some ions from the main discharge plasma are accelerated back

into the keeper plasma region. The ions which enter the keeper plasma through the aperture have a kinetic energy equal to the voltage drop across the transition region; i.e., they constitute a monoenergetic ion beam. A cross section of the hollow cathode ion thruster is shown in Figure 28. This figure shows the direction and relative magnitude of the velocity vectors for the ions and electrons in different parts of the ion thruster. The lower part of Figure 28 shows the plasma potential distribution along the dashed line passing through the aperture in the cross section.

It was also shown in Chapter III that the arc voltage is 180° out-of-phase with the arc current and that the arc voltage reaches its minimum value during a sharp rise (pulse) in the arc current. The phase relationship is believed to be caused by the voltage drop across the current regulator in the main discharge power supply. These facts set the stage for explaining the plasma fluctuation mechanism.

Proposed Plasma Fluctuation Mechanism

It is proposed that an ion acoustic wave is launched at the interface between the transition plasma and keeper plasma region during the "pulse" in the arc current; i.e., when the voltage drop across the transition region is at a minimum. The ion acoustic wave is believed to be caused by so-called ion beam-plasma instability condition which takes place when the ions passing through the transition region are accelerated to a velocity approximately equal to the ion acoustic velocity in the keeper plasma region. It will be shown that the ion energy required for instability is only a few electronvolts; consequently, the voltage drop across the transition region must drop to within a certain range to drive the instability.

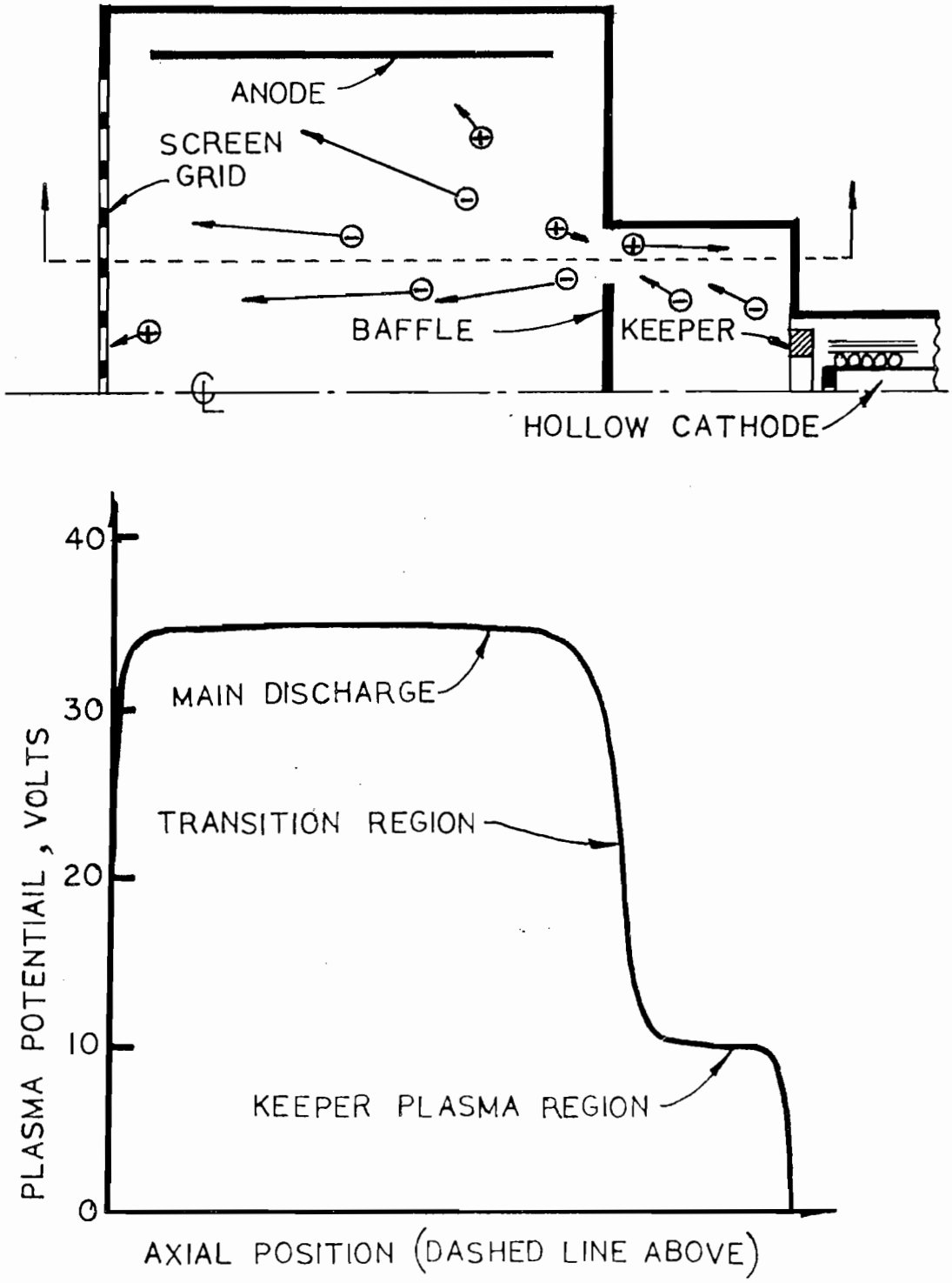

Figure 28 - Cross section of hollow cathode ion thruster showing plasma potential distribution along dashed line.

It is also proposed that the ion acoustic wave moves from the transition-keeper plasma interface to the region of the hollow cathode. Furthermore, the ion acoustic wave is believed to interact with the hollow cathode in such a way as to produce the next arc current "pulse," thus causing a repitition of the cycle.

In Chapter III it was shown that the pulse in the arc current is momentarily preceeded by an increase in the keeper plasma potential which is believed to cause an increase in electron emission from the cathode. The nature of the interaction between the ion acoustic wave and the hollow cathode which produces such a rise in potential is not clearly understood. However, there are several possibilities.

(1) The ion acoustic wave may induce some type of "instantaneous" feedback mechanism between the cathode and the transition plasma region causing the interface to move into the keeper plasma region, producing a rise in the plasma potential in that region. The word "instantaneous" implies that the time is very short compared to the period of the fluctuation. Such feedback mechanisms might include electrostatic waves or electron transport. This type of feedback mechanism has been proposed by Fujita[53] to explain an observed self-oscillation phenomenon in an ion beam-plasma system where wave reflections were not possible, i.e., standing waves were not observed. Additional observations of an "instantaneous" feedback mechanism have been reported by Alport and D'Angelo[54] for an ion beam-plasma system similar to that used by Fujita.

(2) Ion acoustic waves are composed of alternate planes of compressed and rarefied ions which are continuously reversing

roles due to the presence of electric fields. Electrons are carried along with the wave and substantially quench the oscillating space charge electric fields. However, if the ion acoustic wave moves into a region where the potential is rapidly decreasing, then the ions and electrons will part company. Specifically, if the ion acoustic wave enters the region between the keeper electrode and the interior of the hollow cathode, then the ion acoustic wave will transform into planar ion bunches. Consequently, these ions may cause an increase in the plasma potential in the entire keeper plasma region by virtue of the additional positive space charge added to the cathode fall region.

Fluctuations in the keeper plasma region produce changes in the electron density and plasma potential at the baffle aperture and consequently will modulate the energy and density of the electrons entering the main discharge plasma. These electrons acquire an energy in the range of 5 to 30 electronvolts and therefore are capable of communicating any disturbance at the baffle aperture throughout the main discharge within a period of a few tenths of a microsecond. However, the period of the fluctuation in the keeper region is typically on the order of 100 microseconds (10 kilohertz). Thus plasma potential or electron density fluctuation measurements taken within the main discharge would appear to be in phase with each other. In other words, it would appear that the main discharge responds instantaneously to fluctuations in the keeper plasma.

It has been shown in previous chapters that the magnitude of the observed fluctuations of various thruster parameters can be substantial in

comparison with the average values. This implies that the dynamics occuring within the plasma are essentially nonlinear in character. However, in several similar cases,[55-57] linear kinetic theory has been used and proved very successful in predicting the general behavior of an ion beam-plasma system. In the following, it will be shown that essentially the same results can be derived by a simpler method, i.e., the linearized fluid theory. The analysis will begin with a general derivation of the linearized equation of motion and continuity using Fourier techniques. These equations shall then be applied separately to the three species involved, i.e., electrons, plasma ions, and beam ions, to produce an expression for the density fluctuations. This will in turn be substituted into the linearized Poisson equation and solved for the dispersion equation. This type of analysis, and the graphical method used to find the roots of the dispersion relation, are very similar to an approach which has been used to analyze the electron two-stream instability.[58]

Analysis of Ion Beam-Plasma System

In linear analysis, a changing quantity can be separated into two parts: an "equilibrium" part indicated by the subscript 0, and a "perturbation" part indicated by a subscript 1. For example, the density of the jth species can be represented by:

$$N_j = N_{j0} + N_{j1} \quad , \quad M^{-3} \tag{8}$$

In addition, any periodically changing quantity can be decomposed by Fourier analysis into a superposition of sinusoidal oscillations with different frequencies and wavelengths. The "perturbed" quantity is

usually expressed in exponential form. For example, the density perturbation is given by:

$$N_{j1} = \bar{N}_{j1} \exp\left[i(Kx - \omega t)\right] \quad , \quad M^{-3} \tag{9}$$

where $\bar{N}_{j1}$ is the magnitude of the density perturbation, k is the propagation constant (or wave number), and ω is the frequency in radians. This is used with the convention that the real part of the expression is the measurable quantity. Similar expressions can be given for the electric field and the velocity of each species.

The main advantage of using the Fourier technique is that the equations containing space and time derivatives can be reduced to simple algebraic expressions. For example, the density gradient is given by:

$$\nabla N_j = \frac{\partial}{\partial x}\left[N_{jo} + N_{j1}\right] = \frac{\partial}{\partial x}\left[N_{j1}\right] = iKN_{j1} \quad , \quad M^{-4} \tag{10}$$

Where it is noted that the gradient of the equilibrium term is zero. In a similar fashion, the time derivative of velocity is:

$$\frac{\partial V_j}{\partial t} = \frac{\partial}{\partial t}\left[V_{jo} + V_{j1}\right] = \frac{\partial}{\partial t}\left[V_{j1}\right] = -i\omega V_{j1} \quad , \quad M\,S^{-2} \tag{11}$$

The equation of motion for the jth species is given by:

$$M_j N_j \left[\frac{\partial V_j}{\partial t} + (V_j \cdot \nabla) V_j\right] = Q_j N_j E - \nabla P_j = -Q_j N_j \nabla\phi - \gamma_j K_b T_j \nabla N_j \quad , \quad N\,M^{-3} \tag{12}$$

where: M_j = mass of jth species, kilogram

N_j = number density of jth species, meter^{-3}

V_j = velocity of jth species, meters second^{-1}

ϵ_o = permittivity of free space, 8.85×10^{-12} Farad m^{-1}

E = electric field, Volts $meter^{-1}$

P_j = partial pressure of jth species, Newton $meter^{-2}$

Q_j = charge of jth species, Coulombs

ϕ = electric potential, Volts

γ_j = reversible polytropic process exponent for the jth species

k_b = Boltzmann's constant, 1.38×10^{-23} Joules °$Kelvin^{-1}$

T_j = temperature of jth species, °Kelvin

e = electron charge, 1.60×10^{-19} Coulombs

The final expression on the right hand side of Equation (12) has been developed using the assumptions that;

$$E = -\nabla\phi \quad , \quad VM^{-1} \tag{13}$$

and $$\nabla P_j = \gamma_j K_b T_j \nabla N_j \quad , \quad NM^{-3} \tag{14}$$

where the later can be derived from the equation of a reversible polytropic process;

$$P_j = C\left[N_j\right]^{\gamma_j} \quad , \quad NM^{-2} \tag{15}$$

where C is a constant. The polytropic process exponent, γ_j, is equal to the ratio of specific heats for an isentropic process and unity for an isothermal process.

Application of the process of linearization to the equation of motion gives;

$$M_j N_{jo}\left[-i\omega V_{j1} + iKV_{jo}V_{j1}\right] = -iKQ_j N_{jo}\phi_1 - iK\gamma_j K_b T_j N_{j1} \quad , \quad NM^{-3} \tag{16}$$

where the products of "perturbation" terms are assumed to be small and are therefore neglected.

The equation of continuity for the jth species is given by;

$$\frac{\partial N_j}{\partial t} + \nabla\cdot\left[N_j V_j\right] = \frac{\partial N_j}{\partial t} + N_j\cdot\nabla V_j + V_j\cdot\nabla N_j = 0 \tag{17}$$

which can be linearized to give;

$$-i\omega N_{j1} + iKN_{j0}V_{j1} + iKV_{j0}N_{j1} = 0 \tag{18}$$

The expression for Poisson's equation is given by;

$$\nabla\cdot\vec{E} = (e/\epsilon_0)\left[N_{i1} - N_{e1}\right] \tag{19}$$

where the subscripts i and e are for the ion and electron species respectively.

The assumption was made here that the "equilibrium" ion and electron densities are equal and that only the "perturbation" terms may differ; therefore, they are the only terms necessary to consider. The left hand side can be linearized as follows:

$$\nabla\cdot E = \frac{\partial}{\partial x}\left[E_0 + E_1\right] = \frac{\partial}{\partial x}\left[E_1\right] = iKE_1 = -iK\nabla\phi_1 = -i^2K^2\phi_1 = K^2\phi_1 \tag{20}$$

Thus the linearized Poisson equation is given by:

$$K^2\phi_1 = (e/\epsilon_0)\left[N_{i1} - N_{e1}\right] \tag{21}$$

The Dispersion Equation of the Ion Beam-Plasma System

The derivation of the dispersion equation begins with the following definitions:

N_b = ion beam density = $N_{b0} + N_{b1}$

N_p = plasma ion density = $N_{p0} + N_{p1}$

N_i = total ion density = $N_b + N_p$

$\frac{N_b}{N_i}$ = ion beam fraction = α

thus; $N_b = \alpha N_i$; $N_p = (1 - \alpha) N_i$;

V_b = ion beam velocity = $V_{b0} + V_{b1}$

V_p = plasma ion velocity = $V_{p0} + V_{p1} = V_{p1}$

where the "equilibrium" plasma ion velocity is zero for all intents.

In the following derivation, the plasma and ion beam temperature have been set equal to zero because they would complicate the algebra considerably and, in the final analysis, have little effect on the results providing the ratio of the electron temperature to the ion temperature is greater than a factor of 5. Lower temperature ratios change the dispersion relation sufficiently enough to prevent the growth of the instability.[55] The temperature ratio in the keeper plasma region of the ion thruster is typically around 20.

Thus, assuming that the temperature of the beam ions is zero, the linearized equation of motion for the beam ions is:

$$M_i N_{bo}\left[-i\omega V_{b1} + iKV_{bo}V_{b1}\right] = -iKeN_{bo}\phi_1 \tag{22}$$

where the mass of beam ions and plasma ions is M_i. This equation reduces to:

$$V_{b1} = \left(eK\phi_1\right) / \left[M_i\left(\omega - KV_{bo}\right)\right] \tag{23}$$

Using the definitions above, the linearized equation of continuity for the beam ions is:

$$-i\omega N_{b1} + \alpha N_{io} iKV_{b1} + iKV_{bo} N_{b1} = 0 \tag{24}$$

which can be rearranged to give the following expression for N_{b1}:

$$N_{b1} = \frac{\alpha N_{io} KV_{b1}}{(\omega - KV_{bo})} \tag{25}$$

Combining this with Equation (23) gives:

$$N_{b1} = \frac{\alpha N_{io} K^2 e\phi_1}{M_i(\omega - KV_{bo})^2} \tag{26}$$

Assuming the temperature of the plasma ions is zero, the linearized equation of motion for the plasma ions is given by:

$$M_i N_{po}\left[-i\omega V_{p1}\right] = -iKeN_{po}\phi_1 \tag{27}$$

where the "equilibrium" plasma ion velocity is zero. The above equation reduces to:

$$V_{p1} = \frac{eK\phi_1}{M_i\omega} \tag{28}$$

Again, assuming that V_{p0} equals zero, the linearized equation of continuity for the plasma ions is given by:

$$-i\omega N_{p1} + (1-\alpha)N_{io} iKV_{p1} = 0 \tag{29}$$

which reduces to:

$$N_{p1} = \frac{(1-\alpha)N_{io} KV_{p1}}{\omega} \tag{30}$$

Combining this with Equation (28) yields:

$$N_{p1} = \frac{(1-\alpha)N_{io} K^2 e\phi_1}{M_i\omega^2} \tag{31}$$

Finally, the total ion density perturbation term can be found by combining Equations (26) and (31) to get;

$$N_{i1} = \frac{N_{io} K^2 e \Phi_1}{M_i} \left[\frac{\alpha}{(\omega - K V_{bo})^2} + \frac{(1-\alpha)}{\omega^2} \right] \tag{32}$$

The frequency of the fluctuations in the ion thruster is small in comparison to the electron plasma frequency. In such cases, the inertial term in the electron equation of motion can be set to zero which reduces the expression to a simple balance between the electric potential and the electron thermal energy as follows;

$$M_e N_{eo} \left[-i\omega V_{e1} + iK V_{eo} V_{e1} \right] = -iK(-e) N_{eo} \Phi_1 - iK \gamma_e K_b T_e N_{e1} \tag{33}$$

which reduces to:

$$N_{e1} = \frac{N_{eo} e \Phi_1}{K_b T_e \gamma_e} \tag{34}$$

where it has been assumed that the electrons are so mobile that their heat conductivity is almost infinite, i.e., the electron thermal speed is much higher than the phase velocity of the wave. Thus for isothermal electrons $\gamma_e = 1$.

Using Equations (32) and (34) the linearized Poisson equation becomes:

$$K^2 \Phi_1 = (e/\epsilon_o) \left[\frac{N_o K^2 e \Phi_1}{M_i} \left(\frac{\alpha}{(\omega - K V_{bo})^2} + \frac{(1-\alpha)}{\omega^2} \right) - \frac{N_o e \Phi_1}{K_b T_e} \right] \tag{35}$$

where it is assumed that $N_{i0} = N_{e0} = N_0$.

Equation (35) can be manipulated to give:

$$\left[\frac{N_o e^2}{\epsilon_o K_b T_e} \right] K^2 \left(\frac{K_b T_e}{M_i} \right) \left[\frac{\alpha}{(\omega - K V_{bo})^2} + \frac{(1-\alpha)}{\omega^2} \right] = K^2 + \left[\frac{N_o e^2}{\epsilon_o K_b T_e} \right] \tag{36}$$

Using the definition of the Debye length:

$$\lambda_D = \left[\frac{K_b T_e \epsilon_o}{N_o e^2}\right]^{1/2} \tag{37}$$

and the ion acoustic frequency:

$$\omega_s = KV_s = K\left(\frac{K_b T_e}{M_i}\right)^{1/2} \tag{38}$$

Equation 36 can be simplified to give:

$$\omega_s^2\left[\frac{\alpha}{(\omega - KV_{bo})^2} + \frac{(1-\alpha)}{\omega^2}\right] = K^2\lambda_D^2 + 1 \tag{39}$$

which is the dispersion equation for the ion beam-plasma system.

The propagation constant k can be assumed to be on the order of L^{-1} where L is the characteristic dimension of the plasma. In the case of the keeper plasma region the Debye length is approximately 10^{-6} meters and the propagation constant is on the order of 10 meters^{-1}; therefore, $k^2\,D^2$ is much less than one and Equation (39) becomes:

$$\omega_s^2\left[\frac{\alpha}{(\omega - KV_{bo})^2} + \frac{(1-\alpha)}{\omega^2}\right] = 1 \tag{40}$$

which is the appropriate form of the dispersion equation for the keeper plasma region of an ion thruster.

Graphical Method of Solving Dispersion Equation

The above equation has four roots. Two of the roots are always real. The remaining two may be real or complex conjugates. Equation (40) can be solved graphically for all of the real roots, i.e., two or four as the case may be. If only two real roots exist, then the complex conjugates can be found in a straight-forward manner using the values of the two real roots.

The graphical solution of Equation (40) is simplified by first normalizing the frequency, ω and the product kV_{bo} with respect to the ion acoustic frequency ω_s. Thus we define the normalized frequency as:

$$X = \frac{\omega}{\omega_s} \tag{41}$$

and the normalized ion beam velocity:

$$Y = \frac{KV_{bo}}{\omega_s} \tag{42}$$

which simplifies Equation (40) to the following:

$$\frac{\alpha}{(X-Y)^2} + \frac{(1-\alpha)}{X^2} = F(X,Y) = 1 \tag{43}$$

where F(x,y) represents the left hand side of the equation. In most cases, the four roots can be found directly by plotting F(x,y) as a function of x for selected values of α and y and by determining the value of x when F(x,y) = 1. This technique is shown in Figure 29A. However, there are only two real roots for some values of y. An example of this is shown in Figure 29B. In such cases, the two remaining unknown roots are complex conjugates which can be easily calculated using the two known real roots and the value of y. In this case, the real part of the complex number is given by

$$R = Y - \left(\frac{r_1 + r_2}{2}\right) \tag{44}$$

where r_1 and r_2 are the two real roots which were determined graphically. The imaginary part of the complex number is given by

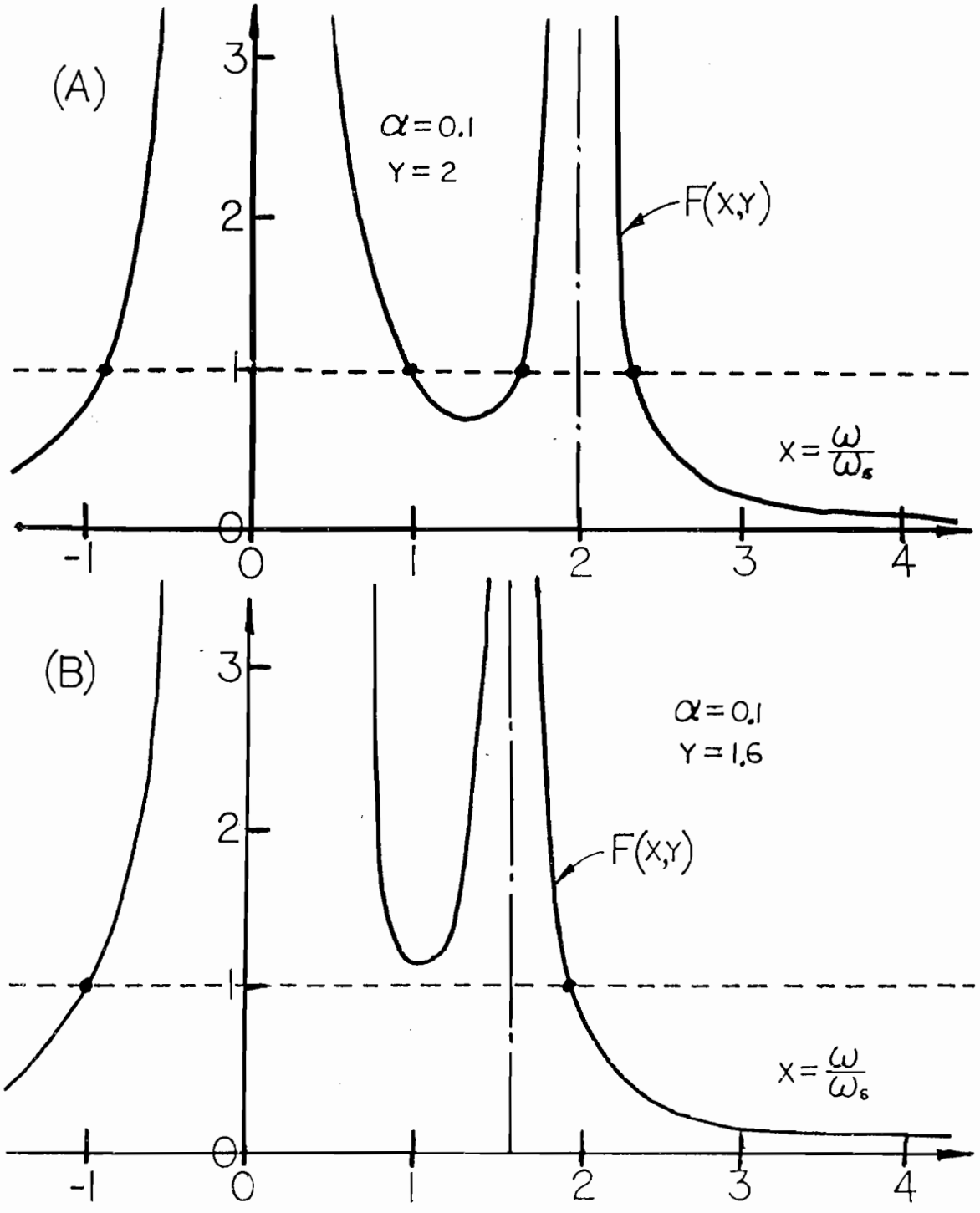

Figure 29 - F(x,y) as a function of the non-dimensional frequency x for (A) y = 2 (4-real roots) and (B) y = 1.6 (2 real roots, 2 complex conjugate roots).

$$I = \left(\gamma^2 - 1 - R^2 - 2R(r_1 + r_2) - r_1 r_2\right)^{1/2} \tag{45}$$

The Dispersion Equation for the Keeper Plasma Region

The value of α, the ion beam fraction, must first be determined for the keeper plasma region before the roots of the dispersion equation can be found. The procedure for finding α, is given in the following.

The density of the ion beam entering the keeper plasma region from the main discharge can be estimated by the following relation for continuity through the transition region,

$$N_b = N_+ \left(\frac{\epsilon_i}{\epsilon_i + \Delta V}\right)^{1/2} \tag{46}$$

where ϵ_i is the mean energy of ions approaching the transition region from the main discharge. N_+ is the ion density in the main discharge, and ΔV is the voltage drop across the transition region. If N_i is the total ion density in the keeper plasma region, then α, the ion beam fraction is,

$$\alpha = \frac{N_b}{N_i} = \frac{N_+}{N_i}\left(\frac{\epsilon_i}{\epsilon_i + \Delta V}\right)^{1/2} \tag{47}$$

The value of ϵ_i should obey the modified Bohm sheath criterion,[59]

$$\epsilon_i \geq \frac{K_b T_{em}}{2e}\left(\frac{N_+}{N_{em}}\right) = \frac{K_b T_{em}}{2e}\left(\frac{N_+}{N_+ - N_{ep}}\right) \tag{48}$$

where T_{em} and N_{em} are the Maxwellian electron temperature and density respectively in the main discharge, e is the charge on the ion, k_b is the Boltzmann's constant, and N_{ep} is the primary electron density in the main discharge. The final expression on the right-hand side of Equation (48) was derived using the equality:

$$N_+ = N_{em} + N_{ep} \tag{49}$$

When ΔV is much greater than ϵ_i, Equations (48) and (49) can be combined to give the following approximate value for α:

$$\alpha \simeq \frac{N_+}{N_i}\left(\frac{\epsilon_i}{\Delta V}\right)^{1/2} = \frac{N_+}{N_i}\left[\frac{K_b T_{em}}{2e\Delta V}\left(\frac{N_+}{N_+ - N_{ep}}\right)\right]^{1/2} \tag{50}$$

For example, if the primary electron density, N_{ep}, in the main discharge is 10% of the total electron density (i.e., 0.1 N_+) the maxwellian electron temperature is 2eV, the ratio of the ion density in the main discharge to the ion density in the keeper discharge (N_{mi}/N_i) is 0.1, and the voltage drop through the aperture (ΔV) is 25 volts, then Equation (50) will give a value of α of about 0.02.

The roots of the dispersion equation can now be determined as a function of the normalized ion beam velocity by using the graphical procedure described above. A plot of the roots of Equation (43) is shown in Figure 30A for an ion beam fraction α of 0.02. The single negative root is not shown because it has no physical meaning. In this example, one real root and two complex congugate roots appear between y = 0 and y = 1.3. The real part of the complex root is shown by the dashed line and the magnitude of the imaginary part is shown by the dotted line. One of the complex roots has a positive imaginary part and therefore is unstable; i.e., it will grow without bound. When y is greater than 1.3 there are three distinct roots indicative of the three stable frequency modes which are possible within the plasma.

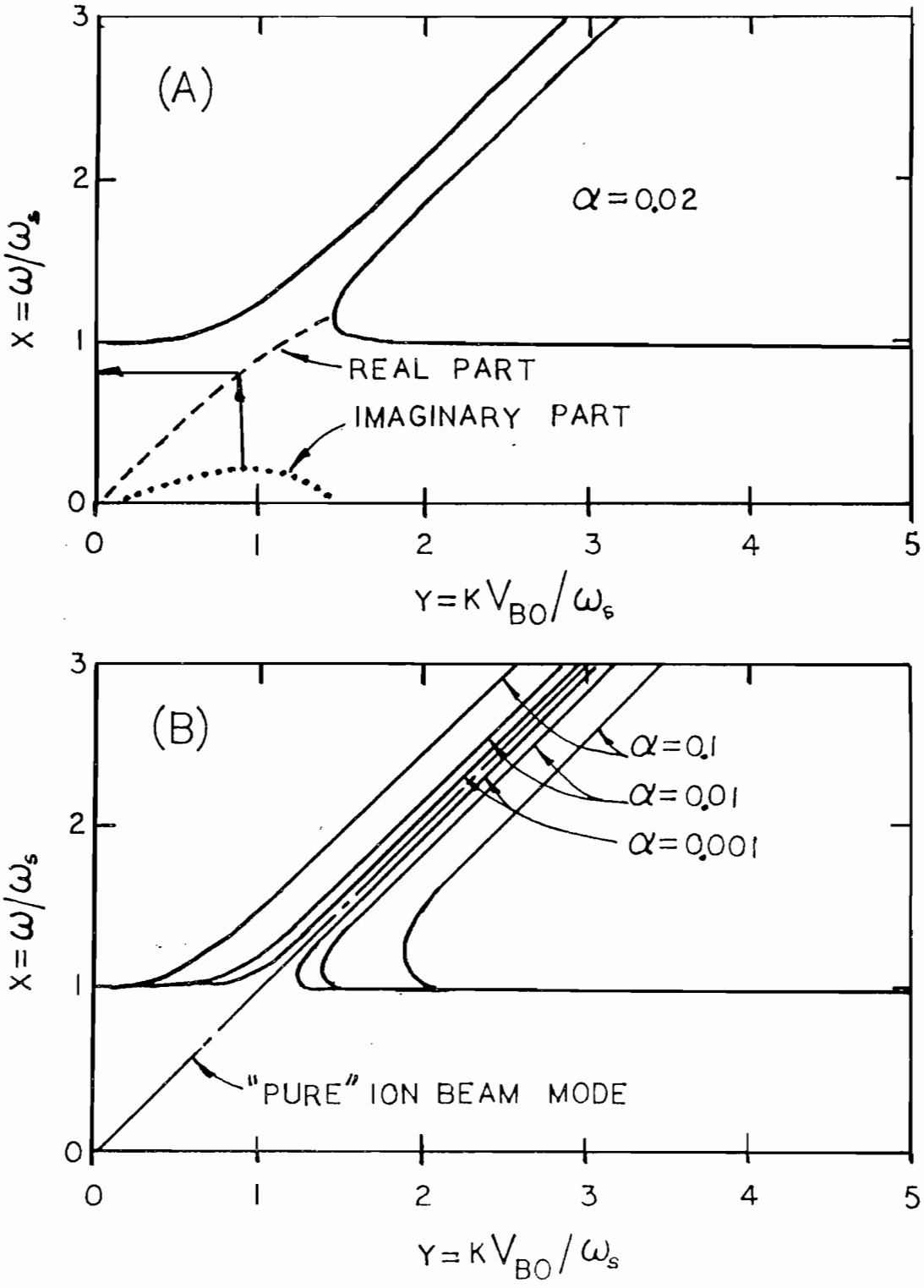

Figure 30 - Dispersion equation for ion beam-plasma system: (A) α = 0.02, showing complex roots, (B) for several values of α .

Figure 30A shows that for α = 0.02, the complex component reaches a maximum at a normalized beam velocity of about 0.9. This corresponds to the beam velocity with the highest growth rate for instability.[60] The real part of the complex frequency associated with the highest growth rate is therefore the most probable frequency to be produced if an instability commences. For the case shown in Figure 30A, the most probable instability frequency is at X = 0.8 or 0.8 times the ion acoustic frequency. The most probable frequency increases very slowly with decreasing values of the ion beam fraction, α, and approaches X = 1.0 for very small values of α. Therefore, at small α, the frequency of the instability approaches the ion acoustic frequency.

The analysis above predicted complex roots which extend down to a nondimensional beam velocity of zero. This cannot be true, because the ion beam is supposedly driving the instability. This error is a result of using the fluid equations which do not take into account a phenomenon known as Landau damping which takes place when the ion beam velocity is lower than the thermal velocity of the ions. A more exact kenetic-theory analysis[56] indicates that the lower limit for the ion beam-plasma instability occurs at a nondimensional ion beam velocity of about 0.6 for an electron to ion temperature ratio of 20 and an ion beam ratio of 0.1.

The value of y, the normalized ion beam velocity in the keeper plasma region, can be found by using the following equation:

$$Y = \frac{KV_{bo}}{\omega_s} = \frac{KV_{bo}}{KV_s} = \left(\frac{2e\Delta V}{K_b T_e}\right)^{1/2} \tag{51}$$

where ΔV is the voltage drop from the main discharge to the keeper discharge region and T_e is the electron temperature. For example, in the

keeper plasma region, the electron temperature is approximately 20,000°K and the voltage drop, ΔV, for the beam ions in the aperture is about 25 volts. This produces a value of y of about 5. Thus, for the conditions existing in the ion thruster, there are three stable frequency modes which are possible. The lowest mode is the ion acoustic frequency. The two higher frequency modes are commonly called the upper and lower ion beam mode, respectively. The difference between the upper and lower ion beam modes is twice the ion acoustic frequency when $\alpha = 1$. This difference decreases as decreases with both modes approaching the so-called "pure" ion beam mode. This characteristic is exemplified in Figure 30B which shows the dispersion equation, less the complex roots, for three different values of α.

It was shown that a typical value for y, the nondimensional ion beam velocity, in the keeper plasma region is about 5. There are three stable roots for this value; i.e., a wave will travel with the three distinct phase velocities associated with these roots. Experiments[61] have demonstrated this effect using time-of-flight measurements of a voltage pulse applied to an ion beam-plasma system. In this case, a single pulse evolved into three separate pulses traveling through the plasma at the three phase velocities associated with this state. Other measurements[56] have shown this characteristic using a voltage exciter held at a constant frequency. These measurements showed a superposition between the respective modes.

It is apparent from the above results that in the range of interest for the ion thruster; i.e., y = 5, the analysis predicts that there will

be certain effects on externally stimulated waves but does not indicate any unstable condition which would bring about a self-induced ion beam-plasma resonance. In fact, it would appear that the keeper plasma region should be stable. However, there are two mechanisms which may cause instability. These will be described in the following section.

Conditions Which May Lead to Ion-Beam Plasma Instability

There are at least two conditions in the keeper plasma which may cause an ion beam-plasma instability to develop. First, there are several processes such as charge exchange which will reduce the velocity of at least a small fraction of the ion beam coming through the aperture. The net effect of this is that a fraction ($\sim$1%) of the total ion beam will have velocities in the proper range to drive the instability. Secondly, it was shown that the voltage drop across the transition region varies during the plasma fluctuations. In fact, during part of the cycle, the voltage drop is in the range which should cause an instability. This periodic stimulus may be sufficient to maintain a resonance in the keeper plasma region. These two cases are depicted in Figure 31.

In the first case, the ion beam ratio, α, of the fraction of low energy ions with the proper velocity for instability is about two orders of magnitude lower than the value of α for the total ion beam. However, it can be shown that the growth rate for the instability (Im /Re) is reduced by only a factor of 5 for this change in the beam ratio. In the second case, it would be necessary that the temporal behavior of the plasma fluctuations would bring about a return to the low voltage drop condition across the transition region required to drive the instability periodically. This later case has been proposed as playing a role in the plasma fluctuations earlier in this chapter.

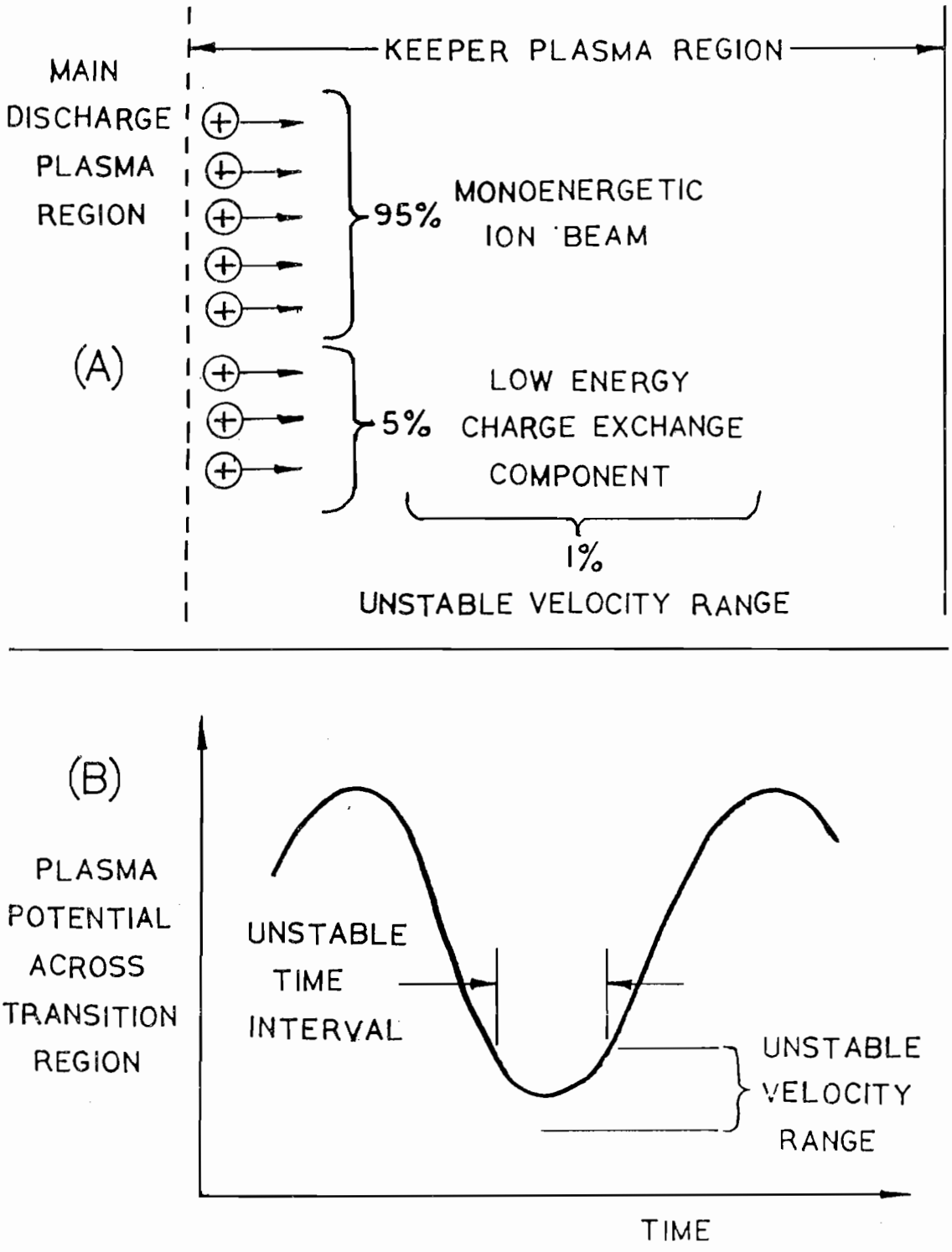

Figure 31 - Two examples of conditions in the hollow cathode ion thruster which may cause an ion beam-plasma instability.

It was mentioned that the average value of the normalized beam velocity in the keeper region is about 5, and that three stable roots exist at this condition. This general condition in the keeper plasma region would not necessarily inhibit the growth of an instability by the two processes given above. In fact, contrary to a static plasma, the ion beam-plasma system provides a medium where the wave will travel with very little attenuation at the three phase velocities associated with this state.

Ion beam-plasma experiments[53-57,60,61] have generally been conducted in plasmas which are two to three orders of magnitude lower in density than the keeper plasma region. In these cases, the ion beam-plasma conditions were produced by using a dual plasma device which is equipped with a set of fine mesh grids between the respective plasmas. The ion beam is produced by simply biasing one plasma with respect to the other. The ion beam ratio, and normalized ion beam velocity could be controlled very well in this apparatus; therefore, it was relatively easy for the experimenters to maintain and examine the behavior of waves at different ion beam-plasma conditions. However, the grids were biased in such a way to preclude the flow of electrons in the opposite direction. Therefore, these experiments differ in two ways from the conditions that exist in the ion thruster: (1) There is no transition plasma region and (2) there is no counterstreaming electron current. The lack of a transition region would eliminate the first instability mechanism proposed. The absence of a counterstreaming electron current effectively prevents the transfer of fluctuations into the second (ion beam source) plasma region. The later

effect would also preclude the possibility of a current "pulse" which was proposed to provide the feedback required to start the next fluctuation cycle.

None of the above mentioned conditions for instability have been proven experimentally. In fact, it would be very difficult to make definitive measurements in the large plasma fluctuations present in the ion thruster plasma. This would require a carefully designed experimental set-up comparable to the dual plasma device described in the last paragraph. This should be the subject of future study. The purpose of this section was to show that there are mechanisms present in the keeper plasma region which may be capable of driving an ion beam plasma instability and consequently producing an ion acoustic wave in the keeper plasma region.

Current Driven Ion Acoustic Waves

Another mechanism for driving an ion acoustic wave, briefly mentioned in Chapter II, is the electron current itself.[34,36-42] This can occur when the electron drift velocity exceeds a certain critical value which is a function of the thermal velocity of the electrons and the ratio of electron to ion temperature. There were several problems with this mechanism which will be discussed in the following.

The electron drift velocity (and the condition for instability) increases as the ratio of electric field to pressure (E/P) increases. Rough calculations indicate that this ratio is about an order of magnitude lower in the keeper plasma region than it is in transition and main discharge regions. Consequently, the electron drift velocity is also about an order of magnitude lower. In addition, the ratio of electron to ion temperature (T_e/T_i) is lower (more stable) in the keeper and

transition regions than in the main discharge. Therefore, the main discharge would appear to be more susceptable to spontaneous ion acoustic wave growth than the keeper and transition plasma regions. However, the results described in Chapter II appear to dispel the idea of ion acoustic waves in that region.

Refractory cathode ion thrusters generally operate with very stable discharges up until the magnetic field is raised above a certain critical value[17,26,28] which also corresponds to the minimum energy per beam ion extracted (eV/ion). The instability which developes in this case has been described by Cohen[26] and is not related to the ion acoustic instability. However, plasma measurements[17,19-21] in refractory cathode ion thrusters often indicate greater cause for the ion acoustic instability, i.e., higher values of (E/p) and (T_e/T_i) than that found by comparable measurements in hollow cathode ion thrusters. Therefore, it is difficult to explain why the electron drift would induce an ion acoustic instability in the hollow cathode thruster and not in the refractory cathode thruster.

In spite of this predicament, calculations do indicate that the conditions in the keeper plasma should be marginally unstable with respect to an electron drift induced ion acoustic instability. Therefore, it cannot be dismissed entirely as a possible cause. As with the ion beam induced mechanisms, the electron drift mechanism must be examined under more carefully controlled plasma conditions than are presently available with the ion thruster.

The ion beam-plasma instability mechanism is also favored because the ion beam-plasma condition is unique to the keeper plasma region of the hollow cathode ion thruster. Refractory cathodes are bombarded by ions accelerated through the sheath. However, this region is not a true

plasma, and is not bounded by physical structure such as the baffle in a hollow cathode thruster. Theory indicates[62] that cathode sheaths should be stable with respect to the ion acoustic instability. In addition, it was mentioned in Chapter III that the fluctuation frequency was often changed by the presence of Langmuir probes in the keeper plasma region. This observation is similar to that described by workers[53,54] studying the ion beam-plasma instability whereas the probe apparently establishes a new boundary condition and consequently changes the frequency.

Derivation of Expression for Fluctuation Frequency

The proposed fluctuation mechanism given earlier in this chapter was composed of a sequence of events which occur during one fluctuation period. However, the fluctuation period can be broken down into two stages; i.e., (1) the time of flight for an ion acoustic wave to move from the aperture (transition) region to the cathode, and (2) the time required for the arc current "pulse" to reach its maximum value. It was assumed that the next ion acoustic wave was launched from the transition/keeper plasma interface when the voltage drop across the transition plasma was at a minimum; i.e., when the arc current "pulse" was at a maximum. Temporal measurements of the electron density and plasma potential fluctuations in the keeper plasma region (see Figures 25-27 in Chapter III) indicate that the ion acoustic wave stage amounts to about 75% of the fluctuation period. The limited experimental data available show reasonable consistency with this 75%/25% time breakdown between the two stages over the frequency range encountered in this study. Therefore, for simplicity, it will be assumed that the total period of the fluctuation is 4/3 times the time-of-flight of the ion acoustic wave (stage one) from the aperture to the cathode.

The time-of-flight for the ion acoustic wave to move from the transition/keeper plasma interface near the aperture to the cathode is,

$$\tau_s = \frac{(L^2+R^2)^{1/2}}{V_s} \tag{52}$$

where the numerator is the diagonal distance between the two points stated, and v_s is the ion acoustic velocity as defined by Equation (38). The diagonal distance is calculated from the length of the keeper discharge chamber, L, and the radius of the opening of the aperture, R. The actual location of the double sheath at the aperture is somewhat speculative. It is known that the sheath generally protrudes back into the keeper plasma region; therefore, one would expect that the actual diagonal length will be slightly smaller than that calculated with the physical boundaries.

The period of the fluctuation would be 4/3 times the value given in Equation (52). The fluctuation frequency is the reciprocal of the period. Thus, the fluctuation frequency is given by,

$$F = \frac{3}{4}\frac{V_s}{(L^2+R^2)^{1/2}} = \frac{3}{4}\frac{(K_b T_e/M_i)^{1/2}}{(L^2+R^2)^{1/2}} \tag{53}$$

As a simple check of this equation, the data in Figure 24 (Chapter III) were replotted as a function of the inverse diagonal distance. This is shown in Figure 32. The two sets of data represent the two different keeper discharge chamber diameters used in these experiments. However, the aperture geometry was identical; therefore, the same radius was used for the opening of the aperture. The radius of the aperture opening was arbitrarily chosen to be the mean between the inner and outer radius of the aperture; i.e., 2.61 centimeters. Figure 32 includes four solid

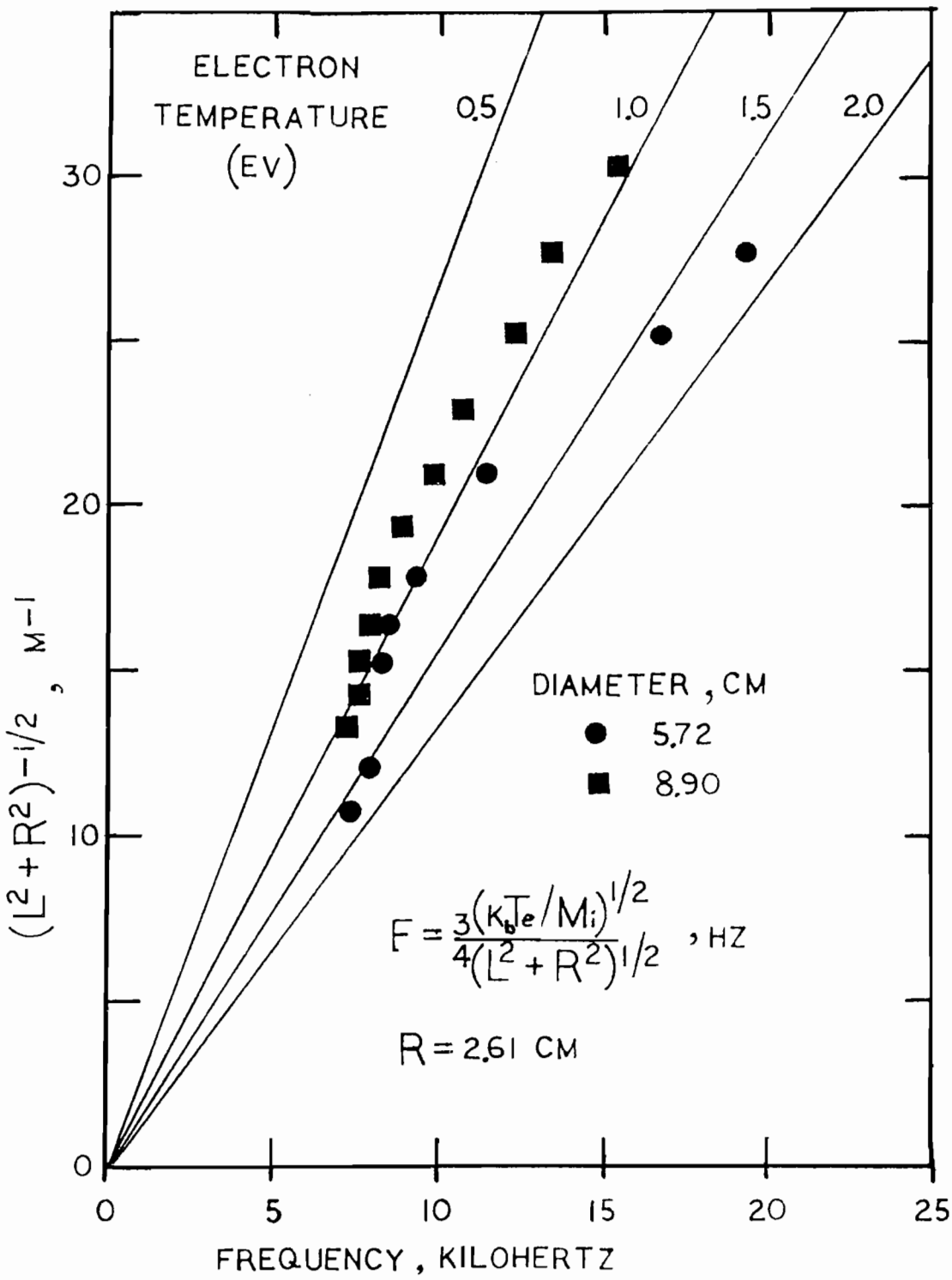

Figure 32 - Replot of data from Figure 24 as a function of the inverse distance from the aperture to the cathode.

lines which represent Equation (53) for four values of electron temperature from 0.5 to 2.0 electronvolts. The data for the large diameter case falls within a range of electron temperatue which is quite typical of those measured in the keeper plasma region. Electron temperature measurements were not available for the small chamber diameter. However, they would be expected to be about the same. Therefore, it is very likely that the effective aperture radius and the chamber lengths are smaller in this case; i.e., the double sheath protrudes farther into the keeper plasma region.

For a more exact comparison between the proposed theory and the measurements, it was necessary to take electron temperature measurements for an accurate determination of the ion acoustic velocity. However, it was mentioned in Chapter III that the presence of the probes often appeared to alter the frequency of the fluctuations. Consequently, in such cases, it was necessary to compare the fluctuation frequency, in the absence of the probes, with the electron temperature taken at the same operating point. This method was used to compare the theoretically predicted value of the fluctuation frequency, i.e., Equation (53), with the measured values. This comparison is shown in Figure 33 for the large diameter keeper chamber case for a wide variety of discharge conditions and keeper chamber lengths.

The solid line on Figure 33 represents the theoretically predicted frequency. All of the data shown in solid symbols were taken at an arc voltage of 30 volts, an arc current of 5 amperes, a magnet current of 2 amperes, and a keeper current of 1 ampere.

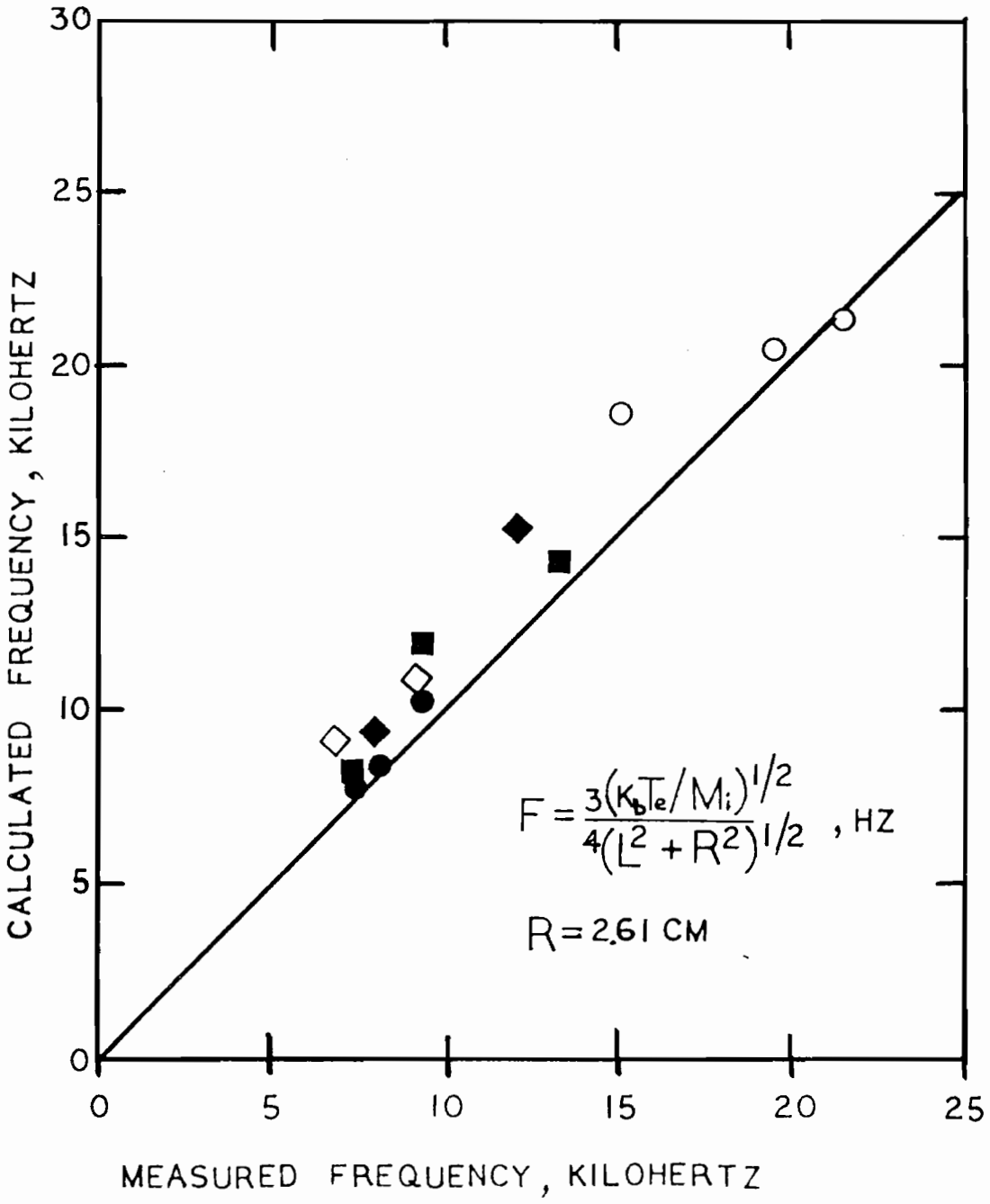

Figure 33 - Plot of frequency calculated from proposed theory as a function of the actual measured frequency.

The solid circles in Figure 33 were derived from electron temperature measurements in the center of the keeper plasma region, 1.5 centimeters from the baffle. The three points, shown in order of increasing frequency on the figure, were taken at 7, 6, and 4.5 centimeter chamber lengths respectively. These results closely parallel the predicted frequency.

The solid squares in Figure 33 represent data taken at a different time in the same location described in the last paragraph. In this case, the data were taken at chamber lengths of 7, 4, and 2.5 centimeters respectively. These results closely track the theoretically predicted frequency value.

The data represented by the solid diamonds in Figure 33 were taken at a chamber length of 6 and 3 centimeters respectively in the same location as described above. These results are in good agreement with the predicted frequency.

The open diamond symbols represent data taken at an arc voltage of 30 volts, a magnet current of 2 amperes, but with the probe located 1.0 centimeter from the baffle at the center of the keeper chamber. In this case the chamber length was held constant at 7 centimeters, and the arc and keeper currents were changed. The lower frequency (6.9 kilohertz) was measured when the arc and keeper currents were 5 and 3 amperes respectively. The higher frequency (9.2 kilohertz) was measured with the arc and keeper currents at 7 and 1 amperes respectively. These results are in reasonably good agreement with the predicted frequency.

Figure 33 also contains some data taken using the experimental test setup shown in Figure 9. The open circles represent the predicted

frequency taken from temperature measurements with the probe located at the center of the keeper plasma about 1 centimeter from the baffle. The three measurements, shown with increasing values of frequency, were taken at arc currents of 5.0, 7.5 and 10.0 amperes, respectively. The arc voltage was 25.5 v, the magnet current was 1.5 amperes, and the chamber length was fixed at 3.81 centimeters. These results are also in good agreement with the predicted frequency.

Discussion of Results

The comparison betwen the theoretically predicted frequency and the measured frequency in Figure 33 indicates that the proposed fluctuation mechanism concept is reasonable. The predicted frequency, on average, was slightly higher than the measured frequency by about 10%. However, the predicted frequency closely parallels the measured frequency over a wide range of discharge conditions and keeper chamber length. These results are therefore considered as strong evidence as to the validity of the proposed theory.

The fluctuation frequency was observed to increase slightly when the arc current was increased. Langmuir probe measurements indicated a small increase in the electron temperature in the keeper plasma region which apparently is sufficient to account for the increased fluctuation frequency. A similar increase in frequency is seen when the arc voltage is increased. This is also believed to be caused by an increase in the electron temperature. However, the relationship between the arc voltage and the temperature were not directly evaluated in this series of experiments because the changes in the frequency spectra were more complex (see Figure 12). Physically, it seems reasonable to expect that an increase in the arc current or the arc voltage will increase the amount of

energy transferred (joule heating) to the electron population. Hence, a rise in the electron temperature (and fluctuation frequency) would be expected.

There was no attempt at changing the length and diameter of the main discharge chamber during this series of experiments. It was concluded that the discharge chamber geometry was not related to the fluctuation frequency. This conclusion was made on the basis of extensive plasma measurements within the main discharge region. First, after due consideration to several types of fluctuation mechanisms, it was found that the ion acoustic resonance frequency was the only candidate close enough to the measured frequency to be considered. However, the predicicted frequency was a factor of 2 or 3 times lower than the measured frequency. Secondly, changes in the arc current and arc voltage did not affect the electron temperature in the main discharge region sufficiently enough to justify the change in the measured frequency. Finally, the discovery of a relationship between the length of the keeper discharge chamber and the frequency obviated the requirement to test the effects of the main discharge dimensions on the fluctuation frequency.

The bell-jar ion source experimental results were found to be different from the previous ion thruster tests in one respect. The fluctuation frequency increased significantly when the magnetic field intensity was increased in the ion thruster, but had no effect on the fluctuation frequency in the bell-jar ion source. The magnetic field in both ion sources has a strong effect on the dynamics of the electrons; consequently, it is believed that the position of the interface between the transition and keeper plasma regions is affected by the magnetic field shape and strength. Thus, the distance between the double sheath and the

cathode, i.e., the distance traveled by the ion acoustic wave, would be affected by the magnetic field.

The JPL 20-centimeter ion thruster was equipped with a magnetic pole piece. The field line distribution for such a configuration has been shown[20,44] to commence at the inside wall of the pole piece and follow a path radially inward and axially downstream. Field lines originating at the back end of the pole piece generally pass through the baffle. The so-called "critical field line" is an expression which was coined to describe the field line which passes the edge of the baffle. It is postulated that the double sheath boundary moves into the keeper plasma region, i.e., closer to the cathode, as the magnetic field strength is increased. Therefore, the distance traveled by the ion acoustic wave would be reduced as the magnetic field is increased which would produce an increase in the frequency. This type of behavior would not be expected to occur in the bell-jar ion source because the magnetic field is uniformally axial; consequently, the double sheath might be expected to expand back from the aperture, parallel to the axis. However, such a change would have to be compensated by a reduction in the electron temperature in order to keep the time of flight of the ion acoustic wave constant. These types of measurements have not been made; therefore this is speculation at this time.

Serafini also observed[50] a similar effect with the Hughes 30-centimeter thruster which was equipped with a hollow cathode and a magnetic baffle. The magnetic baffle is a specially designed magnetic circuit which controls the position and the field strength of the "critical field line." Serafini found that the fluctuation frequency

increased when the magnetic baffle current was increased. This is believed to be a manifestation of the same effect described above.

Suggestions for Future Work

The results shown in Figure 33 is strong evidence that the plasma fluctuations in ion thrusters equipped with hollow cathodes is caused by the presence of an ion acoustic wave generated in the keeper plasma region. However, there are many detailed questions left unanswered. For example, earlier in this chapter it was pointed out that the instantaneous feedback which sets the stage for the next "pulse" is not clearly understood. In addition, there were suggested reasons given for the effects of changes in the keeper chamber geometry and the magnetic field on the fluctuation frequency, but these have yet to be proven experimentally. These types of questions will require carefully designed experiments to resolve. Such experiments may lead to a better understanding of the keeper/transition plasma region and to a thruster design which eliminates the fluctuations all together.

V. CONCLUSIONS

An investigation was made to determine the source of certain electrical fluctuations which have been observed in the main discharge of an ion thruster utilizing a hollow cathode. It was experimentally determined that the fluctuations were produced by a cyclic disturbance in the keeper plasma region. This in turn modulated the electron current flow going into the main discharge, producing large fluctuations in the arc voltage and arc current. The cyclic disturbance in the keeper plasma region is believed to be caused by the presence of an ion acoustic wave. It was proposed that the ion acoustic wave is produced at the interface of the keeper and transition plasma regions by means of an ion beam-plasma instability condition which is present during a "pulse" in the arc current. It was also proposed that the ion acoustic wave moves towards the hollow cathode where it triggers the next "pulse" in the arc current. The nature of the feedback mechanism was not clear and could not be resolved with the present experimental setup. However, there was very good agreement between the proposed theory and experiments over a wide range of discharge conditions and keeper chamber lengths. It was also proposed that changes in the fluctuation frequency due to the changes in the magnetic field strength in the ion thruster were caused by a change in the position of the keeper/transition plasma interface. This idea was not evaluated in this study.

References

1. Fitzgerald, D. J., "Plasma Fluctuations," from Annual Report on JPL Contract 952685, Research on Hollow Cathodes in Mercury Ion Thrusters, Report 15, College of Engineering, Colorado State University, Fort Collins, Colorado, Sept. 1970, pp. 29-32.
2. Cohen, A. J., "An Electron Bombardment Thruster Operated with a Cusped Magnetic Field," NASA Technical Note TN D-5448, Sept. 1969.
3. Thomassen, K. I., "Turbulent Diffusion in a Penning Type Discharge," Physics of Fluids, Vol. 9, No. 9, Sept. 1966, pp. 1836-1842.
4. Macie, T. W., and Whittlesey, A., "Electromagnetic Interference Onboard an Electrically Propelled Spacecraft," AIAA Paper 73-1128, Nov. 1973.
5. Cowgill, R. M., and Macie, T. W., "Magnetic Compatibility of Solar Electric Propulsion Module with Spacecraft and Science," AIAA Paper 75-373, Mar. 1975.
6. Stuhlinger, E., "Ion Propulsion for Space Flight," McGraw-Hill Book Company, New York, 1964.
7. Jahn, R. G., "Physics of Electric Propulsion," McGraw-Hill Book Company, New York, 1968.
8. Langmuir, B. D., Stuhlinger, E., and Sellen, J. M. Jr., Editors of "Electrostatic Propulsion," from Progress in Astronautics and Rocketry, Vol. 5, Academic Press, New York, 1961.
9. Brewer, G. R., "Ion Propulsion," Gordon and Breach Science Publishers, New York, 1970.
10. "Study of a Solar Electric Multi-Mission Spacecraft," Final Report on JPL Contract 952394, TRW Inc., Document 09451-6001-R0-02, Jan. 1970.

11. Sauer, C. G. and Atkins, K. L., "Potential Advantages of Solar Electric Propulsion for Outer Planet Orbiters," AIAA Paper 72-423, Apr. 1972.

12. Husmann, O. K., "Diffusion of Cesium and Ionization on Porous Tungsten," Electrostatic Propulsion (see Reference 8).

13. Kaufman, H. R., "An Ion Rocket with an Electron-Bombardment Ion Source," NASA Technical Note TN D-585, Jan. 1961.

14. Crawford, F. W. and Freeston, I. L., "The Double Sheath at a Discharge Constriction," Proceedings International Conference Phenomena Ionized Gases, 6th Paris, Vol. 1, 1963, pp. 461-464.

15. Andrews, J. G. and Allen, J. E., "Theory of a Double Sheath between two Plasmas," Proceedings Royal Society, London, A.320, 1971, pp. 459-472.

16. Kemp, R. F. and Sellen, J. M. Jr., "Plasma Potential Measurements by Electron Emissive Probes," Review of Scientific Instruments, Vol. 37, No. 4, Apr. 1966, pp. 455-461.

17. Strickfadan, W. B. and Geiler, K. L., "Probe Measurements of the Discharge in an Operating Electron Bombardment Engine," AIAA Journal, Vol. 1, No. 8, Aug. 1963, pp. 1815-1823.

18. Tonks, L. and Langmuir, I., "Oscillations in Ionized Gases," Physical Review, Vol. 33, Feb. 1929, pp. 195-210.

19. Masek, T. D., "Plasma Characteristics of the Electron Bombardment Ion Engine," Technical Report 32-1271, Jet Propulsion Laboratory, Pasadena, CA, April 15, 1968.

20. Poeschel, R. L., Ward, J. W., and Knauer, W., "Study and Optimization of 15 cm Kaufman Thruster Discharges," AIAA Paper 69-257, March 1969.

21. Masek, T. D., "Plasma Properties and Performance of Mercury Ion Thrusters," AIAA Paper 69-256, March 1969.

22. Denisse, J. F. and Delcroix, J. L., "Plasma Waves," No. 17, Interscience Publishers, John Wiley & Sons, New York, 1963.

23. Saheli, F., Palumbo, G., and Mickelsen, W. R., "Conical Solenoid and Shield," from Annual Report on JPL Contract 952685, Research on Hollow Cathodes in Mercury Ion Thruster, Report 15, College of Engineering, Colorado State University, Fort Collins, CO, Sept. 1970, pp. 24-28.

24. Hoh, F. C., "Instability of Penning-Type Discharges," Physics of Fluids, Vol. 6, No. 8, Aug. 1963, pp. 1184-1191.

25. Simon, A., "Instability of a Partially Ionized Plasma in Crossed Electric and Magnetic Fields," Physics of Fluids, Vol. 6, No. 3, Mar. 1963, pp. 382-388.

26. Cohen, A. J., "Onset of Anomalous Diffusion in Electron Bombardment Thruster," NASA Technical Note TN D-3731, Nov. 1966.

27. Kadomtsev, B. B. and Nedospasov, A. V., "Instability of the Positive Column in a Magnetic Field and the 'Anomalous' Diffusion Effect," Journal of Nuclear Energy, Part C: Plasma Physics, Vol. 1, Pergamon Press Limited, 1960, pp. 230-235.

28. Martin, A. R., "Indicators of Anomalous Diffusion in an Ion Engine Discharge," Plasma Physics, Vol. 14, No. 2, Feb. 1972, pp. 123-132.

29. Fitzgerald, D. and Vahrenkamp, R., "Performance Mapping of 20-cm Hollow Cathode Mercury Ion Thruster," under NASA Grant NGR06-002-032, Advanced Electric Propulsion Research, Report No. 8, College of Engineering, Colorado State University, Fort Collins, CO, May 1969, pp. 3.1-3.31.

30. Pawlik, E. V., Costague, E. N., and Schaefer, W. C., "Operation of a Lightweight Power Conditioner with a Hollow Cathode Ion Thruster," AIAA Paper 70-648, June 1970.

31. Alexeff, I. and Neidigh, R. V., "Observations of Ionic Sound Waves in Plasmas: Their Properties and Applications," Physical Review, Vol. 129, No. 2, Jan. 1963, pp. 516-527.

32. Jones, W. D. and Alexeff, I., "A Study of the Properties of Ionic Sound Waves," Proceedings International Conference Phenomena Ionized Gases, 7th Belgrade, Vol. II, 1965, pp. 330-335.

33. Crawford, F. W. and Kuhler, R. J., "Some Results on Electrostatic Sound Wave Propagation," Proceedings International Conference Phenomena Ionized Gases, 7th Belgrade, Vol. II, 1965, pp. 326-329.

34. Tanaca, H., Hirose, A., and Koganei, M., "Ion-Wave Instabilities in Mercury-Vapor Plasma," Physical Review, Vol. 161, No. 1, Sept. 1967, pp. 94-101.

35. Wong, A. Y., Motley, R. W., and D'Angelo, N. D., "Landau Damping of Ion Acoustic Waves in Highly Ionized Plasmas," Physical Review, Vol. 133, 1964, pp. A436-442.

36. Little, P. F., and Jones, H. G., "Waves and Noise in a Plasma Column," Proceedings Physical Society, Vol. 85, 1965, pp. 979-996.

37. Stringer, T. E., "Electrostatic Instabilities in Current Carrying and Counterstreaming Plasmas," Journal of Nuclear Energy, Part C, Plasma Physics, Vol. 6, Pergamon Press Limited, 1964, pp. 267-279.

38. Crawford, F. W. and Lawson, J. D., "Some Measurements of Fluctuations in a Plasma," Journal of Nuclear Energy, Part C, Plasma Physics, Vol. 3, Pergamon Press Limited, 1961, pp. 179-185.

39. Kaufman, H. R., "Electron Diffusion in a Turbulent Plasma," Journal of Nuclear Energy, Part C, Plasma Physics, Vol. 3, Pergamon Press Limited, 1961, pp. 179-185.

40. Ilic, D. B., Wheeler, G. M., Crawford, F. W., and Self. S. A., "Ion-Acoustic Instability of the Positive Column," Journal of Plasma Physics, Vol. 12, Part 3, 1974, pp. 433-444.

41. Karatzas, N. T., Anastassiadis, A. J., and Papadopoulos, K., "Generation and Behavior of Large-Amplitude Ion-Acoustic Waves," Physical Review Letters, Vol. 35, No. 1, July 1975, pp. 33-36.

42. Fenneman, D. B., Raether, M., and Yamada, M., "Ion-Acoustic Instability in the Positive Column of a Helium Discharge," Physics of Fluids, Vol. 16, No. 6, June 1973, pp. 871-878.

43. Gary, S. P., Alexeff, I., and Hsieh, S. L., "Ion Acoustic Waves at a Plasma Sheath," Physics of Fluids, Vol. 19, No. 10, Oct. 1976, pp. 1630-1634.

44. Wells, A. A., "Current Flow Across a Plasma 'Double Layer' in a Hollow Cathode Ion Thruster," AIAA Paper 72-418, April 1972.

45. Beattie, J. R., "Numerical Procedure for Analyzing Langmuir Probe Data," AIAA Journal, Vol. 13, No. 7, July 1975, pp. 950-952.

46. Poeschel, R. L. and Knauer, W., "A Variable Magnetic Baffle for Hollow Cathode Ion Thrusters," AIAA Paper 70-175, Jan. 1970.

47. Poeschel, R. L., "The Variable Magnetic Baffle as a Control Device for Kaufman Thrusters," AIAA Paper 72-488, April 1972.

48. Serafini, J. S., and Terdan, F. F., "Plasma Fluctuations in a Kaufman Ion Thruster," AIAA Paper 73-1056, Nov. 1973.

49. Serafini, J. S. and Nakanishi, S., "Preliminary Measurements of Plasma Fluctuations in an 8-cm Mercury Ion Thruster, AIAA Paper 75-396, Mar. 1975.

50. Serafini, J. S., Mantenieks, M. A., and Rawlin, V. K., "Dynamic Characteristics of a 30-cm Mercury Ion Thruster," Journal Spacecraft, Vol. 13, No. 10, Oct. 1976, pp. 579-584.

51. Doucet, H. J., and Jones, W. D., "Linear Ion Acoustic Waves in a Density Gradient," Physics of Fluids, Vol. 17, No. 9, Sept. 1974, pp. 1738-1743.

52. Brophy, J. R. and Wilbur, P. J., "Electron Diffusion Through the Baffle Aperture of a Hollow Cathode Thruster," AIAA Paper 79-2060, Nov. 1979.

53. Fujita, T., Ohnuma, T. and Adachi, S., "Self-Oscillations Excited by Two Stream Ion-Ion Instability," Plasma Physics, Vol. 19, 1977, pp. 875-887.

54. Alport, M. J., and D'Angelo, N., "Feedback Mechanism in Self-Oscillations Excited by the Ion-Ion Stability," Plasma Physics, Vol. 21, 1979, pp. 379-387.

55. Kiwamoto, V., "Plasma Turbulence Generated by Ion-Ion Two-Stream Instability," Journal Physical Society of Japan, Vol. 37, No. 2, Aug. 1974, pp. 466-474.

56. Gresillon, D. and Doveil, F., "Normal Modes in the Ion Beam-Plasma System," Physical Review Letters, Vol. 34, No. 2, Jan. 1975, pp. 77-80.

57. Sato, N., Sugai, H., and Hatakeyama, R., "Spacial Evolution of Velocity-Modulated Ion Beams in a Plasma," Physical Review Letters, Vol. 34, No. 15, April 1975, pp. 931-934.

58. Chen, F. F., "Introduction to Plasma Physics," Plenum Press, New York, 1974, pp. 186-189.

59. Masek, T. D., "Plasma Properties and Performance of Mercury Ion Thrusters," Technical Report 32-1483, Jet Propulsion Laboratory, Pasadena, CA, June 15, 1970.

60. Romesser, T., and Hershkowitz, N., "Experimental Observation of Ion-Ion Beam Instability in a Cylindrical Geometry," Physics of Fluids, Vol. 18, No. 10, Oct. 1975, pp. 1354-1361.

61. Taylor, R. J. and Coroniti, F. V., "Ion Heating via Turbulent Ion Acoustic Waves," Physical Review Letters, Vol. 29, No. 1, July 1972, pp. 34-38.

62. Chen, F. F., "Electrostatitic Stability of a Collisionless Plane Discharge," Nuovo Cimento, Vol. 26, No. 4, Nov. 1962, pp. 698-716.